THE MOLECULAR AND BIOCHEMICAL BASIS OF DARK-CUTTING BEEF

By

FRANK KIYIMBA

Bachelor of Science in Agriculture
Makerere University
Kampala, Uganda
2017

Master of Science in Animal Science
Oklahoma State University
Stillwater, Oklahoma
2019

Submitted to the Faculty of the
Graduate College of the
Oklahoma State University
in partial fulfillment of
the requirements for
the Degree of
DOCTOR OF PHILOSOPHY
December, 2022

THE MOLECULAR AND BIOCHEMICAL BASIS OF

DARK-CUTTING BEEF

Dissertation Approved:

Dr. Ranjith Ramanathan

Dissertation Adviser

Dr. Gretchen. G. Mafi

Dr. Steven. D. Hartson

Dr. Robert Burnap

ACKNOWLEDGEMENTS

First, I give glory to **God,** the almighty for the gift of life. **He** has granted unto me and for leading me successfully through this challenging time. Thank you, Lord.

In a special way, my heart will always rejoice for the support of my mother Miss. **Nampiima Specioza**. Mammy, thank you and I know you are happy with the Lord. My siblings Richard Ssebuliba, William Ssimbwa, Michael Buyondo, and Angella Nakabuubi whose tireless and selfless efforts to support me through this journey financially and spiritually can only be rewarded by the Almighty God. Words cannot express my sincere gratitude to you all.

I will forever be thankful for my academic supervisor Dr. Ranjith Ramanathan. He believed in me and gave me this opportunity to work and grow as a researcher. I have accumulated surmountable intellectual and personal skills working with you. Thank you for your guidance, mentorship, continuous support, and commitment to training and developing me as an independent researcher. Dr. Ram continues to instill the lessons of curiosity, professionalism, and personal development every time we have a private meeting and within lab meetings. I am here now because of you.

I am very fortunate to have Dr. Steven Hartson, Dr. Gretchen Mafi, and Dr. Robert Burnap in my committee. I am thankful for your tremendous input into my projects and for the fair intellectual criticism, competent guidance, and unfailing generosity right from experimental setup, through experimentation, data analysis, and presentation. Thank you for the invaluable

advice and guidance through my graduate studies. You have been consistently generous with time and useful suggestions.

I would like to thank the faculty at Makerere University Kampala-Uganda more specifically, Professor Donald. R. Kugonza, who gave me my first shot at research as an undergraduate research scholar working under the Regional University's Forum research projects (RUFORUM) and has continued to support me both financially and spiritually throughout my graduate studies.

Aside from my professional acknowledgments, I must thank the support network that I made along the way and the network I grew in Stillwater-Oklahoma. I would not have managed to finish this process without the support of Drs. Joel Komakech and Emmanuel Nsamba who have continued to support me in school and outside school. Valerie Novak, Cheyenne Edmondson, Melanie Whitemore, Anna GoldKamp, Jing Liu, Dr. Mohamed Habibi, Parniyan Goodarzi, Ivan Santiago, Dr. Daniel Jjuko, and my fellow lab mates you have helped me to endure this process. Thank you!

Finally, to Laura Ruiz, I want to thank you for becoming part of my life. You have continued to show me how to become a better man and a significant other. I appreciate your patience and support. I hope my actions will inspire you, the same way yours have inspired me.

Name: FRANK KIYIMBA

Date of Degree: DECEMBER, 2022

Title of Study: THE MOLECULAR AND BIOCHEMICAL BASIS OF DARK-CUTTING BEEF

Major Field: ANIMAL SCIENCE

Abstract: Dark-cutting beef is a meat quality defect where beef fails to have a characteristic bright-red color typical of normal-pH beef. The occurrence of dark-cutting beef is associated with a high muscle pH resulting from defective glycogen metabolism pre-slaughter. Although the factors predisposing animals to muscle darkening have been previously examined, the molecular and mechanistic basis for this occurrence remains largely unknown. In this work, we investigate the molecular and biochemical basis of dark-cutting beef by integrating proteomics, metabolomics, and enzyme assays coupled with bioinformatics analyses. Here, we show that dark-cutting beef is caused, in part, as a consequence of over-proliferation of mitochondria supported by the up-regulation of proteins involved in mitochondrial biogenesis, mitochondrial electron transport, calcium homeostasis, and fatty acid metabolism. However, in atypical dark-cutting beef, "a condition where beef has slightly above normal-pH but present dark-colored muscles", we show that the enzymes involved in glycogen metabolism create a threshold for muscle darkening rather than the metabolites expression profiles. Furthermore, examination of postmortem wet-aging of dark-cutting beef suggests enhanced muscle proteolysis compared with normal-pH beef supported by up-regulation of the proteasome and oxidative proteins and more abundance of TCA-, nucleotide-, and free amino acids metabolites. This implies that the greater mitochondrial content in dark-cutting beef could contribute to more oxidative stress during postmortem aging. Finally, we observed that the inherent substrate inhibition mechanisms in dark-cutting beef regulate muscle pH decline. Therefore, by supplementing glycogen in an in-vitro system, we showed that postmortem muscle pH decline could be restored in dark-cutting muscles. Thus, findings from this study show that understanding the pathways and biochemical processes underpinning muscle darkening in beef, can increase detection and help in designing strategies to minimize the occurrence while improving economic benefit.

Keywords: Dark-cutting, meat color, proteomics, metabolomics, glycogen, pH decline, mitochondria oxygen consumption, mass spectrometry, bioinformatics

TABLE OF CONTENTS

Chapter Page

LIST OF TABLES

Table Page

LIST OF FIGURES

Figure Page

Figure Page

Figure Page

CHAPTER I

INTRODUCTION

Meat color is the most important quality attribute consumers associate with both freshness and wholesomeness (Boykin et al., 2017; Ramanathan et al., 2022; Ramanathan et al., 2020a; Salim et al., 2019; Sammel et al., 2002; Węglarz, 2018). Consumers are willing to pay extra for high-quality meat in order to have a good eating experience (Troy & Kerry, 2010; Wang et al., 2022). Therefore, any deviation in meat surface color is associated with a perceived reduction in quality, and thus discolored meat is discounted in price, especially at retail. The color of meat is primarily determined by myoglobin, a water-soluble sarcoplasmic protein. Myoglobin naturally exists in three forms: oxymyoglobin, deoxymyoglobin, and metmyoglobin (AMSA, 2012). Oxymyoglobin is the form responsible for the desired cherry bright-red color in fresh beef. Discoloration results from accumulation of metmyoglobin. However, predominant deoxymyoglobin is associated with a dark-cutting meat color appearance (Ashmore et al., 1972; Kiyimba et al., 2021; McKeith et al., 2016; Ramanathan et al., 2020b).

The dark-cutting beef phenotype has a worldwide occurrence. Although the prevalence has reduced over the years, dark-cutting beef still occurs in the beef industry. In the United States, an average occurrence rate of 1.9% was reported in the 2016 National Beef Quality Audit (Boykin, et al., 2017). However, in certain months some beef packers reported an occurrence of 2-5%. In Brazil, an occurrence rate of 30% was reported (Rosa et al., 2017), while in South Chile, incidences of 17- 40% of dark-cutting beef was reported to occur annually (Gallo et al., 2003).

Various studies have determined protein, metabolite, and mitochondrial profiles to understand the biochemical basis of dark-cutting beef (Cônsolo et al., 2021; Kiyimba et al., 2021, 2022; Ramanathan et al., 2020b; Wu et al., 2020). Several proteins and metabolites associated with glycogen degradation were found to be less abundant in dark-cutting compared with normal-pH beef counterparts. On the other hand, proteins and metabolites associated with mitochondrial oxidative phosphorylation were found to be overabundant in dark-cutting beef muscles. Therefore, based on findings from previous studies, the current understanding implicates defective glycogen metabolism to contribute to muscle darkening. As a result, dark-cutting beef has a greater than normal muscle pH in excess of 5.8.

The high muscle pH contributes to muscle darkening via sustaining mitochondrial respiration postmortem. Mitochondria remain functional in postmortem muscle, and the increased mitochondrial function postmortem increases the muscles' oxygen consumption while decreasing oxygen available to bind myoglobin. Thus, this maintains myoglobin in a deoxymyoglobin state when exposed to oxygen (Ashmore et al., 1972; Mancini et al., 2018; McKeith et al., 2016; Ramanathan et al., 2009; Tang, et al., 2005). The greater than normal muscle pH also influences myofibril shrinkage by affecting the water held within the muscle.

In-turn, this can reduce the muscle's capacity to scatter light and hence have a dark color appearance (English et al., 2016; Lawrie, 1958; MacDougall, 1982). Therefore, the biochemical and physical characteristics of dark-cutting beef are in part, caused by a high ultimate muscle pH which influences the muscle's postmortem metabolism and the overall color appearance. However, there is a gap in our understanding of how these processes are triggered/initiated and maintained in dark-cutting beef.

In this dissertation, I sought to elucidate the molecular and biochemical basis of dark-cutting phenotypes in beef. The overall goal was to utilize an integrative omics approach combining proteomics and metabolomics profiling coupled with enzyme assays and bioinformatics analyses to better understand the molecular basis of muscle darkening in beef.

Four broad aims included:

(i) To characterize changes in mitochondrial protein profiles of dark-cutting beef compared with normal-pH beef to further understand the contribution of mitochondria in muscle darkening.

(ii) To define the changes in protein and metabolites profiles associated with muscle darkening at a slightly elevated pH.

(iii) To examine the impact of postmortem wet-aging on muscle proteolysis in dark-cutting beef compared with normal-pH beef.

(iv) To evaluate the impact of glycogen supplementation on muscle pH decline in dark-cutting beef using an in-vitro system.

The results of aims 1 to 4 are presented in Chapters 3, 4, 5, and 6, respectively. Together, these results implicate energy adaptation mechanisms pre-slaughter to contribute to dark-

cutting phenotypes in beef. Thus, any fluctuations in energy level pre-slaughter trigger adaptive mechanisms in dark-cutting beef, inducing changes in mitochondrial function, protein, and metabolite profiles that ultimately regulate meat quality characteristics of dark-cutting beef under postmortem conditions.

CHAPTER II

REVIEW OF LITERATURE

Surface color characteristics of dark-cutting beef

Meat color is the most important quality attribute influencing consumers' purchasing decisions. A bright red-color is associated with freshness and wholesomeness. However, dark-cutting beef is a meat quality defect where beef fails to have a characteristic bright red color typical of normal-pH beef (Apple et al., 2011; McKeith et al., 2016; Wills et al., 2017; Kiyimba et al., 2021). As a result, dark-cutting beef is discounted during grading, and the meat is not sold in retail due to its appearance and reduced shelf-life. Dark-cutting beef has a dark appearance due to less reflectance on the meat surface as compared with normal pH meat (English et al., 2016).

The objective measurement of color used in meat research utilizes the Commission Internationale de l'Eclairage (CIE) color system based on three coordinates (L^*-, a^*-, and b^*-values; AMSA, 2012). The L^*-values represent brightness or darkness corresponding to the quantity of light reflected off the meat surface with a range between 0 (all light absorbed) and 100 (all light is reflected). The a^*-values represent muscle color red intensity, and positive values ($+a^*$) represents red color while negative values ($-a^*$) give a green color. Thus, the greater the positive values, the more the red intensity.

The *b**-values represent muscle yellowness and range from blue (-*b**) to yellow (+*b**) values. Other color coordinates, such as hue (lightness) and chroma (light saturation index), are calculated using the *a**- and *b**-values (AMSA, 2012). Using the CIE color system measurements, dark-cutting beef exhibits lower *L**- *a**-, *b**-, hue, and chroma values compared with normal-pH (English et al., 2016; Kiyimba et al., 2021; Cônsolo et al., 2020). The *L**- and *a**- values of 25.2 and 18.4, respectively, compared with 38.2 and 28.4 in normal-pH beef, were used to classify meat as dark-cutting (Mitacek et al., 2018). In addition to the CIE color indicators, biochemical characteristics such as muscle pH, oxygen consumption, and metmyoglobin reducing activity are utilized to classify meat as dark-cutting. For example, muscle lightness can increase depending on the holding temperature, carcass fatness, and time allowed for the meat to oxygenate.

Dark-cutting beef surface color can be improved relative to normal-pH beef by utilizing post-harvest techniques such as enhancements and modified atmospheric packaging. For example, Denzer et al. (2022) showed that nitrite-embedded packaging in combination with glucono delta-lactone enhancements improved surface redness of dark-cutting beef steaks. In another study, extended wet-aging of dark-cutting steaks increased surface color attributes of dark-cutting beef (English et al., 2017). Furthermore, Apple et al. (2011) and Sawyer et al. (2009) tested the capacity of various organic acids to improve surface color properties of dark-cutting beef. They reported that enhancing dark-cutting steaks with 0.35% and 0.5 lactic acid at 112% of fresh weight improved fresh and cooked color of dark-cutting beef close to that of control (normal-pH beef).

The introduction of case-ready meats enables beef purveyors to utilize modified gas composition within the packages to improve meat color and shelf-life. Therefore, the effects of modified atmospheric packaging using high oxygen and carbon monoxide packaging have also been evaluated with regard to improving muscle lightness (L^*-values) and redness (a^* values) of dark-cutting beef (Zhang et al., 2018; Mitacek et al., 2018). Although several of these strategies has the potential to improve dark-cutting beef meat color characteristics, the molecular and mechanistic basis for the occurrence is still unknown.

Muscle biochemistry of dark-cutting beef

Although the biochemical basis for muscle darkening in beef is unknown, the widely accepted model for muscle darkening is that chronic stress before slaughter reduces muscle glycogen (Fuente-García et al., 2021; Kiyimba et al., 2021; Mahmood et al., 2018; Poleti et al., 2018; Ponnampalam et al., 2017). The low glycogen content reduces the muscle's capacity to accumulate lactic acid under postmortem conditions resulting in a greater than normal-muscle pH in excess of 5.8 (Hamilton et al., 2003). The typical dark-cutting beef (regular dark-cutters) have pH ranges from 6.0 and extreme values above 6.4, while the atypical dark-cutters have slightly elevated muscle pH close to normal (5.7) but exhibit a dark meat color (Lei et al., 2020; Mahmood et al., 2018; Roy et al., 2022). Hence, depending on muscle pH, muscle darkening can vary from a slight dark red color to a coffee-bean dark color.

The effect of high postmortem pH on meat color is twofold; the high pH affects muscle's reflectance capacity by allowing muscle proteins to hold more water, limiting the

muscle's capacity to scatter light (Lawrie, 1958; MacDougall, 1982). Hence, dark-cutting beef has low reflectance and appears dark. The high muscle pH can support mitochondrial function, enhancing oxygen consumption and myoglobin deoxygenation. Thus, muscle oxygen consumption is greater in dark-cutting compared with normal-pH beef (English et al., 20017; McKeith et al., 2016; Ramanathan and Mancini., 2019). Furthermore, the high pH can stabilize the activity of proteolytic systems mostly the alkaline-dependent caspases which degrade muscle proteins. Therefore, the activity of caspase 9 and 3/7 in high-pH meats is evaluated as a way to explain the meat characteristics and biochemical attributes of dark-cutting beef (Fuente-García et al., 2022).

Several proteins and metabolites involved with glycogen catabolism are less abundant in dark-cutting groups compared with normal-pH counterparts, while proteins and metabolites associated with mitochondrial oxidative metabolism are overabundant (Cônsolo et al., 2021; Fuente-García et al., 2021; Gagaoua et al., 2021; Kiyimba et al., 2021; Ramanathan et al., 2020b; Wu et al., 2020). Therefore, the overabundance of mitochondrial proteins and metabolites in dark-cutting beef suggests enhanced oxidative metabolism. Thus, evaluation of muscle fiber characteristics showed that dark-cutting beef has a greater abundance of type I fibers than normal-pH (Roy et al., 2022).

Causes and factors contributing to muscle darkening

Pre-slaughter and post-slaughter factors influence muscle metabolism and physical properties. Pre-slaughter factors, including: stocking density, housing or management practices, environmental conditions/seasons, transportation conditions, time at the lairage, stunning, and slaughter protocols, among several others, contribute to the occurrence of

dark-cutting phenotypes in beef (Egbert & Cornforth, 1986; Gagaoua et al., 2021; Knee et al., 2007; Hendrick et al., 1959; Ponnampalam et al., 2017). In addition, nutritional regimes, as well as feeding systems, also can contribute to muscle darkening. For example, animals that are fed on pastures (grass-fed diets) are more susceptible to produce dark-cutting beef compared with grain-fed animals (feed lot diets; Huges et al., 2015 and Muir et al., 1998). This is attributed to the low energy density of pasture diets and the greater energy maintenance requirements for pasture-fed animals relative to the feed-lot animals (Ponnampalam et al., 2017; Priolo et al., 2001). In addition, grain-fed diets are associated with more subcutaneous fat which allows the carcasses to chill at a slower rate thus increasing the rate of protein degradation and facilitating greater and faster pH decline (Farouk & Lovatt, 2000; Priolo et al., 2001). Therefore, feeding with high-energy diets has been examined as a potential strategy to reduce dark-cutting in pasture-fed beef (Knee et al., 2005). Other pre-slaughter factors include: animal genetics, age, and sex of the animal. Older animals have much more concentration of myoglobin compared to young animals and, bulls are more susceptible to stress than heifers (Field, 1971). Additionally, physical activity, nutritional status, and tolerance to various stressors vary between animals of different sex, age, and genetics (Kadim et al., 2004; Kim et al., 2003).

The post-slaughter factors are mostly associated with the intrinsic components within the muscle that impact overall postmortem muscle metabolism. Following slaughter, the animal's metabolism shifts from aerobic to anaerobic metabolism. This phase is associated with several changes that impact muscle quality characteristics. For example, pre-slaughter stress induces changes in (i) muscle glycogen storage, (ii) mitochondrial respiratory capacity (McKeith et al., 2006; Tang et al., 2005; Kiyimba et al., 2022), and (iii) muscle

fiber characteristics (Roy et al., 2022). These changes regulate the muscles' intrinsic properties, such as: muscle pH, color, and oxygen consumption. However, how the pre-slaughter factors and post-slaughter factors interact on a molecular and mechanistic level is largely unknown.

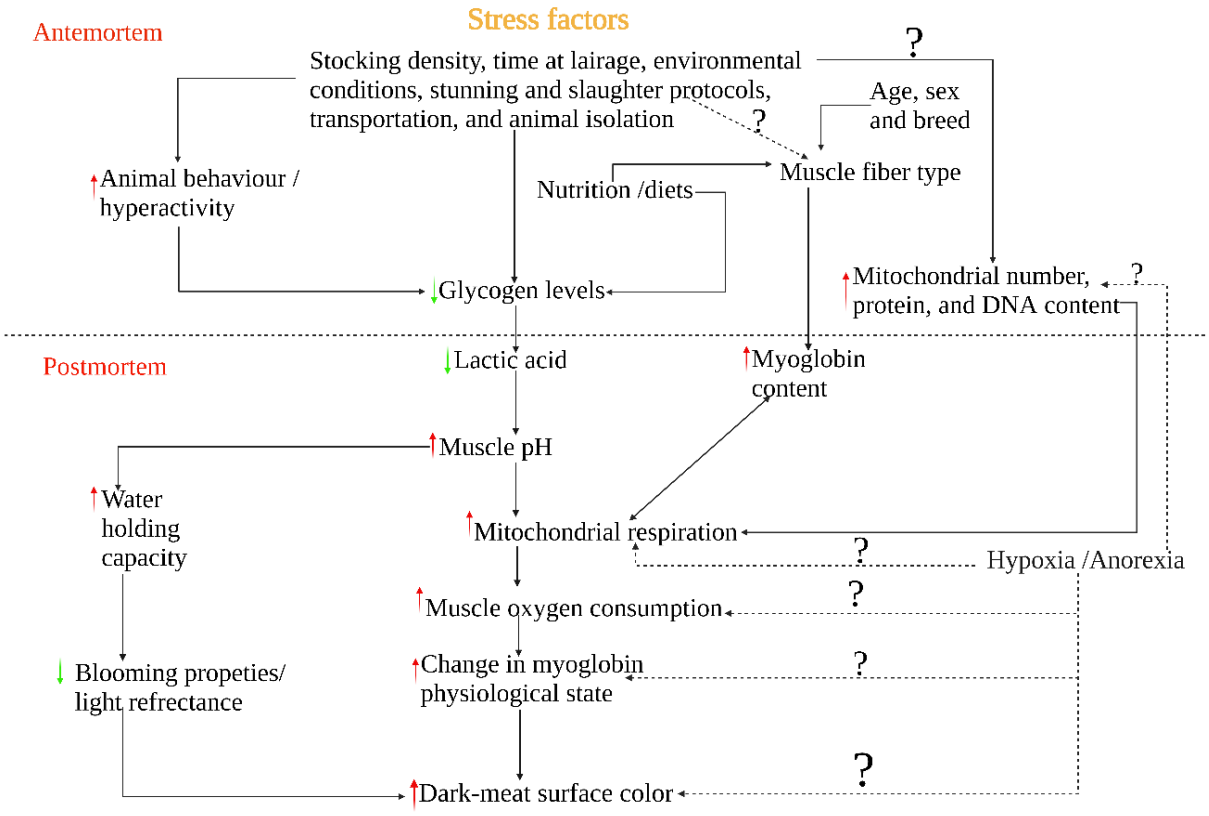

Figure 1: Schematic representation of pre- and post-slaughter factors contributing to muscle darkening.

The green arrow indicates decreased levels, while the red arrow indicates increased levels. The broken allows shows missing/unconnected gaps in knowledge for the etiology of dark-cutting phenotypes in beef. The double-headed arrows show the potential reversible influence between two factors.

Role of stress in muscle darkening

The stressors within the animal's environment disrupt cellular energy balance and stimulate a stress response. For example, in postmortem muscles, the loss of cellular homeostasis results in several changes in the muscle's biochemical mechanisms that regulate postmortem metabolism. However, in a pre-slaughter environment, the recognition of the threat to cellular homeostasis triggers several events that activate the hypothalamus-pituitary-adrenal axis (HPA) and sympathetic-adreno-medullar axis (SAM) through neural input from the thymus and amygdala (Engler et al., 1989; Scheinman et al., 1997; Tsigos & Chrousos, 2002). Therefore, animals that are under stress respond with a number of physiological, physical, and behavioral changes. These events subsequently result in release of glucocorticoids and catecholamine, which are important mediators of the stress coping mechanisms.

Although acute and mild stressors are relatively adaptive, chronic stressors have the potential to induce negative consequences on the energy balance and overall cellular metabolism. Thus, animals that are exposed to chronic stressors are more susceptible to muscle darkening (Hendrick et al., 1959; Ponnampalam et al., 2017; Priolo et al., 2001). For example, chronic heat stress induces enhanced glycolysis and creatine kinase activity in postmortem muscles (Petracci et al., 2001; Zhang et al., 2012). The enhanced glycolysis pre-slaughter depletes the glycogen reserves leading to less accumulation of lactic acid necessary to initiate post-mortem pH decline (Mahmood et al., 2018; Ponnampalam et al., 2017; Wulf et al., 2002; Kiyimba et al., 2021; Ramanathan et al., 2020b). Hence, dark-cutting beef has a greater than normal muscle pH in excess of 5.8.

The differences in levels of stressors (chronic vs. mild) coupled with the prevalence of animal's ability to cope with stress contribute to different levels of dark-cutting phenotypes in beef on the basis of ultimate pH (Ijaz et al., 2022; Holdstock et al., 2014; Roy et al., 2022). To understand how stress contributes to dark-cutting beef, Hendrick et al. (1959) investigated active manipulation of the animal's physiology via epinephrine treatment to induce stress in the animals. The logic was that among other factors, if the stress was the causative factor for the dark-cutting phenomenon, then animals injected with epinephrine should produce darker beef and present with the hallmark characteristics of muscle darkening (a greater than normal muscle-pH). However, if dark-cutting conditions do not occur in epinephrine-treated animals, then stress cannot be the cause. They found that cattle fasted for 24 h and injected with epinephrine 5 h before slaughter presented with symptoms of stress. In addition, administration of epinephrine at doses of 2.5 or 5 mg reduced muscle glycogen and produced a shady meat surface color. However, increasing the concentration of epinephrine produced dark-carcasses. Thus, this study showed that longer periods of stress are required to sufficiently deplete muscle glycogen. Hence, dark-cutting beef phenotype in beef is associated with long term stress before slaughter.

Effects of hypoxia and oxidative stress on meat color

The loss of blood flow and antioxidant systems in postmortem muscles induces hypoxic and oxidative stress. The resultant hypoxic conditions, particularly at slaughter, lead to a limited substrate and oxygen supply at the mitochondrial cytochrome *c* oxidase, which reduces the rate of electron transport. Therefore, the decrease in mitochondrial oxidative capacity leads to less ATP, low energy balance, and increased production of reactive oxygen species (ROS; Zorov et al., 2014). This imbalance between ROS

production and the cells' ability to readily detoxify leads to a rise in ROS beyond the physiological threshold, a process called oxidative stress.

The resultant oxidative stress can activate several cellular pathways, including (i) mitochondrial degeneration and apoptosis (Orrenius et al., 2007), (ii) cell cycle and proliferation (Kim et al., 2001), (iii) growth and transcriptional factor signaling (Ježek & Hlavatá, 2005). In addition, the ROS produced during hypoxia and oxidative stress plays important roles in stabilizing hypoxia transcription factors (HIF-1α and HIF-2α), and in activating mitochondrial protein kinases (Bell et al., 2005; Han et al., 2011; Zhang et al., 2008). Therefore, the hypoxic conditions within postmortem muscles induce the expression of hypoxia inducible factor -1 α (HIF-1 α), which activates glycolysis by regulating changes in enzyme activities and mitochondrial function (Xin et al., 2022). Furthermore, HIF-1 α modulates the inhibition of F_0, F_1-ATPase complex via S-nitrosylation post-translational modification and through binding of regulatory proteins such as G0S2 and the ATPase inhibitory factor 1 (García-Bermúdez & Cuezva, 2016). Therefore, the inhibition of the F_0, F_1-ATPase complex leads to low energy balance and increases the production of ROS via electron leakage (Zorov et al., 2014).

In postmortem muscles, hypoxic and oxidative stress can influence meat color by regulating oxygen demand within the muscle. Oxygen from the atmosphere and within the muscle is utilized by myoglobin and the mitochondria (Ramanathan et al., 2020b; Tang et al., 2005). Therefore, with increasing hypoxic and oxidative stress postmortem, the competition between mitochondria and oxygen-consuming enzymes with myoglobin for available oxygen increases. This might deoxygenate myoglobin and hence contribute to dark-cutting phenotypes via predominant deoxymyoglobin. In addition, hypoxic

conditions/metabolic stress, initiates the apoptosis cascade mainly via the activation of caspase 9 followed by activation of executioner caspases 3/7. In dark-cutting beef, greater expression of caspase 3 large subunit at 24 h postmortem was observed (Diaz-Luis et al., 2021).

Antioxidant activities vary across muscles of different fiber compositions (Chen et al., 2020; Yu et al., 2018; Zhai et al., 2020; Zhang et al., 2018). For example, the oxidative muscles (Type I), due to their greater mitochondrial content, have greater antioxidant capacity relative to glycolytic muscle fibers (Type II; Powers et al., 1994).Therefore, the greater mitochondrial protein and DNA content observed in dark-cutting phenotypes (Ramanathan et al., 2020b; McKeith et al., 2016) suggest that dark-cutting beef is more susceptible to ROS-induced oxidative damage. However, the impact of the molecular signals produced during hypoxia and oxidative stress on postmortem metabolism more specifically in dark-cutting beef is yet to be well described.

Impact of heat stress on meat color

Heat stress occurs when the amount of heat generated by the animal's body exceeds the capacity of the animal's heat regulatory mechanisms to restore the homeostatic set point. Therefore, heat stress adversely affects physiological and immune responses of livestock by altering the animal's biological function. The main biological responses to heat stress involve the activation of the hypothalamus-pituitary-adrenal axis (HPA) and sympathetic-adreno-medullar axis (SAM; Butcher & Lord, 2004; Ulrich-Lai & Herman, 2009).

Depending on the level, magnitude, and frequency of heat stress, the glucocorticoids produced can stimulate the release of several factors and hormones. For example, animals exposed to elevated temperatures respond by releasing heat shock proteins (HSPs) which are important in activating the heat shock response (HSR) pathway (Gidalevitz et al., 2011). In addition, excess heat can increase the production of cellular ROS, which in-turn might contribute to protein degradation and myofibrillar disorganization (Abdelnour et al., 2019). These changes can lead to metabolic disorders associated with a decrease in adenosine triphosphate (ATP) synthesis and an altered supply of gluconeogenesis precursors (Abdelnour et al., 2019; Baumgard & Rhoads, 2013; Skibiel et al., 2018). Although the extent of heat stress in animals that produce dark-cutting beef and its contribution to muscle darkening has not been examined, one could speculate that the dysregulated glycogen metabolism in dark-cutting beef muscles might as well be associated with pre-slaughter heat stress conditions.

Cellular stress adaptation mechanisms

The physiological memories of the environmental and cellular stressors can help animals predict future environmental changes and also in developing stress adaptation mechanisms. Therefore, animals that are directly exposed to stressful conditions during key windows of development, especially early in life, can develop long-lasting reprogramming mechanisms in their energy metabolic axis. These changes can persist longer, even after the initial stimulus is lifted (Fawcett et al., 2019).

The adaptation to cellular stressors involves several levels including: morphological, behavioral, physiological, biochemical, neural, and metabolic responses

(Sejian et al., 2018; Young et al., 1989). In skeletal muscle, an example of metabolic adaptation to stress-induced disrupted energy homeostasis is mitochondrial biogenesis (Lee and Wei, 2005; Remels et al., 2010; Zong et al., 2002). Thus, the overabundance of mitochondrial bioenergetics and biogenesis proteins in postmortem dark-cutting muscles suggests pre-slaughter stress adaptive metabolic response (Kiyimba et al., 2022). However, how these responses are activated and maintained postmortem is yet to be well described.

The role of mitochondria in stress adaptation and energy balance

Mitochondria structure

Mitochondria are membrane-bound organelles responsible for energy production within cells. Many of the metabolic pathways, including ATP synthesis, heme and iron cluster synthesis, and metabolism of lipids, amino acids, and other metabolites, are localized in the mitochondria (Rutter & Hughes, 2015). In addition, mitochondria are highly dynamic cellular organelles capable of building large interconnected intracellular networks (Bereiter-Hahn, 1990), with numerous fusion and fission processes (Westermann, 2010). The outer membrane comprises of a phospholipid membrane that separates the organelle from the cytoplasm. Within the outer membrane, small voltage-gated channels span the membrane and facilitate the transportation of small uncharged molecules into the mitochondria.

The mitochondrial inner membrane comprises two sub sections, the bound membrane and the cristae. The surface membrane of the cristae creates a proton gradient necessary for oxygen diffusion and mitochondrial respiration (Osellame et al., 2012). Several proteins

responsible for oxidative phosphorylation are also localized with in the inner mitochondrial membrane. The pores localized within the inner membrane form the mitochondria membrane permeable transport pore (MPTP). These pores regulate calcium overload and mitochondrial membrane permeability as well as function (Bernardi and Di Lisa, 2015; Osellame et al., 2012; Palmer et al., 2011). In addition, contact sites including: (i) the translocases import proteins such as the outer membrane (TOM) and inner membrane (TIM) import proteins, (ii) adenine nucleotide translocases, and (iii) voltage-dependent anion channels also align the mitochondrial membranes (Brdiczka et al., 1990, Krener and Hoppel, 2000).

Mitochondria uniporter

The mitochondrial uniporter (MCU), also referred to as the mitochondrial calcium uniporter, regulates calcium entry into the mitochondria. The MCU is ubiquitously expressed among organisms and has two transmembrane helices connected with a short lope consisting of several acidic residues called the DIME motif (Baughman et al., 2011; Dong et al., 2017; Patron et al., 2013). The well-characterized proteins of the MCU include: (i) MICU1, whose expression regulates MCU-mediated calcium uptake. (ii) MICU2, which depends on MICU1 expression levels, (iii) MCUR1, a regulator protein, and (iv) EMRE an essential MCU regulator protein that mediates the interaction between MUC1 and MUC2 (Baughman et al., 2011; Dong et al., 2017; Patron et al., 2013; Tomar et al., 2016). Although the role of MCU in mitochondrial function and bioenergetics has been examined, how the postmortem signaling events that lead to the activation of MCU, its role in the muscle contractile machinery and postmortem metabolism remains to be elucidated.

Mitochondrial oxidative phosphorylation apparatus and bioenergetics

Cellular stress adaptation and cellular metabolic processes require energy in the form of adenosine triphosphate (ATP). Energy is generated via glycolysis, a series of reactions that generate pyruvate from glucose, and also via mitochondrial oxidative phosphorylation machinery. The mitochondrial oxidative phosphorylation apparatus (electron transport chain) comprises five protein complexes located in the inner membrane (Osellame et al., 2012). The bioenergetics mechanisms within the mitochondria facilitate the transfer of electrons from one complex to the next. Pyruvate from glycolysis is imported into the mitochondria via special channels called the mitochondria pyruvate channels (MPCs; McCommis & Finck, 2015). In the mitochondria, pyruvate is incorporated into the tri-carboxylic acid cycle (TCA) metabolites with a production of reducing equivalents such as nicotinamide adenine dinucleotide (NADH) and Flavin adenine nucleotide (FAD).

Mitochondrial complex 1 consists of 46 subunits that aid in NADH oxidation and initiate electron flow. Electrons picked up by NADH and FADH are transferred from NADH-Coenzyme Q-reductase (Complex I) to succinate dehydrogenase (complex II), cytochrome bc1 (complex III), and finally to cytochrome *c* oxidase (Complex IV; González et al., 2005; Jung et al., 2002; Osellame et al., 2012; Palmer et al., 2011). The proton gradient across the inner membrane is then utilized to phosphorylate adenosine diphosphate (ADP) by complex V generating ATP. Therefore, the structure, content, and function of the mitochondria are important in determining the efficiency of muscle metabolism (Erlich et al., 2016). Hence, the changes in mitochondrial structure can reduce mitochondrial bioenergetics and influence postmortem muscle metabolism.

Mitochondria biogenesis

Mitochondrial biogenesis is a complex pathway that requires a coordinated system of activation of both nuclear and mitochondrial encoded gene expression necessary to assemble large sets of proteins, lipids, import and assembly of mitochondria networks (Palikaras et al., 2015; Pohjoismäki et al., 2012). In skeletal muscles, the peroxisome proliferator-activated receptors (PPR; PGC-1α) is the main regulator of mitochondrial biogenesis (Lehman et al., 2000; Wu et al., 1999). However, other transcriptional and post-translational factors such as the nuclear respiratory factors, NRF1 and NRF 2 (Gill & La Merrill, 2017; Wenz, 2013) and cellular stress signaling molecules including, adenosine mono-phosphate (AMP)-activated protein kinase (Zong et al., 2002; Lee and Wei, 2005), and sirtulin-1 nicotinamide adenine nucleotide (NADH) dependent deacetylases (SIRT1;Gurd, 2011; Menzies et al., 2013; Yuan et al., 2016) also alter the expression of PGC factors. These modulate and direct the mitochondrial gene expression of nuclear-encoded mitochondrial proteins (mtTFA/TFAM, mtTFBI, and mtFBII) and several mitochondrial RNA polymerases involved in mitochondrial biogenesis.

Mitochondrial biogenesis can be activated by various environmental and cellular factors including adaptive thermogenesis especially during low temperatures and excessive caloric intake (Wu et al., 1999). Additionally, mitochondrial biogenesis is activated in response to increased exposure of muscle cells to exercise (Calvo et al., 2008; Holloszy, 1967; Steiner et al., 2011) and during electrical stimulation (Sanders et al., 1987). The well-described processes regulating mitochondrial biogenesis include: fusion and fission. These are necessary for proper morphology and function but can also play roles in cell division and apoptosis (Osellame et al., 2012). Fusion of mitochondria is regulated by

mitofusin proteins (Mfn1 and Mfn2; Cartoni et al., 2005; Kawalec et al., 2015; Romanello & Sandri, 2010; Schrepfer & Scorrano, 2016), while mitochondrial fission is mediated via the action of dynamin-related proteins such as Dmn1 and mitochondrial fission 1 protein (FIS1). FIS1 is an outer mitochondrial membrane protein important in recruiting Dmn1 to the membrane at the site of division (Romanello & Sandri, 2010). Several of these proteins are overabundant in dark-cutting beef (Kiyimba et al., 2022), suggesting enhanced mitochondrial biogenesis in dark-cutting beef phenotypes.

Signaling pathways regulating mitochondrial biogenesis

Several signaling pathways tightly regulate mitochondrial biogenesis. However, the complete pathways are still largely unknown. The most commonly described pathways included: (i) adenosine monophosphate-activated protein kinase (AMPK)-PGC-1α and (ii) the Sirtuin-1[SIRT1, NADH dependent deacetylase]- PGC-1α pathways (Gurd, 2011; Marcinko & Steinberg, 2014; Marin et al., 2017; Menzies et al., 2013; Yuan et al., 2016; Zong et al., 2002). AMPK is an energy-sensing molecule activated when cytosolic ratios of [ATP]/[ADP] change during starvation, endurance exercise, and via physiological stimuli such as hypoxia and oxidative stress. When activated, AMPK can direct the phosphorylation of PGC-1α, which is then translocated into the nucleus to turn on gene regulation that mediates mitochondrial biogenesis. However, the activation of Sirtulin -1 is dependent on fluctuations in the $[NAD]^+$/[NADH] levels (Gurd, 2011). The other pathways involving calcium signaling and sensing molecules such as calcium/calmodulin-dependent protein kinase (CAMK) and mitochondrial fatty acid oxidation protein such as carnitine palmitoyltransferase-1(CPT1). Carnitine palmitoyltransferase-1 can modulate mitochondrial fission through active translocation of long-chain fatty acids into the

mitochondria for oxidation (Chin, 2004; Jain et al., 2014). A representation of pathways depicting factors involved in mitochondrial biogenesis and the association with muscle darkening is shown in Figure 2.

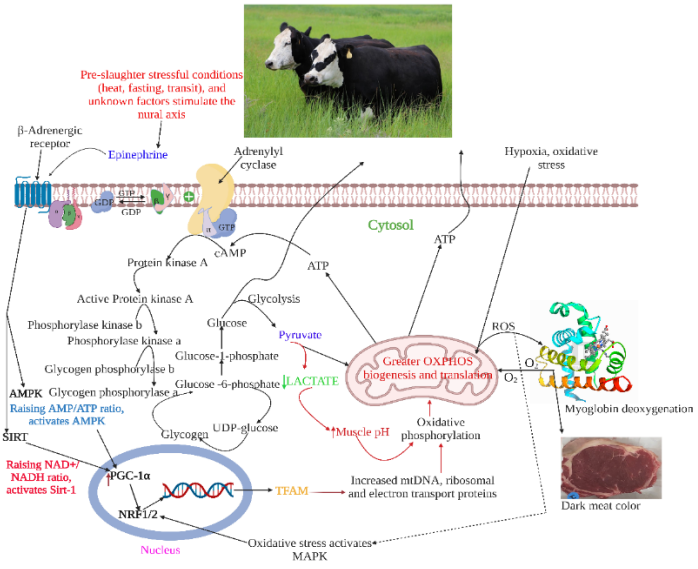

Figure 2: A simplified representation of components involved in activation of mitochondrial biogenesis and enhanced bioenergetics pathways contributing to muscle darkening.

The diagram depicts pre-slaughter stress activation of a stress response mechanism that promotes energy utilization pathways and the interaction with the energy-sensing molecules (SIRT1, AMPK) that drive mitochondrial biogenesis via activation of nuclear factors to ensure a steady energy supply. The hypoxic conditions at slaughter can increase mitochondrial oxidative output postmortem, accelerating ROS production. The ROS produced can induce mitochondrial biogenesis via the mitogen-activated protein kinase (MAPK) pathway, while greater oxygen consumption results in muscle darkening postmortem.

Epigenetics reprogramming of mitochondrial biogenesis

The metabolic intermediates driving epigenetic regulation are derived from metabolic pathways that are localized in the mitochondria (Picard et al., 2018). The well-reported epigenetic mechanisms involved in physiological and metabolic stress response include; post-translational histone modifications, DNA methylation patterns (Matilainen et al., 2017), and altered expression of noncoding RNAs (Jain et al., 2014). The epigenetic modifications that occur early in the developmental process, especially when animals are exposed to stressors, can persist long after the initial stimulus is lifted, enhancing a more robust response. Therefore, stressors experienced by the dam during gestation are capable of changing DNA methylation patterns in the offspring (Karlsson et al., 2019; Tachibana et al., 2015). For example, prenatal transportation stress altered DNA methylation patterns in Brahman heifers leading to long-term phenotypic changes via regulation of cell signaling, immune response, and metabolic pathways in the offspring (Baker et al., 2020).

The impact of epigenetic reprogramming on mitochondrial biogenesis is through modifications of critical pathways and regulatory processes associated with mitochondrial function and redox signaling. For example, DNA methylation reprogramming in the PPARGC1A, a gene that encodes PGC-1α (mediator of mitochondrial biogenesis) has been reported in different tissues (Barrès et al., 2009; Ling et al., 2008; Pirola et al., 2013). In addition, hypermethylation of PPARGC1A was found to cause gene down-regulation and lower mitochondrial content (Barrès et al., 2009).

Cross talks between mitochondrial biogenesis and muscle darkening

In postmortem muscles, the accumulating biochemical and molecular evidence allows speculation that muscle darkening in beef could result from upstream pre-slaughter regulation of the stress adaptive responses. Evidence includes that (i) dark-cutting beef compared with normal-pH beef has greater expression of mitochondrial biogenesis and bioenergetics proteins, (ii) mitochondrial DNA copy number is greater in dark-cutting muscles, and (iii) increased oxidative metabolism is observed in dark-muscles (Ramanathan et al., 2020b; Wu et al., 2021; Kiyimba et al., 2021; Consolo et al., 2021; Fuente-Garcia et al., 2021). Therefore, in order to add evidence that suggests muscle darkening is caused as a consequence of energy adaptation, one would need a method that monitors energy levels during the developmental stages and mapping those changes to the resultant muscle phenotypes postmortem. However, no current research has been conducted in postmortem skeletal muscles to further explore these possibilities. In addition, how and when these adaptation processes are triggered, regulated by specific signaling pathways, and maintained through postmortem in dark-cutting beef muscles is yet to be described.

Mitochondrial biogenesis is a metabolic stress response to fluctuating energy levels. Thus, the number of mitochondria in cells is regulated by changes in metabolic demand (Kelly and Scarpulla, 2004). Muscles with a high-energy demand are more likely to have greater mitochondrial content and lower color stability. Although the cross-talks between mitochondrial biogenesis and muscle darkening have not been investigated, enhanced mitochondrial biogenesis can promote meat darkening via increased mitochondrial respiration (Ramanathan et al., 2020b). The exchange of oxygen between oxymyoglobin

and mitochondria occurs at the mitochondrial outer membrane when the oxygen partial pressures are between 2-5mm Hg (Postnikova et al., 2009). The increase in oxygen flux into mitochondrial cells results from a greater mitochondrial cytochrome *c* oxidase affinity for oxygen than myoglobin's affinity to bind oxygen (Sidell 1998). Thus, oxygen consumed by the mitochondria darkens muscle by lowering oxygen partial pressures while encouraging maintenance of myoglobin in a deoxymyoglobin state (Ashmore et al., 1971; Tang et al., 2005). However, mitochondrial oxygen consumption can also provide reducing equivalents necessary for metmyoglobin reducing activity enhancing muscle color stability (Mitacek et al., 2019). Therefore, enhanced mitochondrial biogenesis could also be associated with an increase in color stability due to greater levels of NADH regeneration. Hence, a balanced mitochondrial activity is necessary for enhanced bright and stable red color.

Evaluation of biochemical and molecular markers of muscle darkening

Integrative and system biology approaches, including proteomics, transcriptomics, and metabolomics, are currently incorporated in meat science research to elucidate the molecular and biochemical basis of meat quality. The relationship between up-regulation or down-regulation of specific pathways related to energy metabolism, muscle structure, and cell proliferation is of interest to meat researchers. For example, proteomics analyses utilizing gel-based and label-free quantification coupled with liquid chromatography mass spectrometry (LC-MS) have identified several markers associated with energy metabolism, muscle contraction, stress response, and mitochondrial function in dark-cutting phenotypes compared with normal-pH beef (Wu et al., 2021; Kiyimba et al., 2021; Fuente-Garcia et al., 2021). A recent review examining the integromics meta-analysis at the proteome level

to decipher the underlying pathways regulating muscle darkening revealed 130 protein biomarkers and highlighted oxidation-reduction, TCA cycle, and muscle structure proteins as key pathways regulating muscle darkening in beef (Gagaoua et al., 2020). Biochemically, muscle darkening in beef is characterized by the reduction in glycolytic and increased abundance of mitochondrial metabolites. Several TCA metabolites, such as fumarate, malate, and citrate, were found overabundant while glycolytic metabolites were low in dark-cutting beef compared with normal-pH beef (Ramanathan et al., 2020b; Consolo et al., 2021).

To date, limited studies have evaluated the genomic profiles of muscle darkening in beef. Lei et al. (2017) evaluated the genetic contribution to muscle darkening via analysis of single nucleotide polymorphism (SNPs) using a case-genome wide association study (GWAS). They found that the identified SNPs were harbored in genes involved in calcium, Poly A (RNA), and GTP- binding molecular functions. However, no evidence was found for the association of a large genetic effect on beef dark-cutting phenotypes. This suggests that animal genetics contributes less to the dark-cutting phenomenon. Hence, dark-cutting beef is a polygenic trait with other conserved makers co-segregating within the dark-cutting beef phenomenon.

The exhaustive identification of biochemical and molecular markers associated with muscle darkening from a single omics tool is limited. Therefore, integrating multiple omics tools may provide a comprehensive understanding of molecular makers driving muscle darkening. However, there are still limitations in the quantitative assessment of omics data in terms of analysis and interpretation of high throughput data. Several platforms for proteomics and metabolomics analyses utilize mass-spectrometry based methods such as

GC-MS/MS (Abraham et a., 2017; Ramanathan et al., 2020b; Tan et al., 2021; Ueda et al., 2019) and LC-MS/MS (Jia et al., 2021; Li et al., 2021; Liao et al., 20222; Subbaraj et al., 2016). With advances in technology, new approaches such as near magnetic resonance spectrometry (NMR; Brescia et al., 2002; Kim et al., 2016) and rapid evaporative ionization mass spectrometry (REIMS; He et al., 2021; Setyabrata et al., 2022; Verplanken et al., 2017) have also been used in meat quality research.

Bioinformatics analyses for interpreting proteomics and metabolomics data

The explosion of molecular sequence data and the development of databases such as the European Molecular Biology Laboratory nucleotide sequence database (EMBL), GenBank, Protein Information Resource (PIR), SWISS-PROT, and the National Center for Biotechnology Information (NCBI), among others, have contributed to increased application of bioinformatics tools in biological research. Bioinformatics is utilized in meat research to reveal meaningful insight into biological processes involved in gene expression, physiological response, enzyme, and metabolomics activities that regulate meat quality.

Statistical analyses of omics data employ various free online bioinformatics platforms to identify protein, metabolite or gene expression changes. Among several platforms, proteomics data pipeline uses Perseus (https://maxquant.net/perseus/; Pang et al., 2021; Tyanova & Cox, 2018) and Mass profiler (https://www.thermofisher.com/). Metabolomics data utilize MetaboAnalyst (https://www.metaboanalyst.ca) and R-package based programs such as Metabox (https://kwanjeera.githun.io/metabox/). Within these platforms, univariate analyses such as straight forward student T-test, ANOVA,

linear modeling, Wilcoxon rank sum, and volcano plots analyses can be conducted. In addition, multivariate analyses such as principal component analysis (PCA), partial least square discriminative analysis (PL-SDA), deep learning algorithms, Bayesian clustering and hierarchical clustering are also conducted to aid in interpreting of relevant information on tested samples.

In addition to statistical analysis, GO enrichment is employed to translate the collected omics data into meaningful biological knowledge. The classical enrichment algorithms utilize Fisher's exact test. However, bioinformatics software and platform developments have enabled adoption of several enrichment algorithms such as the Kolmogorov-Smirnov, Wilcoxon, and hypergeometric statistical tests based on Fisher's exact test principles. Summaries of bioinformatics tools used in meat research studies are indicated in Table 1 and 2.

Table 1: Database searching, functional, pathway enrichment, and protein-protein network analysis platforms used in meat color proteomics studies.

Proteomic platform	**Muscles used**	**Bioinformatics analysis**	**Platform used**	**References (Author)**
LC-MS/MS	Dark-cutting vs Normal-pH	Database searching Differential analysis Functional enrichment Pathway enrichment Protein-protein interaction	MaxQuant (https://www.maxquant.org/) Perseus V1.6.2.1(https://omictools.com/perseus-tool) David (https://david.ncifcrf.gov/) Wikipathway in Cytoscape (https://cytoscape.org) STRING in Cytoscape (https://cytoscape.org) GOprofiler (https://biit.cs.ut.ee/gprofile/)	Kiyimba et al., 2021

		ID conversion tool		
LC-MS/MS	Dark-cutting vs Normal-pH	Pathway analysis Protein-protein interaction	KEGG (http://www.genome.jp/kegg/) STRING (http://string-db.org/)	Wu et al., 2020
	Meta-analysis	GO analysis Protein-protein ID conversion tool	ProteINSIDE (http://www.proteinside.org) STRING (http://string-db.org/) BioMart (http://www.ensembl.org/biomart/)	Gagaoua et al., 2020
Liquid Isoelectric focusing (OFFGEL)	Dark-cutting vs Normal-pH	Gene Ontology	AmiGO (http://amigo.geneontology.org/amigo/) STRING (http://string-db.org/)	Fuente-Garcia et al., 2019

		Protein-protein interaction		
2D-gel electrophoresis	Canadian AA, Dark-cutting (B4) and atypical (B4)	Protein-protein interaction	STRING (http://string-db.org/)	Mahmood et al., 2018
TMT labelling tag with LC-MS/MS	Muscle-specific in beef (LL vs PM)	Protein-protein interaction Pathway analysis	STRING (http://string-db.org/) Reactome (https://reactome.org) KEGG (http://www.genome.jp/kegg/)	Zhai et al., 2020
ITRAQ phosphoproteomics using LC-MS/MS	Muscle-specific in yak (LL vs PM)	Database searching GO analysis	Mascot v2.2 (https://www.matrixscience.com/sever.html) Blast2GO(https://ww.blast2go.com/)	Yang et al., 2020)

		Pathway analysis Protein-protein interaction	KEGG (http://www.genome.jp/kegg/) STRING (http://string-db.org/)	
LC-HRMS		Database searching GO analysis Protein-protein networks	Mascot v2.2 (https://www.matrixscience.com/sever.html) MZmine 2 v.2.53 (http://mzmine.github.io/download.html) AmiGO (http://amigo.geneontology.org/amigo/) STRING in Cytoscape (https://cytoscape.org)	Sentandreu et al., 2021

Table 2: Database searching, functional, pathway enrichment analysis platforms used in meat color metabolomics studies.

Metabolomics platform	**Muscles used**	**Bioinformatics analysis**	**Platform used**	**References (Author)**
GC-MS non targeted approach	Dark-cutting vs Normal-pH	Differential analysis and Principal component analysis (PCA) Pathway enrichment	MetabolAnalyst V4.0 (https://www.metaboanalyst.ca)	Ramanathan et al., 2020
GC-MS non targeted approach	Muscle-specific in beef (LL vs PM)	Metabolome identification	AMDIS(https://chemdata.nist.gov/)	Abraham et al., 2017
NMR-based metabolomics	Dark-cutting vs Normal-pH of Angus X Nellore crossbreed cattle	Differential analysis and Principal component analysis (PCA) Pathway enrichment	MetabolAnalyst V4.0 (https://www.metaboanalyst.ca)	Cônsolo et al., 2021

Summary

The occurrence of dark-cutting condition in meat is associated with elevated pH levels resulting from the depletion of glycogen postmortem. The high ultimate pH influences the biochemical and physical properties of postmortem dark-cutting beef. However, the mechanistic basis for the occurrence is still unknown. Despite increased applications of omics tools in understanding postmortem metabolism, limited research has utilized an integrative approach to characterize the biochemical and molecular basis of dark-cutting beef. The overall goal of this dissertation was to utilize an integrative omics approach combining proteomics and metabolomics profiling coupled with enzyme assays and bioinformatics analyses to get a better understanding of the molecular and mechanistic basis of dark-cutting beef.

CHAPTER III

DARK-CUTTING BEEF MITOCHONDRIAL PROTEOMIC SIGNATURES REVEAL INCREASED BIOGENEIS PROTEINS AND BIOENERGETICS CAPABILITIES

Frank Kiyimba, Steven D. Hartson, Janet Rogers, Deborah L. VanOverbeke, Gretchen G. Mafi, and Ranjith Ramanathan

Published: Journal of Proteomic, 265(2022)104637

https://doi.org/10.1016/j.jprot.2022.104637

Abstract

Mitochondria remain active in postmortem muscles and can influence meat color via oxygen consumption. Previous studies have shown that dark-cutting compared with normal-pH beef has greater mitochondrial protein and DNA content per gram of muscle tissue. However, the mechanism regulating mitochondrial content in dark-cutting vs. normal-pH beef is still unknown. Therefore, the objective was to compare mitochondrial proteomes of dark-cutting vs. normal-pH beef using LC-MS/MS-based proteomics and mitochondrial respiratory capacity using a Clark oxygen electrode. Dark-cutting compared with normal-pH beef has up-regulation of proteins involved in mitochondrial biogenesis, oxidative phosphorylation, intracellular protein transport and cellular calcium ion homeostasis.

Mitochondria isolated from dark-cutting phenotypes showed greater mitochondrial complex II respiration and uncoupled oxidative phosphorylation. However, mitochondrial membrane integrity and respiration at complexes I and IV were not different between normal-pH and dark-cutting beef. These results indicate that dark-cutting beef has greater mitochondrial biogenesis proteins that normal-pH beef, increasing mitochondrial content and contributing to dark-cutting beef.

Significance: Defective glycogen metabolism resulting from chronic stress before slaughter coupled with the greater mitochondrial protein and DNA content per gram of muscle tissue promotes muscle darkening in dark-cutting phenotypes in beef. However, the mechanistic basis for this occurrence in dark-cutting phenotypes is still unknown. In this work, we show that dark-cutting beef phenotype is caused, in part, as a consequence of over-proliferation of mitochondria. This is supported by the up-regulation of proteins involved in mitochondrial biogenesis, mitochondrial electron transport, calcium homeostasis, and fatty acid metabolism. Hence, the study of mitochondrial proteomes changes provides a set of mitochondrial biogenesis proteins that could be used as potential candidate biomarkers for detecting changes in pre-slaughter development events contributing to dark-cutting phenotypes in beef.

Keywords: Dark-cutting beef, Mitochondrial biogenesis, oxygen consumption, Beef color, Proteomics

Introduction

Meat color is an important sensory attribute that influences consumer perception of quality and acceptance. Dark-cutting beef is a color defect in which muscle exposed to air does not have a characteristic cherry bright-red color. The dark-cutting condition results from a combination of several factors. For example, the predominately existing pre-slaughter stressful conditions such as; extreme weather conditions, poor animal management, nutrition, long transportation hours, lairage times before slaughter among others, contribute to postmortem muscle biochemical changes reported in dark-cutting phenotypes in beef (Kiyimba et al., 2021; Mahmood et al., 2018; Ponnampalam, et al., 2017; Roy et al., 2022; Wulf et al., 2002). Therefore, early identification of molecular changes in the pre-slaughter developmental events could be a useful strategy to lower the incidences of dark-cutting phenotypes.

The interaction between mitochondria and myoglobin is a key determinant of postmortem meat color (Postnikova et al., 2009; Ramanathan and Mancini, 2018; Tang et al., 2005). There is competition for available oxygen between mitochondria and myoglobin. Actively respiring mitochondria, as in case of dark-cutting beef, decrease oxygen availability to myoglobin and results in darker meat color due to more deoxymyoglobin. Dark-cutting muscles have greater mitochondrial protein and DNA content per gram of muscle tissue compared with normal-pH beef (McKeith et al., 2016; Ramanathan, et al., 2020b). However, the underlying molecular mechanisms of greater mitochondrial content in dark-cutting phenotypes is still unknown.

Transcriptional and posttranscriptional factors that regulate mitochondrial biogenesis respond to diverse environmental, metabolic, and cellular stimuli. The most described regulators of mitochondrial biogenesis are a set of nuclear transcription factors such as the nuclear respiratory factors (NRF1 and NRF 2; Gill and La Merrill, 2017; Wenz, 2013), mitochondria transcriptional factor A (TFAM), and the peroxisome proliferator-activated receptors (Huang et al., 2018; Kelly & Scarpulla, 2004; Sakellariou et al., 2016; Wu et al., 1999). In addition, mitochondrial biogenesis also involves activation of transmembrane proteins necessary to import and assemble large sets of proteins, lipids, and mitochondrial networks (Palikaras et al., 2015; Pohjoismäki et al., 2012).

Although markers of mitochondrial biogenesis in skeletal muscles have been described previously (Honda et al., 2005; Ishihara et al., 2004; Neutzner et al., 2008; Santetl et al., 2003; Yun & Finkel, 2014), the molecular signals and the expression profiles of key regulators that drive mitochondrial biogenesis in dark-cutting phenotypes compared with normal beef are not fully understood. Here, we propose a model in which the dark-cutting phenomenon, in part, is caused by over-proliferation of mitochondria. The hypothesize of the current study was that mitochondrial biogenesis in dark-cutting beef phenotypes is due to, in part, up-regulation of nuclear-encoded genes and proteins which control mitochondrial properties. The hypothesis was tested by comparing the mitochondrial proteomes of dark-cutting vs. normal-pH beef, and characterized differences in mitochondrial respiration capacity. The results demonstrated that dark-cutting relative to normal-pH beef have greater expression of mitochondrial biogenesis proteins, suggesting over-proliferation of mitochondria in dark-cutting phenotypes. These results provide a set of mitochondrial biogenesis proteins that could be used as candidate markers

for identifying changes in pre-slaughter developmental events contributing to dark-cutting phenotypes in beef.

Materials and methods

Sample collection and preparation

Eleven normal-pH and 11 dark-cutting beef loins (*longissimus lumborum*; IMPS #180, NAMP, 2002; grain finished, spray chilled) from mature carcasses were obtained within 72-h post-mortem from Creekstone Farms, Arkansas City, KS on two different occasions (five normal-pH and dark-cutting loins during first time and six dark-cutting and normal-pH loins during the second time). Loins were transported on ice, and upon arrival, three 2.54-cm-thick steaks from each animal were cut from the anterior end of the loin. The first steak from each animal (dark-cutting and normal-pH beef) was utilized for color and biochemical analysis. The second steak was utilized for mitochondrial LC-MS/MS proteomics studies (six replications out of 11 loins were randomly selected for proteomic studies). The third steak from each animal was used to determine muscle pH and proximate compositions.

Determination of surface color characteristics and biochemical properties

The pH of each steak (dark-cutting vs normal beef) was recorded using an Accumet 50 pH meter (Fisher Scientific, Fairlawn, NJ). The pH probe was calibrated with buffers at pH 4 and 7. The proximate compositions were determined using an Association of Official Analytical Chemist-approved (Official Method 2007.04; Anderson, 2007) near-infrared spectrophotometer (Foss Food Scan 78800; Dedicated Analytical Solutions, DK-

3400 Hillerød, Denmark). Protein, moisture, and fat contents were reported on a percent (%) basis.

The surface color was measured using a HunterLab MiniScan spectrophotometer (Kiyimba et al., 2021; AMSA, 2012). Following surface color measurements, each steak was cut in half. The first half was used to estimate muscle oxygen consumption, and the second half was utilized to measure metmyoglobin reducing activity. The greater postmortem muscle pH (above 5.8) seen in dark-cutting beef influence muscle reflectance properties (AMSA Color Guide; AMSA, 2012). Hence, a modified method was utilized to measure oxygen consumption and metmyoglobin reducing activity (Ramanathan et al., 2019). The steak half was bloomed for 1 h at 4 °C. Following blooming, each steak section was vacuum-packaged and incubated at 25 °C for 30 min to promote oxygen consumption. After incubation, surface color readings were taken and the deoxymyoglobin level was measured to determine muscle oxygen consumption (AMSA Color Guide; AMSA, 2012). A greater number indicates greater metmyoglobin reducing activity.

Mitochondrial isolation

Mitochondria from skeletal muscle were isolated according to the method of Smith (1967) with minor modifications. Five grams of muscle tissue visibly devoid of fat and connective tissue from each normal-pH and dark-cutting beef loin (n = 11 each from normal-pH and dark-cutting) were minced using a blade. Following mincing, samples were suspended in 10 mL ice-cold suspension buffer (250 mM sucrose and 12 mM HEPES, pH 7.4), containing 1.25 µg/mL trypsin (5 µL of proteinase 0.25% (w/v) trypsin) for each 1 mL of suspension buffer in a 250 mL beaker. The beaker containing the tissue

suspension mixture was placed on a 500 mL beaker prefilled with ice and stirred gently for 15 min. After incubation, 40 mL of ice-cold mitochondria isolation buffer (67 mM sucrose, 10 mM EDTA, 50 mM Tris, 50 mM KCl, and 0.2% bovine serum albumin (BSA), pH 7.4) was added to the suspension mixture, and the pH was readjusted to 7.2. The samples were homogenized two times, first using a pinpointed glass/Teflon Potter Elvehjem homogenizer and secondly with a round-bottomed glass/Teflon Potter Elvehjem homogenizer, tightly fitted on Potter-Eberbach tissue grinder (Model E7000, Volt 130, St. Belleville, MI) at 160 rpm.

The homogenate was then centrifuged at 800 g for 10 min at 4°C. The pellet was discarded, and the supernatant was decanted through a double-layered cheesecloth. The collected supernatant was then centrifuged at 10,000 g for 10 min at 4°C, and the supernatant was discarded. The mitochondrial pellet was washed twice, and gently resuspended in 75 mM sucrose, 10 mM Tris and 0.1 mM EDTA, pH 7.4. The mitochondrial protein content was determined using a bicinchoninic acid assay following the manufacturer's recommended protocol (Thermo-Fisher, Waltham, MA).

Analysis of mitochondrial respiratory activity

A Clark Oxygen type electrode (DW 1, Hansatech, Norfork, UK) with a polarizing voltage of 0.6 V and 8 mL incubation chamber was utilized to measure the mitochondrial respiratory capacity of dark-cutting and normal-pH beef. The reaction chamber was maintained at 25°C. A 10 mm Teflon covered bar was used to stir the chamber at 600 rpm. The electrode was attached to a Rank Brothers digital model 20 oxygen controller (Cambridge, England), connected to a personal computer and data logger. Mitochondrial

respiration experiment measurements were initiated by suspending 2 mg of mitochondria in 1 mL respiration buffer (250 mM sucrose, 5 mM potassium monophosphate, 5 mM magnesium chloride, 0.1% BSA, 0.1 mM EDTA and 20 mM HEPES, pH 7.4). After 1 min equilibration period in the incubation chamber, mitochondria respiration in dark-cutting and normal beef samples was evaluated using complex specific substrates at complex I (5 mM glutamate and malate 2 mM), II (5 mM succinate), and IV (6 mM ascorbate and 300 µM TMPD).

Determination of mitochondrial respiratory control ratio (RCR) and ADP/O ratio

To evaluate state III and IV mitochondrial respiration, mitochondria (2 mg/mL) isolated from dark-cutting and normal-pH beef was suspended in the respiration buffer (250 mM sucrose, 5 mM potassium mono phosphate, 5 mM magnesium chloride, 0.1% BSA, 0.1 mM EDTA and 20 mM HEPES, pH 7.4). Mitochondrial complex I was first blocked using rotenone (2 µM). State III oxygen consumption was initiated by the addition of ADP at a final concentration of 100 µM after a 1-minute incubation with the oxidizable substrates (5 mM succinate). State IV oxygen consumption was allowed to proceed for 2 minutes after completion of state 3 respiration and the rate of oxygen consumption was measured. The ratio between mitochondrial oxygen consumption under state III and state IV, was calculated to determine the respiratory control ratio (RCR) as previously described (Estabrook, 1967). The number of nanomoles of ADP phosphorylated by the nanomoles of oxygen consumed per mg mitochondria (ADP/O) ratio was also calculated according to (Estabrook, 1967), using 235 nmol O_2/mL as the value of oxygen solubility at 25°C.

Evaluation of mitochondrial outer membrane permeability and uncoupled oxidative phosphorylation

To characterize the integrity of the outer mitochondrial membrane, oxygen consumption of isolated mitochondria from dark-cutting and normal beef was monitored following the addition of cytochrome *c* at a final concentration of 10 µM. Briefly, mitochondrial (2 mg/mL) suspended in respiration buffer (250 mM sucrose, 5 mM potassium monophosphate, 5 mM magnesium chloride, 0.1% BSA, 0.1 mM EDTA and 20 mM HEPES, pH 7.4), was supplemented with rotenone (2 µM, to abolish complex I endogenous substrates contribution). The assay was started in a coupled state with succinate (5 mM), and State III was initiated by the addition of ADP. Then cytochrome *c* was added at a final concentration of 10 µM and the response to cytochrome *c* addition was determined. The degree of coupling between the electron transport chain (ETC), and the oxidative phosphorylation machinery (OXPHOS) through FCCP-induced maximal uncoupler-stimulated respiration was initiated by the addition of FCCP at a final concentration of 100 µM.

Mitochondrial protein extraction and digestion

To determine the molecular signals and the expression profiles of key regulators driving mitochondrial biogenesis in dark-cutting phenotypes compared with normal beef, 6 out of the 11 isolated mitochondrial protein samples were randomly selected from each animal group (n = 6 dark-cutting and n = 6 normal-pH beef) for LC-MS/MS proteomics analysis. The samples were dissolved in 8 M urea, 100 mM Tris-HCL 5 mM Tris (2-carboxyethyl) phosphine pH = 8.5 and reduced at room temperature for 20 min. After

reduction, samples were alkylated by the addition of iodoacetamide to 10 mM and incubated for 15 min at room temperature. Samples were then diluted with three volumes of 100 mM Tris-HCl pH 8.5, digested at 37°C overnight with 4 µg/ml trypsin/LysC (Promega, Madison, WI), and digested further by a second addition of trypsin/LysC (2 µg/ml) for 6 hr. Digested samples were acidified to 1% trifluoroacetic acid, and purified by reversed-phase chromatography using monolithic C18 affinity media (Pierce™ C18 Tips, 100 µL bed, #87784, Thermo-Fisher, Waltham, MA).

Peptides were separated on an Acclaim PepMap RSLC column (2 µm C18 particles, 75 µm ID x 50 cm length; Thermo-Fisher, Waltham, MA), loaded in 0.1% aqueous formic acid, and developed using an acetonitrile gradient of 2.5% - 30% acetonitrile over 120 min. The column terminated with a stainless-steel emitter within a Nanospray Flex ion source (Thermo-Fisher, Waltham, MA), coupled to a Fusion mass spectrometer programmed for a "Top Speed" analysis using quadrupole isolation, HCD fragmentation, and fragment ion analysis in the ion trap sector.

MS/MS database searching for identification of differentially abundant proteins (DAPs)

The MS/MS spectra from each nano-LC-MS/MS run were searched against a Uniprot *Bos Taurus* proteome database of 23,968 protein sequences (downloaded in March of 2018). The searches were performed using MaxQuant software (V1.5.3.12, Max Planck institute of biochemistry) with the same search parameters as previously reported (Kiyimba et al., 2021). The sequences of common contaminates were included in the searches. The MaxQuant LFQ protein intensities were imported into the Perseus v1.6.3.3 software platform (https://omictools.com/perseus-tool) and analyzed. Protein groups were first

filtered for reverse and potential contaminants. Then protein expression intensities were analyzed within the Perseus framework, using a permutation based method to compare log_2 transformed LFQ protein intensities and the results were visualized on a volcano plot. Proteins were considered significant if the fold change was greater or equal to1.5 with a FDR p-value less than or equal to 0.05.

Principal Component Analysis (PCA) plots and heat map were constructed using Perseus software (V.1.6.3.3) to compare mitochondrial protein expression profiles of dark-cutting and normal-pH beef. David version 6.8 (https://david.ncifcrf.org/) was utilized to determine the functional characterization of the differentially expressed proteins in the mitochondrial proteomes of dark-cutting and normal-pH beef. To acknowledge sampling bias, the gene list of all identified and quantified proteins in all 6 of the 6 compared samples was used as background. Those proteins with limited description in the database were annotated using a blast search. The potential protein-protein interactions (PPI) between the set of differentially abundant proteins in dark-cutting beef vs normal-pH beef were analyzed using STRING database, via the Cytoscape plugin (Szklarczyk et al., 2017; Studham et al., 2014; V.3.7.1; https://cytoscape.org/) for known and predicted protein-protein interactions using a confidence score of 0.8 with zero additional interactors. The collected nodes of the subnetworks were used to create clusters of the corresponding differentially expressed proteins (up-and down-regulated in dark-cutting beef mitochondria proteomes) using the Markov Clustering Algorithm (MCL; Kucera et al., 2016).

Statistical analysis

A completely randomized block design was utilized to determine muscle-specific differences in mitochondrial functional properties and color attributes. The experiment was replicated 11 times (n = 11). Eleven loins were collected during two different phases. There was no significant effect of collection day on mitochondrial functionality. Hence, the collection day was not included in the model. Each loin from normal-pH and dark-cutting beef was considered a block. Least square means and standard error of mean were analyzed using Proc Mixed procedure in SAS (Version 9.1, SAS Institute Inc. Cary, NC). Least square means were separated using the pdiff option and were considered significant at $P < 0.05$. All statistical analyses for the proteomics study were performed using Perseus (V1.6.2.1, https://omictools.com/perseus-tool) biostatistics software.

Results

Intact steak biochemical properties and mitochondrial protein content

Muscle pH and mitochondrial protein content of dark-cutting beef was significantly greater than those of normal-pH beef (Table 1). Moreover, dark-cutting beef demonstrated greater muscle oxygen consumption and metmyoglobin reducing ability relative to normal-pH beef (Table 1). These results confirmed the dark-cutting beef biochemical characteristics (Kiyimba et al., 2021; McKeith et al., 2016; Ponnampalam, et al., 2017; Ramanathan., et al., 2020b).

Dark-cutting phenotype stimulate greater mitochondrial oxygen consumption at complex II

To access the differences in mitochondrial functional properties of dark-cutting and normal-pH beef at complex I, II, and IV, mitochondrial complex-specific substrates were added to the isolated mitochondria, and the resultant mitochondrial oxygen consumption was measured. The addition of glutamate and malate, TMPD and ascorbate to stimulate electron flow at complexes I and IV, respectively, resulted in measurable mitochondrial oxygen consumption in mitochondria isolated from both dark-cutting and normal-pH beef (Figure 1a and 1c). Mitochondria isolated from normal-pH beef had numerically greater ($p = 0.054$) complex I activity than dark-cutting beef. The addition of succinate to stimulate electron flow at complex II resulted in a 35% increase ($p = 0.024$) in dark-cutting mitochondrial oxygen consumption than normal-pH beef (Figure 1b). No differences ($p = 0.534$) in oxygen consumption between mitochondria from normal and dark-cutting was noted for complex IV activity.

To gain further insights into the mitochondrial functional differences in dark-cutting vs. normal-pH beef, we analyzed the mitochondrial oxidative phosphorylation (OXPHOS) capacity by measuring mitochondrial State III and IV oxygen consumption, respiratory control ratio (RCR; the ratio between State III and IV), ADP/O ratio, and uncoupled oxidative phosphorylation. The results showed that mitochondria isolated from dark-cutting beef had a 65% increase in State III oxygen consumption ($p = 0.004$) compared with normal-pH beef (Figure 2a). However, no differences ($p = 0.826$) were observed in mitochondrial State IV oxygen consumption (Figure 2b). Furthermore, mitochondria isolated from dark-cutting beef had an 84% increase in RCR ($p = 0.0008$;

Figure 2c). Increased RCR and State III oxygen consumption suggest more functional mitochondria in dark-cutting beef.

Estimation of the ratio of number of moles of ADP phosphorylated to number of moles of oxygen consumed following addition of ADP (ADP/O ratio) showed that mitochondria from dark-cutting beef had a 64% reduction in the ADP/O ratio ($p = 0.0038$; Figure 2d). Analysis of mitochondrial uncoupled oxidative phosphorylation in presence of FCCP showed that dark-cutting beef mitochondria had almost 68% greater uncoupled oxidative phosphorylation ($p = 0.004$; Figure 2e) compared with normal-pH beef. The lower ADP/O ratio and a greater uncoupled-oxidative phosphorylation suggests an increased capacity for mitochondria in dark-cutting beef to consume more oxygen relative to normal-pH beef.

Dark-cutting conditions does not affect mitochondrial outer membrane integrity

To characterize differences in the mitochondrial outer membrane integrity, we measured responses to the addition of extraneous cytochrome *c*. The addition of cytochrome *c* stimulated an increase in mitochondrial oxygen consumption in both dark-cutting and normal-pH beef (Figure 2f). However, no differences ($p = 0.365$) were observed in mitochondrial respiration between dark-cutting and normal-pH beef isolated mitochondria with addition of extraneous cytochrome *c*. Further, measurement of mitochondrial membrane potential using rodamine 132 fluorescence probe showed no differences in the membrane integrity between dark- cutting and normal-pH beef (data not shown). Therefore, these results suggested that postmortem conditions have no effect on normal-pH and dark-cutting mitochondrial outer membrane integrity.

Dark-cutting conditions up-regulates components of mitochondrial biogenesis influencing mitochondrial protein content and function.

The mitochondrial proteomes of dark-cutting vs. normal-pH beef were compared to determine the molecular signals and the expression profiles of key regulators that drive mitochondrial biogenesis. The LC-MS/MS analysis identified 1,862 proteins (n = 6 dark-cutting and n=6 normal-pH beef). Comparison of protein expression profiles in the mitochondrial proteome of dark-cutting vs. normal-pH beef showed that 174 proteins were differentially expressed, with a clear separation in a volcano plot of p-values vs. fold change (Figure 3). Eighty-nine proteins were up regulated more than 1.5-fold (Supplemental Table A.1), while 61 were down-regulated more than 1.5-fold in the mitochondrial proteome of dark-cutting beef (Supplemental Table A.2).

To gain further insights about the proteomic features responsible for differences in the mitochondrial proteomes of dark-cutting vs. normal-pH beef, the differentially expressed protein profiles were compared using principal component analysis (PCA) plots and by hierarchical clustering analysis (HCA). As depicted in Figure 4 and 5, the red color represents proteins with up-regulation in mitochondrial proteomes of dark-cutting beef while the green color represents down-regulation. The PCA scoring analysis showed clear segregation between the dark-cutting and normal-pH beef samples. This result shows that the samples within each group clearly formed distinguishable clusters. However, the dark-cutting conditions showed lower factor loading ≥ -0.5 with PC1 (70.5% explained variance). In addition, hierarchical clustering analysis showed similar cluster patterns to PCA plot analysis (Figure 5), with correlated differentially expressed

proteins up- and down-regulated in dark-cutting beef clustered together suggesting that these proteins belong to related functional categories.

To determine the functional annotations of the differentially expressed proteins (DEPs) which were over-or underrepresented significantly in the mitochondrial proteomes of dark-cutting compared with normal-pH beef, we utilized gene ontology enrichment (GO) analysis using DAVID (V. 6.8). GO results showed enrichment for several processes that are implicated in mitochondrial protein translation and import mechanisms (Figure 6). These results suggested that dark-cutting beef conditions promote changes in protein expression profiles of processes that are important in the regulation of mitochondrial proliferation.

To further explore the potential protein-protein network interactions between these differentially expressed proteins (DEPs), protein-protein interaction network analyses were carried out using the STRING database and visualized in Cytoscape (Figure 7). Auto-annotation of the protein network revealed that majority of the up-regulated proteins were present in interaction networks that regulate mitochondrial division processes, electron and membrane transport, mitochondrial transcription and translation regulation, fatty acid metabolism, and the calcium homeostasis. Combined, these results suggest that the dark-cutting phenotypes promotes changes in protein expression profiles that are indicative of energy adaptive response mechanisms.

Discussion

A shift from aerobic to anaerobic metabolism triggers several changes in biochemical mechanisms that regulate postmortem metabolism. In dark-cutting

phenotypes, the defective glycogen metabolism resulting from chronic stress before slaughter underlie the occurrence of this phenomenon in beef (Kiyimba et al., 2021; Mahmood et al., 2018; Ponnampalam, et al., 2017; Wulf et al., 2002). The greater mitochondrial protein and DNA content per gram of muscle tissue reported in dark-cutting beef (McKeith et al., 2016; Ramanathan, et al., 2020b) also can promote muscle darkening. In this study we examined and compared mitochondrial respiratory function and mitochondrial protein profiles of dark-cutting relative to normal pH beef to better understand the occurrence of dark-cutting phenotypes in beef.

In the current study, over proliferation of mitochondrial, in part, causes the greater mitochondrial content which in turn promotes muscle darkening in dark-cutting beef (Table 1). In support, our results show that dark-cutting condition exhibit significantly enhanced mitochondrial respiration capacity specifically at complex II (Figure 1b), greater oxidative phosphorylation capacity (Figure 2a and 2c), and reduced mitochondrial ADP/O ratios (Figure 2d). State III oxygen consumption and RCR have been previously evaluated in skeletal muscles and are associated with increased utilization of substrate-dependent respiration (Estabrook, 1967; Gottlieb et al., 2002) and a greater capacity for mitochondrial OXPHOS (Ashmore et al., 1972). However, the lower ADP/O ratio observed in dark-cutting beef mitochondria can lead to less coupling of nucleotides and phosphate transport to the electrochemical proton gradient across the inner mitochondrial membrane (Gottlieb et al., 2002). Therefore, this suggests that mitochondria from dark-cutting tissues have more active ATP synthase and/or increased ability to transport ADP.

Although the post-mortem alterations in the bioenergetics demand in dark-cutting phenotypes has not been characterized, we can assume that maintenance of mitochondrial

function would require comparable amounts of ATP in dark-cutting compared to normal pH beef. Thus, our results suggest that substrate oxidation and oxygen consumption in dark-cutting beef mitochondria is more tightly coupled to energy production. Consistent with this observation, dark-cutting mitochondrial proteomes showed over-expression of enzymes involved in ATPase-coupled proton transport and ATP synthesis (Supplemental Table A.1). Recently, metabolomics studies demonstrated that dark-cutting relative to normal-pH beef has increased abundance of tricarboxylic acid metabolites such as citric acid, fumaric, and malic acid, and lower succinate (Cônsolo et al., 2020; Ramanathan, et al., 2020b). Together, the results show that the predominantly described chronic stress conditions in dark-cutting phenotypes can induce changes in mitochondrial bioenergetics mechanisms that are necessary to supply ATP. However, the increase in mitochondrial respiration capacity coupled with a greater than normal muscle pH (above 5.8, Table 1), becomes a conducive factor for enhanced mitochondrial oxygen consumption contributing to muscle darkening via myoglobin deoxygenation (Kiyimba et al., 2021).

The enhanced over proliferation of mitochondria in dark-cutting phenotypes is evidenced by up-regulation of proteins involved in mitochondrial biogenesis specifically fusion and fission of individual mitochondria (Figure 7, and Supplemental Table A.1) and mitochondrial transmembrane membrane proteins specifically TOM22, TOM40, TMEM43, and TMEM109 (Figure 7, and Supplemental Table A.1). Over-expression of these proteins supports the formation of mitochondrial networks (Cao et al., 2017; Honda et al., 2005; Ishihara et al., 2004; Qi et al., 2016; Braschi et al., 2009; Li et al., 2008; Yun et al., 2014), translocation of cytosolically synthesized mitochondrial pre-proteins (Saeki et al., 2000; Namba, 2019), and assembly of mitochondrial membrane complexes

(Namba, 2019). Therefore, our results suggest that animals experiencing stress could trigger an increase in mitochondrial content via increased expression of mitochondrial biogenesis and translation machineries in order to increase energy production required to overcome the stress. However, the molecular mechanisms driving mitochondrial proliferation in dark-cutting beef are yet to be described.

While these observations argue for increased biogenesis in dark-cutting phenotypes, AMP-activated protein kinase (AMPK), Sirtulin1 (SIRT1, NAD-dependent protein deactylase), and other proteins that activate mitochondrial biogenesis directly such as NRF1, or NRF-2, and TFAM (Huang et al., 2018; Kelly & Scarpulla, 2004; Sakellariou et al., 2016; Wu et al., 1999) did not show significant increase in the mitochondria proteomes of dark-cutting compared with normal-pH beef. Although we did not investigate these proteins' activity, their static expression in dark-cutting vs. normal tissues hints that they may not be the main drivers of dark-cutting beef mitochondrial proliferation. Instead, we saw that PERM1, a PGC-1α and ERR-induced regulator in muscle protein 1, adenylate kinase 4, mitochondrial (AK4), ATPase family AAA domain-containing 1 (ATAD1) activators of AMPK, and proliferation-associated protein 2G4 (PA2G4) were up-regulated in mitochondria from dark-cutting phenotypes (Table A.1). Hence, up-regulation of these proteins suggest that these proteins may be key factors modulating the up-regulation of mitochondrial biogenesis in dark-cutting beef.

Mitochondrial content in skeletal muscles is regulated in accordance to metabolic activity of the cells. Therefore, due to depleted glycogen content in dark-cutting beef phenotypes (Kiyimba et al., 2021; Mahmood et al., 2018; Ponnampalam, et al., 2017;

Wulf et al., 2002), we reasoned that other energy pathways become activated to provide the necessary intermediates required to support mitochondrial proliferation processes. Consistent with this observation, several proteins involved in fatty acid oxidation (Supplemental Table A.1) showed an up-regulation in mitochondria proteomes isolated from dark-cutting tissues while fatty acid synthase protein (FASN) was down-regulated (Supplemental Table A.2). Mitochondrial fatty acid oxidation proteins observed in this study specifically carnitine palmitoyltransferase-1 (CPT1) has been shown to modulate mitochondrial fission processes through its action as a protein that translocate long-chain fatty acids into mitochondria for oxidation (Alam and Saggerson, 1998; McGarry et al., 1978). In addition, the peroxisome proliferator-activated receptor ɣ coactivator 1(PCG-1) can activate fatty acid oxidation pathways (Vega et al., 2000). Therefore, the increased abundance of PERM1, a PGC-1α and ERR-induced regulator in muscle protein 1 could, in part, explain the greater abundance of the fatty acid oxidation proteins in the mitochondrial proteomes of dark-cutting beef.

The expression of many mitochondrial biogenesis factors can be regulated by calcium (Ca^{2+}) concentration. For example, intra-mitochondrial Ca^{2+} uptake has been shown to play a role in oxidative phosphorylation and ATP synthesis (Brookes et al., 2004). Consistent with these findings, we observed in the present study that dark-cutting mitochondrial proteomes showed greater abundance of Ca^{2+} binding and transporting proteins (Figure 6, 7, and Supplemental Table A.1). The Ca^{2+}-regulated signaling pathways can contribute to mitochondrial biogenesis (Chin, 2004; Liu et al., 2020; Wright, 2007) via activation of rate limiting enzymes of the TCA (pyruvate-, α-ketoglutarate-, and NAD-isocitrate- dehydrogenase), and ATP synthase (Jouaville et al.,

1999). Proteins specifically calcium/calmodulin dependent protein kinase (CAMK2A) up-regulated in dark-cutting beef mitochondrial proteomes has been shown to regulate the expression of peroxisome proliferator-activated receptor ɣ coactivator 1(PGC-1), a master regulator of mitochondrial biogenesis in vivo (Wu et al., 2002). Thus, we speculate that up-regulation of calcium proteins is in dark-cutting beef is associated with mitochondrial biogenesis processes. However, the amplitude, duration, and temporal patterns of Ca^{2+} signaling in the dark-cutting phenotypes that are necessary to induce these changes are yet to be described.

Conclusions

In the current study, we have showed that dark-cutting beef is caused, in part, as a consequence of over proliferation of mitochondria. The greater mitochondrial oxidative phosphorylation capacity is supported by up-regulation of proteins involved in mitochondrial biogenesis, mitochondrial electron transport, calcium homeostasis, and fatty acid metabolism. Greater mitochondrial biogenesis and enhanced bioenergetics suggest an energy adaptation mechanisms involved with cellular energy homeostasis pre-slaughter. In addition, the study suggests that PERM1, a PGC-1α and ERR-induced regulator in muscle protein 1, adenylate kinase 4, mitochondrial (AK4), ATPase family AAA domain-containing 1 (ATAD1) activators of AMPK, and proliferation-associated protein 2G4 (PA2G4) may be important mediators in the activation of mitochondrial biogenesis increasing mitochondrial protein content in dark-cutting tissues.

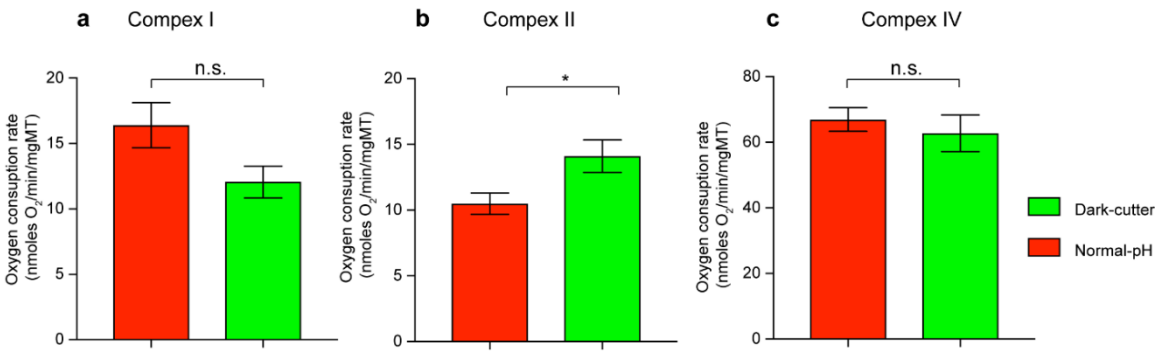

Figure 1: Differences in mitochondrial oxygen consumption rate (OCR) of dark-cutting beef vs. normal-pH beef

Mitochondrial respiration properties at complex I, II and IV of dark-cutting and normal-pH beef were measured as described in Methods. (A) mitochondrial OCR measured at complex I was initiated by the addition of glutamate and malate. (B) mitochondrial OCR measured at complex II was initiated by addition of succinate. (C) mitochondrial OCR measured at complex IV after addition of TMPD and ascorbate. Error bars represent one standard deviation (n = 11), * $p < 0.05$, and ns $p > 0.05$.

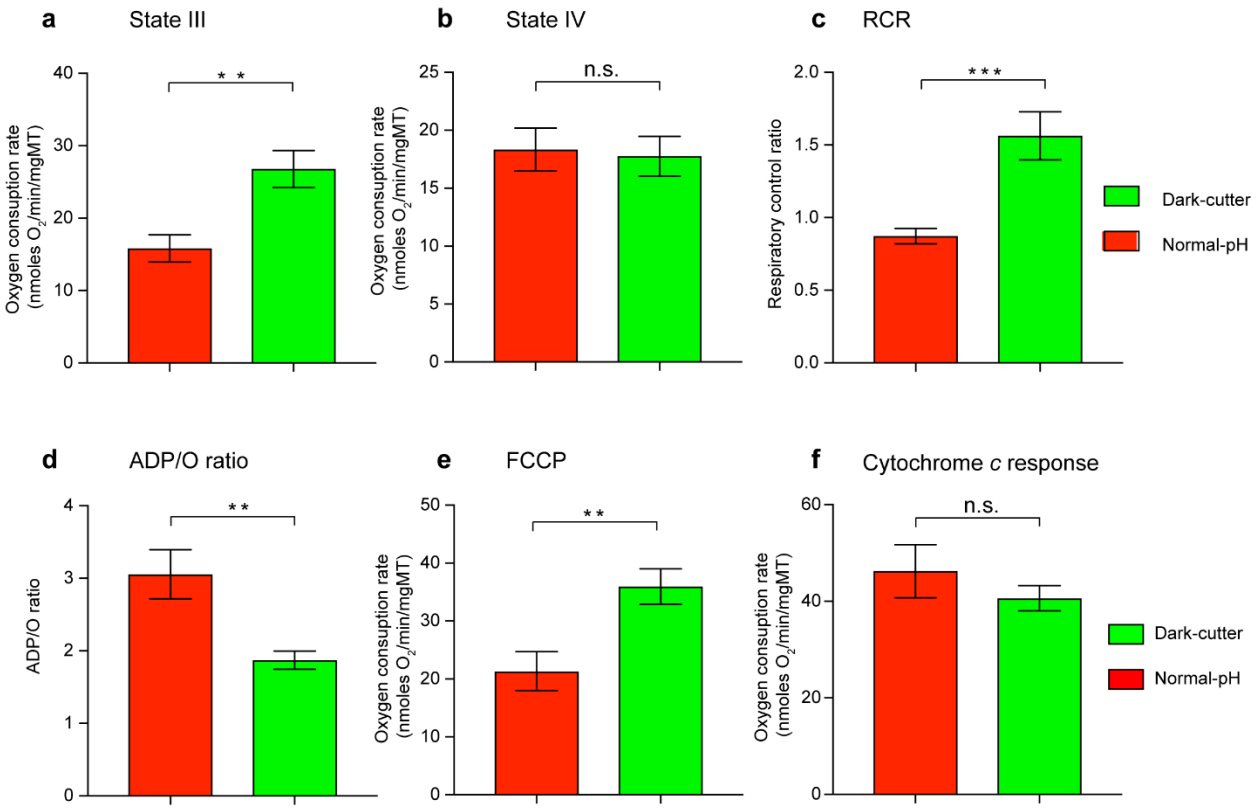

Figure 2: Mitochondrial functional differences in dark-cutting beef vs. normal-pH beef

Mitochondrial State III and IV oxygen consumption of dark-cutting and normal-pH beef was evaluated as described in the Methods. (A) state III OCR determined by measuring the rate of oxygen consumption by mitochondria in presence of succinate and ADP. (B) state IV OCR determined by measuring mitochondrial respiration in presence of succinate. (C) mitochondrial RCR calculated as a ratio between state III and state IV OCR. (D) Mitochondrial coupled oxidative phosphorylation calculated as a ratio between amounts of ADP (nmoles), added under State III OCR to number of oxygen molecules consumed (nmoles). (E) Mitochondrial uncoupled respiration measured by the addition of uncoupler FCCP. (F) mitochondrial membrane integrity measured by adding cytochrome *c* to a final concentration of 10 µM. Error bars represent one standard deviation (n = 11). * $p < 0.05$,** $p < 0.01$, *** $p < 0.001$, and ns $p > 0.05$.

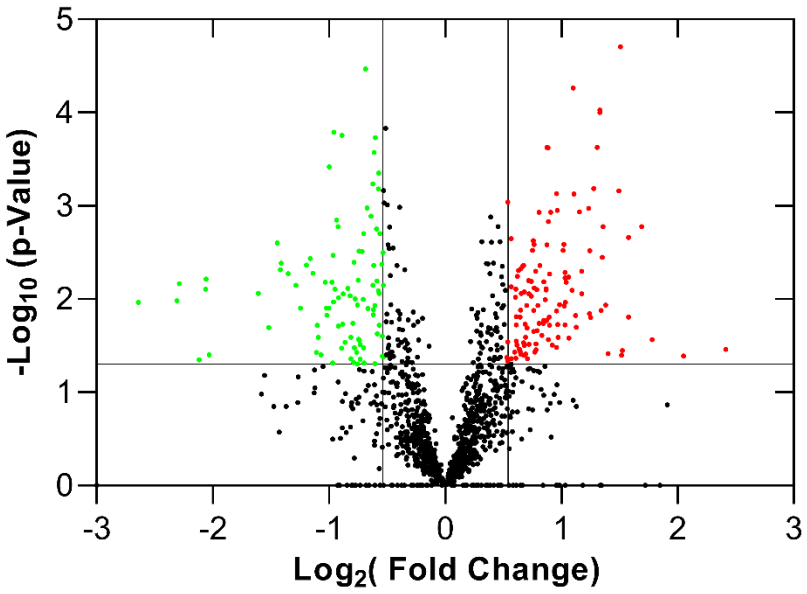

Figure 3: Differentially expressed proteins in the mitochondrial proteome of dark-cutting vs. normal-pH beef

Differences in protein expression profiles in the mitochondrial proteome dark-cutting and normal-pH beef were quantified as described in Methods. (A) Volcano plot representing results of label free quantification of significant differences in the expression of individual proteins in dark-cutting vs. normal-pH beef. The logarithm (base 2) of the ratios of protein intensities in dark-cutting vs. normal-pH beef were plotted against the negative log10 of the p-values. The black lines separate specific red and green dots representing up- and down-regulated proteins significantly expressed respectively in dark-cutting beef from the background proteins (black dots).

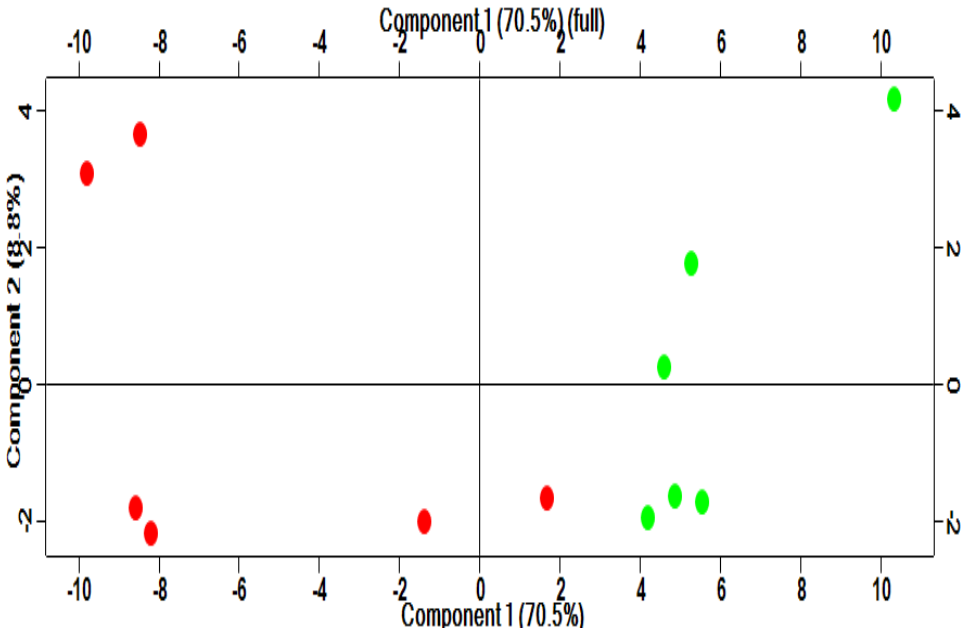

Figure 4: Principal component analysis (PCA) of quantified proteins differentially expressed in the mitochondrial proteome of dark-cutting beef vs. normal-pH beef.

Differences in mitochondrial protein expression profiles of dark-cutting vs. normal-pH beef were quantified as described in Methods. (A) Principal component analysis (PCA) of quantified proteins at total protein level. Red and green dots represent up-regulated and down-regulate proteins differentially expressed ($p \leq 0.05$) respectively, in the mitochondrial proteome of dark-cutting beef vs. normal-pH beef.

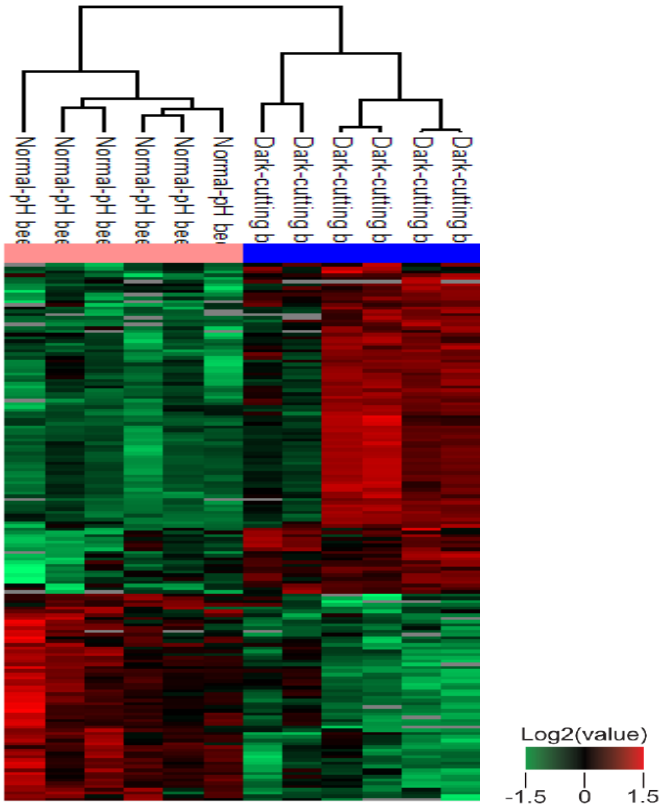

Figure 5: Hierarchical clustering analysis of mitochondrial protein expression profiles in dark-cutting vs. normal-pH beef

Mitochondrial protein expression changes induced by dark-cutting phenotypes were compared to normal-pH beef. Red and green colors represent up-regulated and down-regulate proteins significantly expressed respectively in dark-cutting beef compared to normal-pH beef. Heat map color legend indicated represents the log 2 transformed ratio of dark-cutting to normal-pH beef.

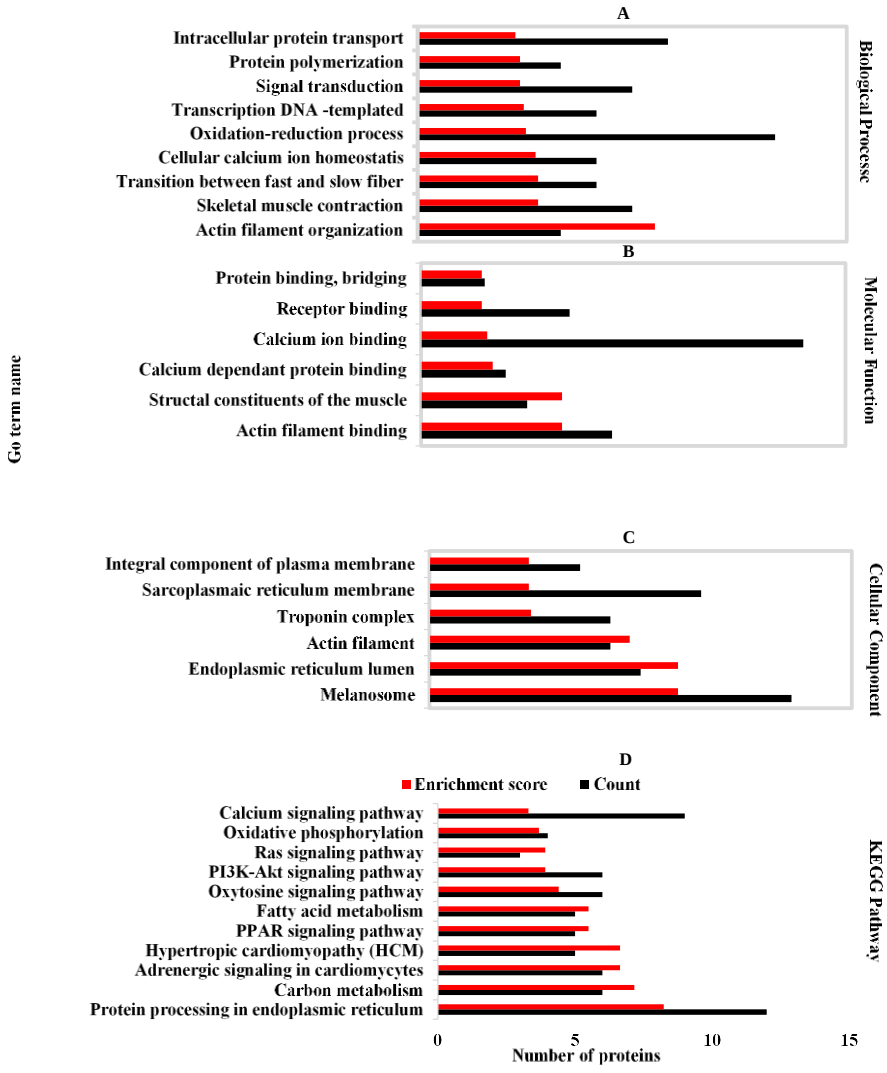

Figure 6: Functional enrichment analysis of GO category of differentially abundant mitochondrial proteins in dark-cutting beef compared to normal-pH beef

Mitochondrial proteins with significantly altered expression in dark-cutting beef compared to normal-pH beef were analyzed for functional enrichment using DAVID. (A) representative subset of proteins enriched in biological processes, (B) enrichemnt of molecular functions, (C) cellular component enrichment, and (D) KEGG pathway enrichment ($P < 0.05$). The red bars represent GO term enrichment score and black bars represent number of proteins in each GO term category.

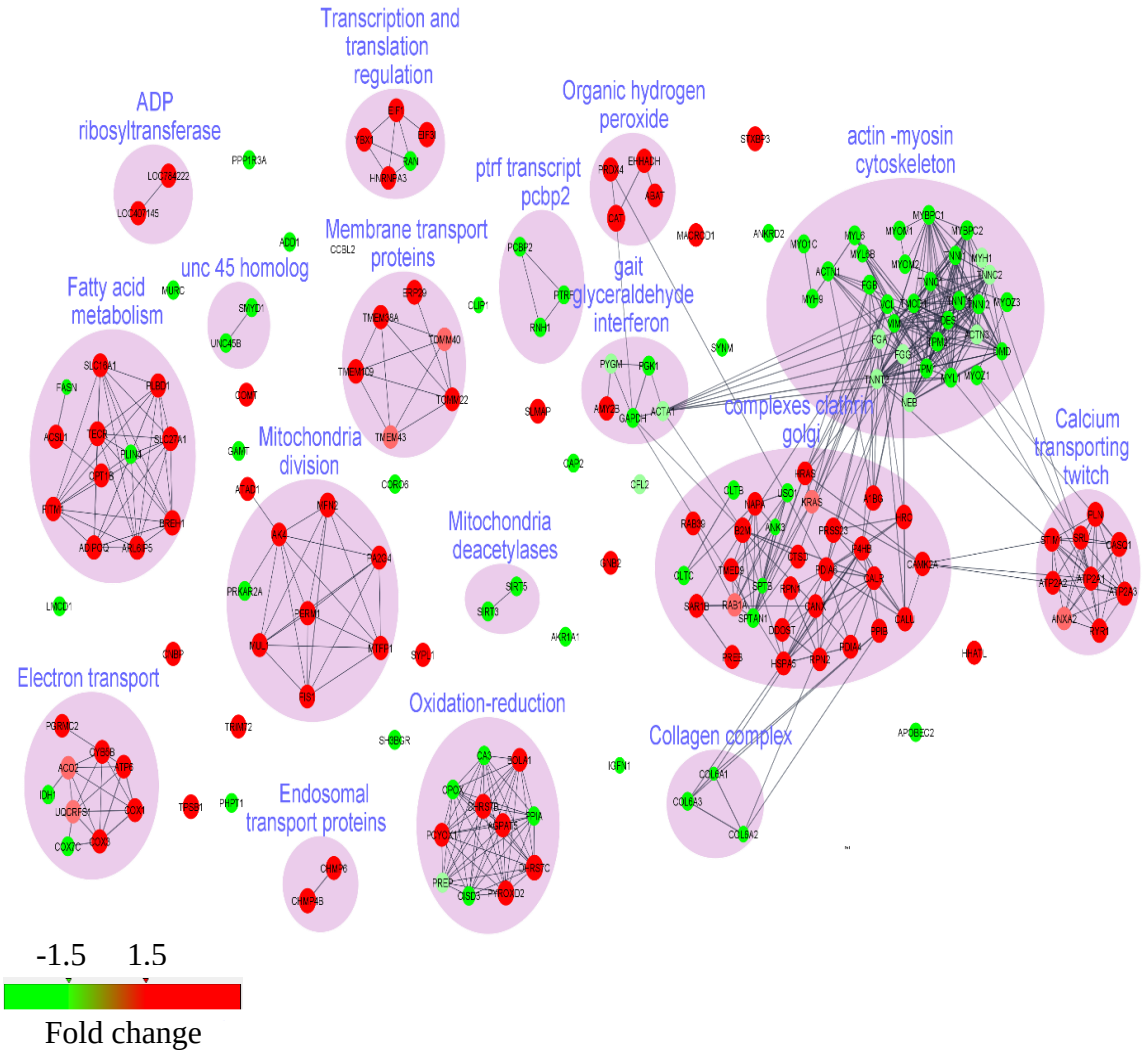

Figure 7: STRING database analysis of differentially abundant mitochondrial proteins in dark-cutting vs. normal-pH beef

Mitochondrial protein expression changes induced by dark-cutting condition in subnetworks identified were compared to normal-pH beef. Red and green colors represent up-regulated and down-regulate proteins significantly ($P \leq 0.05$) expressed respectively in dark-cutting beef mitochondrial proteome relative to normal-pH beef. Proteins in clustered circles exhibit protein-protein interactions while those outside the clusters showed no protein-protein interactions.

Table 1: Comparison of mitochondrial content and biochemical properties of normal and dark-cutting beef longissimus muscle

Parameters		Normal-pH	Dark-cutting beef	SEM	P-value
a) Proximate composition[1]	Moisture (%)	67.1	72.2	0.8	< 0.001
	Protein (%)	23.4	22.6	0.4	0.51
	Fat (%)	8.1	7.9	0.5	0.21
b) Surface color[2]	*L**	41.5	30.4	0.84	< 0.001
	*a**	29.4	22.4	0.93	< 0.001
	Chroma	37.6	29.1	0.92	< 0.001
	Hue	36.8	35.6	0.33	0.01
c) Biochemical properties[3]	pH	5.6	6.4	0.06	< 0.001
	Oxygen consumption (OC)	0.92	1.52	0.20	< 0.001
	Metmyoglobin reducing activity (MRA)	0.62	0.94	0.11	< 0.001
	Mitochondrial protein content (mg/g tissue)	33.85	44.12	3.82	0.01

[1]Proximate composition was determined using a NIR-based Food Scan.

[2] Surface color was measured using a HunterLab MiniScan Spectrophotometer after exposing the steaks in atmospheric oxygen for 1 h at 4 °C. *L** represents lightness, and a lower number represents darker meat color; *a** value represents redness and a lower number indicates less red color, a lower chroma indicates less red intensity, and lower hue indicates less brown or discoloration.

[3] pH was measured using a probe-type pH meter; OC– a greater number indicates more OC. MRA was determined as resistance to form initial metmyoglobin formation, a greater number indicates greater MRA. Mitochondrial protein content was measured using BCA assay. SEM – standard error of mean.

CHAPTER IV

INTEGRATIVE PROTEOMICS AND METABOLOMICS PROFILING TO UNDERSTAND THE BIOCHEMICAL BASIS OF BEEF MUSCLE DARKENING AT A SLIGHTLY ELEVATED pH

Accepted for publication: Journal of Animal Science

Abstract:

Previous studies investigated the biochemical basis of dark-cutting conditions at elevated muscle pH (above 6), but the molecular basis at slightly above normal pH (between 5.6 and 5.8) is still not clear. The objective was to determine protein and metabolite profiles to elucidate postmortem muscle darkening at slightly elevated pH. Loins were selected based on the criteria established in our laboratory prior to sample collections, such as pH less than 5.8, *L** values (muscle lightness) less than 38, and not discounted by the grader (high-pH beef with dark color are discounted and not sold in retail stores). Six bright red loins (*longissimus lumborum*) at normal-pH (average pH = 5.57) and six dark-colored loins at slightly elevated pH (average pH = 5.70) from A mature carcass were obtained within 72-h postmortem from a commercial beef purveyor. Surface color, oxygen consumption, metmyoglobin reducing activity, protein, and metabolite profiles were determined on normal-pH and dark color steak at slightly elevated ph. Enzymes related to glycogen

metabolism and glycolytic pathways were more differently abundant than metabolites associated with these pathways. The results indicated that oxygen consumption and metmyoglobin reducing activity were greater ($P < 0.05$) in darker steaks than normal-pH steaks. Enzymes involved with glycogen catabolic pathways and glycogen storage disease showed low abundance in dark beef. The tricarboxylic acid metabolite, aconitic acid, was overabundant, but glucose derivative metabolites were less abundant. The majority of glycogenolytic proteins and metabolites reported as overabundant in the previous dark-cutting studies at high pH (> 6.4) also did not show significant differences in the current study. Therefore, our data suggest enzymes involved in glycogen metabolism, in part, create a threshold for muscle darkening than metabolites.

Key words: Dark-cutting, normal-pH, meat color, proteomics, metabolomics, mass spectrometry

Introduction

The color of meat is an important factor in consumers' assessment of meat quality. To meat buyers, the bright cherry-red color of meat indicates freshness and wholesomeness (Boykin et al., 2017; Ramanathan et al., 2022; Ramanathan et al., 2020a; Salim et al., 2019; Sammel et al., 2002; Węglarz, 2018). The color of meat is primarily determined by myoglobin, a water-soluble sarcoplasmic protein (AMSA, 2012; Bendall, 1979; Faustman & Cassens, 1990; Suman & Joseph, 2013). Myoglobin exists in three forms, namely oxy-, deoxy-, and met-myoglobin. A greater concentration of oxymyoglobin gives consumers' desired bright cherry-red color. However, predominant deoxymyoglobin is associated with a dark meat color appearance (Ashmore et al., 1972; Kiyimba et al., 2021; McKeith et al., 2016; Ramanathan et al., 2020b). Although the prevalence of dark-cutting beef has reduced over the years, dark-cutting beef still continues to occur in the beef industry. The 2016 National Beef Quality Audit (NBQA) reported an average dark-cutter occurrence of 1.9% (Boykin et al., 2017). However, some beef packers reported an occurrence of 2-5% in certain months (personal communication, 2022). The dark-cutting beef is discounted during grading, and beef is not sold in retail due to its appearance and reduced shelf life. The US beef industry loses $202 million annually due to dark-cutting conditions (calculated based on 2016 NBQA and carcass discount by the American Marketing Service United States Department of Agriculture). However, the molecular and mechanistic basis for the occurrence remains unknown.

The hallmark of dark-cutting conditions is a greater than normal muscle pH. More specifically, depending on the range of ultimate pH, muscle darkening can vary from slight dark red color to a coffee-bean dark color (Lei et al., 2020; Mahmood et al., 2018; Roy et

al., 2022). Thus, meat with an ultimate muscle pH greater than 5.8 results in a visually detectable dark red color (Holdstock et al., 2014; Knee et al., 2007; Mahmood et al., 2018; Steel et al., 2018). Although the trigger for dark-cutting development is not clear, the current knowledge suggests that lower glycogen levels correlate with less glycolysis and greater than normal muscle pH. More specifically, dysregulated glycogen catabolic processes postmortem cause less carbon flow, leading to less postmortem lactic acid accumulation and elevated muscle pH (Fuente-García et al., 2021; Kiyimba et al., 2021). Additionally, dark-cutting beef has increased mitochondrial respiration postmortem than normal pH (Ashmore et al., 1971; English et al., 2016; McKeith et al., 2016; Ramanathan et al., 2020b). Thus, greater than normal-muscle pH in dark-cutting is a conducive factor for enhanced mitochondrial respiration postmortem. Therefore, sustained mitochondria respiration in dark-cutting phenotypes increases competition for available muscle oxygen and produces dark-colored muscles (Ashmore et al., 1972; Egbert & Cornforth, 1986; Ramanathan et al., 2009).

The identification of changes in protein profiles of muscle darkening at elevated muscle pH (> 5.8) noted that several proteins and metabolites involved with glycogen catabolism were less abundant, while proteins and metabolites associated with mitochondrial oxidative metabolism were overabundant in dark-cutting groups compared to normal-pH counterparts (Cônsolo et al., 2021; Fuente-García et al., 2021; Gagaoua et al., 2021; Kiyimba et al., 2021; Ramanathan et al., 2020b; Wu et al., 2020). Additionally, a recent study evaluating muscle fiber characteristics showed that dark-cutting beef has greater type I fibers than normal-pH (Roy et al., 2022).

Different grades of dark-cutting beef are reported based on ultimate pH. Therefore, characterizing protein and metabolite profiles of muscles that produce darker color at slightly elevated pH offers valuable insights into the occurrence of dark-cutting conditions. However, limited research has characterized the protein and metabolite expressional profiles of darker beef at slightly elevated muscle pH (< 5.8). A combination of proteomics and metabolomics can provide a comprehensive and in-depth understanding of complex biological processes regulating muscle darkening at slightly elevated muscle pH. In the current study, we combined proteomics and metabolomics profiling to identify differentially abundant proteins and metabolites in dark-cutting beef at slightly elevated muscle pH compared with normal-pH beef. Furthermore, we utilized bioinformatics analyses to elucidate the pH-dependent effects on muscle darkening in beef.

Materials and methods

Beef loins were purchased from a United States Department of Agriculture (USDA) Food Safety and Inspection Service inspected commercial plant. Therefore, institutional animal care and use committee approval were not requested for this study.

Sample collection and preparation

Six bright red *longissimus lumborum* loins at normal-pH (average pH = 5.57) and six dark-colored loins (Institutional Meat Purchasing Specification #180, NAMP, 2002; grain-finished, spray chilled) at slightly elevated pH (average pH = 5.70) from A maturity carcasses were obtained within 72-h postmortem from a commercial beef purveyor in Amarillo, TX. Dark-colored loins were selected based on the criteria established in our

laboratory before sample collections, such as pH less than 5.8, *L** values (muscle lightness) less than 38, and not discounted by the grader (high-pH beef with dark color are discounted and not sold in retail stores). pH and surface color of dark-colored loins were measured in the meat plant to satisfy conditions before collection. The loins were transported on ice, and loins were also measured for pH and color after packaging. Three 2.54-cm-thick steaks from each animal were cut from the anterior end of the loin. The first steak from each loin type (normal pH and darker at slightly elevated pH) was utilized for surface color, oxygen consumption, and metmyoglobin reducing activity studies. The second steak was utilized for liquid chromatography mass spectrometry/mass spectrometry (LC-MS/MS) proteomics and gas chromatography mass spectrometry (GC-MS) non-targeted metabolomics approach. The third steak from each animal was used to determine muscle pH and proximate compositions. All analyses were conducted 96 h postmortem.

Determination of pH, proximate composition, surface color, metmyoglobin reducing activity, and oxygen consumption

The pH of each steak was recorded using a probe-type Accumet 50 pH meter (Fisher Scientific, Fairlawn, NJ). The pH probe was calibrated with buffers at pH 4 and 7. The pH probe was inserted into the meat at three locations and the average pH was determined for each steak. The proximate compositions were determined using an Association of Official Analytical Chemist-approved (Official Method 2007.04; Anderson et al., 2007) near-infrared spectrophotometer (Foss Food Scan 78800; Dedicated Analytical Solutions, DK-3400 Hilleroed, Denmark). Protein, moisture, and fat contents were reported on a percent (%) basis. From each loin, a 2.5-cm-thick steak was cut, placed onto foam trays with absorbent pads, and steaks were wrapped with polyvinyl

chloride film (oxygen-permeable polyvinyl chloride fresh meat film; 15,500 to 16,275 cm3 O_2/m^2/24 h at 23°C, E-Z Wrap Crystal Clear Polyvinyl Chloride Wrapping Film; Koch Supplies, Kansas City, MO) and stored at 4°C for 30 min.

The surface color was measured using a HunterLab MiniScan spectrophotometer(AMSA, 2012). Following surface color measurements, each steak was cut in half. The first half was used to estimate muscle oxygen consumption, and the second half was utilized to measure metmyoglobin reducing activity. The greater postmortem muscle pH (above 5.8) seen in dark-cutting beef can influence muscle reflectance properties (AMSA, 2012). Hence, a modified method was utilized to measure oxygen consumption and metmyoglobin reducing activity (Ramanathan et al., 2019).

For metmyoglobin reducing activity, samples from the interior of steak halves (approx. 3 × 3 × 1.5 cm tissue with no visible fat or connective tissue) were submerged in a 0.3% w/v solution of sodium nitrite (Sigma Aldrich, St. Louis, MO) for 20 min at 30°C (Fisher Scientific, Model 630F, Waltham, MA) to facilitate metmyoglobin formation (Sammel et al., 2002). The sections were then removed and blotted to remove visible nitrite solution. The level of metmyoglobin content on the surface was determined by using a HunterLab Miniscan spectrophotometer. Resistance to myoglobin oxidation was a better indicator of metmyoglobin reducing activity than post-reduction values (Mancini et al., 2008; O'Keeffe & Hood, 1982). The resistance to myoglobin oxidation was reported as K/S572 ÷ K/S525. A greater number indicates greater metmyoglobin reducing activity. The steak half was bloomed at 4 °C for 1 h. Following blooming, each steak section was vacuum-packaged and incubated at 25 °C for 30 min to promote oxygen consumption.

After incubation, surface color readings were taken, and the deoxymyoglobin level was measured to determine muscle oxygen consumption.

Metabolomics Analysis

The metabolomics analyses were conducted at the National Institute of Health West Coast Metabolomics Center, University of California Davis, CA, USA. In brief, ten milligrams of skeletal muscle tissue from normal-pH and dark-colored beef from slightly elevated pH were freeze-dried and stored at −80 °C until analysis. The samples were mixed with two 3 mm grinder glass beads (Cat.1.04015, Sigma, St. Louis, MO). Metabolites were extracted with 1000 µL of degassed acetonitrile/isopropanol/water mixture (3:3:2, v/v/v). The mixture was homogenized for 30 s and shaken using an automatic shaker for 6 min at 4 °C. The homogenate was centrifuged at 4 °C for 2 min at 14,000 g, and the supernatant was collected. Methyl esters (2 µL of 1 mg/mL) were added as an internal standard, and the samples were dried under a gentle stream of nitrogen gas. The dried samples were derivatized with 10 µL of methoxyamine (Thermo Fisher Scientific, Catalog number TS-45950) in pyridine and subsequently by 90 µL of N-methyl-N-(trimethylsiyl) trifluoroacetamide (Thermo Fisher Scientific, Catalog number TS-48910) for trimethylsilylation of acidic protons. The extracted metabolites were analyzed using gas chromatography-mass spectrometry (Fiehn, 2016; Ramanathan et al., 2020b).

Metabolomics data processing

GC-MS data files were preprocessed directly after data acquisition using ChromaTOF version 2.32 and stored as specific *.peg files, as generic *.txt result files, and

additionally as generic ANDI MS *.cdf files (Skogerson et al., 2011). The files were exported to a data server with absolute spectra intensities and further processed by a filtering algorithm implemented in the metabolomics BinBase database. The BinBase algorithm (rtx5) settings used included: validity of chromatogram (10^7 counts s -1), unbiased retention index marker detection (MS similarity >800, validity of intensity range for high m/z marker ions), and retention index calculation by 5th order polynomial regression. Metabolite quantification was reported as peak height using the unique ion as default. A quantification report table was produced for all KEGG compound database entries that were positively detected in more than 10% of the samples (as defined in the miniX database) for unidentified metabolites. The list of metabolite features quantified and identified in dark-cutting beef at slightly elevated pH and normal-pH beef was uploaded into MetaboAnalyst for differential metabolite expression.

Protein extraction and digestion

Skeletal muscle tissue samples of 0.5 g free of fat and connective tissue collected from normal and dark-cutting beef at slightly elevated pH (n = 6 for each loin type) steaks were extracted as previously described by (Kiyimba et al., 2021). Protein concentration was determined using a tryptophan fluorescence assay (Wiśniewski & Gaugaz, 2015). The extracted samples were alkylated by the addition of 10 mM iodoacetamide and incubated for 15 minutes at room temperature. The solutions were then diluted with three volumes of 100 mM Tris-HCL, pH 8.5, and digested at 37 ºC overnight with 4 µg/mL of trypsin/LysC (Promega, Madison, WI). The samples were further digested by the second addition of trypsin/LysC (2 µg/mL) for 6 h. Further steps in sample preparation and LC-MS/MS analysis were performed as previously described (Kiyimba et al., 2021).

MS/MS database searching for identification of differentially abundant proteins (DAPS)

The raw LC-MS/MS instrument data files were analyzed using MaxQuant software (V1.5.3.12, Max Planck Institute of Biochemistry). The MS/MS spectra from each nano-LC-MS/MS run were searched against a Uniprot *Bos taurus* proteome database of 23,968 protein sequences (downloaded in March 2018) using the same search parameters as previously reported (Kiyimba et al., 2021). The sequences of common contaminate were included in the searches. The obtained MaxQuant label-free quantitation (LFQ) protein intensities were imported into the Perseus v1.6.3.3 software platform.(https://omictools.com/perseus-tool) and analyzed for differential abundance. For this analysis, protein groups were first filtered for reverse and potential contaminants. Then LFQ intensities were analyzed within the Perseus framework, using a two-sample T-test to compare $\log_2$ transformed LFQ protein intensities. Protein expression profiles were considered significant if the p-value was less than or equal to 0.05.

Statistical and Bioinformatics analyses

A completely randomized block design was employed to characterize muscle-specific differences in biochemical properties and color attributes of normal-pH and dark-colored beef at slightly elevated pH. The experiment was replicated 6 times (n = 6). Each loin from normal-pH and dark-colored beef at slightly elevated pH was considered a block. The least square means and standard error of mean were analyzed using the Proc Mixed procedure in SAS (Version 9.1, SAS Institute Inc. Cary, NC). The least squares means were separated using the pdiff option and were considered significant at $P < 0.05$.

To investigate the protein and metabolic changes associated with dark-colored beef at slightly elevated pH, Principal Component Analysis, supervised projections to latent structure-discriminant analysis, and hierarchical cluster analysis were performed to create plots and heat maps for the differentially abundant proteins and metabolites using Perseus software (V.1.6.3.3,https://omictools.com/perseus-tool) and MetaboAnalyst (V.5.0, http://www.metaboanalyst.ca), respectively. The metabolite data sets were normalized by a median, log-transformed, and scaled by Pareto scaling.

The online platform Metascape (https://metascape.org/) was employed to analyze the differentially abundant protein enrichment in the GO annotation and the DisGeNET database (Zhou et al., 2019). To acknowledge sampling bias, the gene list of all identified and quantified proteins in all 6 of the 6 compared samples (dark-colored beef at slightly elevated pH and normal-pH beef) was used as background uploaded into Metascape. The key pathway involved in postmortem metabolism (glycogen metabolism) was further analyzed in Cytoscape (V.3.7.1; https://cytoscape.org/) using the WikiPathway plugin (https://www.wikipathways.org; Szklarczyk et al., 2017). Protein networks were analyzed using the String database plugin in Cytoscape to explore the potential protein-protein biological interactions.

Results

Muscle surface color and biochemical characteristics

The muscle surface color and biochemical attributes of normal-pH and dark-colored beef at slightly elevated pH are summarized in Supplemental Table B.1. A slight elevation in muscle pH (0.13 units; 2.3% greater than normal-pH) of dark beef resulted in

11.72% decrease in lightness (L^*-value difference = 5.11, $P < 0.001$). Dark-colored beef at slightly elevated pH had lower a^*- and b^*-values ($P < 0.01$) than normal-pH beef. The L^*-value is an indicator of muscle lightness, and lower a^* values indicate less red meat. Furthermore, dark-colored beef at slightly elevated pH also showed greater oxygen consumption ($P = 0.03$) and metmyoglobin reducing activity (MRA, $P = 0.02$) compared with normal-pH beef.

Proteomics analysis

The LC-MS/MS proteomic profiling analysis identified 1,080 proteins in the proteomes of dark-colored beef at a slightly elevated pH than normal-pH beef. Among these, 23 proteins were overabundant (Supplemental Table B.2) and 13 proteins were less abundant (Supplemental Table B.3) in dark-colored beef than normal-pH beef ($P < 0.05$; fold change > 1.3). Principal component analysis (Figure 1) showed that 71.1 % variability was explained by the first two components with 59.9% and 11.2% total variation, respectively. The clusters of dark-colored beef at slightly elevated pH showed distinctive separation from the normal-pH beef clusters. In addition, the hierarchal clustering analysis (Figure 2) revealed distinctive clusters of protein groups co-segregating together in dark-colored beef at slightly elevated pH and normal-pH beef.

Gene Ontology (GO) and pathway enrichment analyses were employed using Metascape to explore the functional annotations of the proteins within clusters. The changes in protein abundance showed enrichment in a number of GO processes, including glycogen metabolism, muscle contraction, sarcomere organization, calcium-dependant protein binding, and ATP metabolic processes ($P < 0.001$; Figure 3a). In

addition, the platform of diseases-associated genes and variants analysis (DisGeNET) showed enrichment for proteins associated with the glycogen storage disease ($P < 0.001$; Figure 3b).

To further understand how the differentially abundant proteins might participate in dark color development, we analyzed the extent to which these proteins might cooperate in specific cellular pathways. Results showed enrichment in several metabolic clusters, including seven enzymes (Figures 4 and 5) involved in glycogen catabolic pathway were less abundant in the dark-colored beef. Annotation of the protein network (Figure 5) revealed distinctive interactive clusters of proteins associated with glycogen catabolism, muscle contraction, stress-related, ribosomal, and proteasome proteins. In the glycogen catabolic cluster, several nodes were of less abundant proteins in dark-colored beef at slightly elevated pH. While in the muscle contraction and stress-related protein-protein interaction network clusters, several nodes comprised overabundant proteins in dark-colored beef at slightly elevated pH.

Metabolomics analysis

A GC-MS-based non-targeted metabolomics approach was utilized to evaluate how the changes in protein expression profiles impact dark-colored beef at a slightly elevated pH metabolome. A total of 174 known compounds were identified in the metabolite library. Among these, three were significantly overabundant (Supplemental Table B.4), while five were significantly less abundant with ≥2 fold (Supplemental Table B.4) in dark-colored beef. Principal component analysis (Figure 6a), Partial least-squares discriminant analysis (Figure 6b), and hierarchal clustering (Figure 6c) did not show

distinctive clusters of metabolite groups co-segregating together in dark-colored beef at slightly elevated pH compared with normal-pH beef. Furthermore, several metabolites involved with glycolysis, tri-carboxylic acid cycle, and adenine nucleotides did not show significant abundance in dark-colored beef at slightly elevated pH compared with normal-pH beef (Supplemental Figures B.1-3).

Discussion

Meat color deviation from bright cherry-red leads to economic losses and limits consumer acceptance and marketability (Ramanathan et al., 2022). Previous research noted that a lower abundance of glycolytic enzymes and metabolites in dark-colored beef is associated with greater than normal muscle pH (> 6.4; Cônsolo et al., 2021; Kiyimba et al., 2021; Mahmood et al., 2018; Ramanathan et al., 2020b; Sentandreu et al., 2021). However, limited knowledge is currently available on protein and metabolite expression profiles of dark-colored beef at slightly elevated muscle pH. In the current study, we utilized an integrative approach combining proteomics and metabolomics profiling to identify differentially abundant proteins and metabolites in dark-colored beef at slightly elevated muscle pH compared with normal-pH beef.

Proteomic expression profiling revealed seven enzymes involved in glycogen catabolic pathways were less abundant in dark-colored beef at slightly elevated pH (Supplemental Table B.3). The low abundant enzymes in dark-colored beef (Figures 4 and 5) are associated with glycogen degradation pathways in the muscle (Komoda & Matsunaga, 2015). More specifically, glycogen phosphorylase, muscle isoform (PYGM) catalyzes the rate-limiting step in glycogen catabolism via the phosphorolytic cleavage of

glycogen to produce glucose-1-phosphate was down-regulated. Furthermore, enrichment analysis in the platform of disease-associated genes and variants (DisGeNET) also showed enrichment for proteins involved in the glycogen storage disease (Figure 3B). Thus, lower levels of these proteins can reduce dark-colored muscle's capacity to mobilize glycogen and the ability to accumulate lactate postmortem. Therefore, our data agree with previous findings relating incidences of muscle darkening in beef with defective glycogen metabolism (Fuente-Garcia et al., 2020; Kiyimba et al., 2021).

The central dogma of molecular biology is gene regulates protein, and proteins regulate the metabolites (Crick, 1970; Morange, 2009; Shapiro, 2009). Interestingly, the changes in protein abundance profiles related to glycolytic and tricarboxylic pathways observed in the present study did not coincide with changes with significantly abundant metabolite profiles (Supplemental Figures B.1-3). In addition, the majority of glycogenolytic proteins and metabolites less abundant in the previous dark-cutting studies (Kiyimba et al., 2021; Ramanathan et al., 2020b) at high pH (> 6.4) also did not show significant differences in the current study. Therefore, these data suggest enzyme activities threshold for muscle darkening. Consistent with this observation, several proteins and metabolites implicated in regulating postmortem pH decline, for example, lactate- and pyruvate-dehydrogenases, lactate, and pyruvate, respectively (Apaoblaza et al., 2020; Elkhalifa et al., 1984; Gagaoua et al., 2021; Robergs et al., 2004), were not differentially abundant in dark-colored beef at slightly elevated pH compared with normal-pH bright red steaks. Thus, the lack of significant changes in proteins and metabolites involved in muscle acidification explain a slightly elevated muscle pH observed in dark-colored beef in the present study.

When muscle glycogen content is low, there is a lack of a linear relationship between glycogen content and muscle pH decline (England et al., 2016). Consistent with this disconnect between glycogen content, glycolysis, and muscle pH, we observed that glycolytic metabolite profiles were not significantly different in dark-colored beef at slightly elevated pH and normal-pH bright red steaks (Supplemental Table B.4 and Figure B.1). In support, a recent study characterizing muscle properties of dark-colored beef at slightly elevated pH (approximately 0.21 pH difference) relative to normal-pH beef also revealed no differences between muscle darkening (based on L^* values) and glycogen content (Ijaz et al., 2022). Furthermore, in another study, a similar glucosidic potential was observed in Canadian AB4 (dark beef at pH < 5.9) compared with AA (normal bright red color at pH 5.6; Holdstock et al., 2014). Therefore, we speculate that other pathways, besides muscle glycolysis and glycogen content, might contribute to postmortem muscle pH decline and darkening in dark-colored beef at slightly elevated pH.

Muscle contractile proteins such as alpha-actin-4, xin actin, synaptopodin 2-like protein, and sarcolemma membrane-associated protein were overabundant in slightly elevated beef than normal pH beef (Figure 5 and Supplemental Table B.2). Interestingly in previous research, muscle contractile proteins were not different in dark-cutting beef compared to normal-pH beef (Kiyimba et al., 2021). Even though the mechanistic basis for overabundance is not clear, we speculate that contractile muscle proteins might have helped to increase glycolysis as an energy-adaptive mechanism.

Although the extent of stress in dark-colored beef is unknown in this research, several stress-related proteins, such as heat shock proteins and chaperones (Supplemental Table B.2), were overabundant in dark-colored beef at slightly elevated pH compared

with normal-pH beef. Heat shock proteins are important in protein quality control by mediating folding and refolding of misfolded proteins. Therefore, an overabundance of stress-related proteins in dark-colored beef at slightly elevated pH suggests increased oxidative stress. Previous studies also noted greater mitochondrial content in dark-cutting beef (pH > 6.4) than normal-pH beef (Kiyimba et al., 2021; McKeith et al., 2016; Ramanathan et al., 2020b). In the current research, proteins involved in mitochondrial substrate-level and oxidative phosphorylation (ATP1A2, CYB5R3, NDUFA7, OXCT1; Supplemental Table B.2) were overabundant in dark-colored beef at a slightly elevated pH than normal-pH beef. Therefore, our data suggest that dark-colored beef at slightly elevated pH has greater mitochondrial respiratory capacity compared with normal-pH beef. Consistent with this observation, muscle oxygen consumption was greater in dark-colored beef at slightly elevated pH than normal-pH beef (Supplemental Table B.1). Thus, greater mitochondrial oxygen consumption can result in more deoxymyoglobin and darker meat color (Ashmore et al., 1971; English et al., 2016; McKeith et al., 2016; Ramanathan et al., 2020a; Ramanathan et al., 2020b; Ramanathan & Mancini, 2018). Hence, a slightly elevated pH also can decrease the shrinkage of muscle bundles, which decreases reflectance of light and results in dark muscle.

Conclusions

The current research demonstrates the reduced abundance of proteins involved with glycogen catabolic processes and overabundance of mitochondrial oxidative proteins in dark-colored beef at slightly elevated pH than normal-pH beef. Interestingly, the number of metabolites associated with glycogen, glycolytic, and tricarboxylic pathways were not differentially abundant compared with protein profiles. Previous dark-cutting (pH > 6.4)

vs. normal-pH beef study revealed dysregulation of glycogen and glycolytic proteins and metabolites abundance. Thus, this study shows that, in part, the aberrant regulation of molecular signals driving muscle darkening in postmortem muscles is highly dependent on the changes in protein expression profiles rather than metabolite profiles.

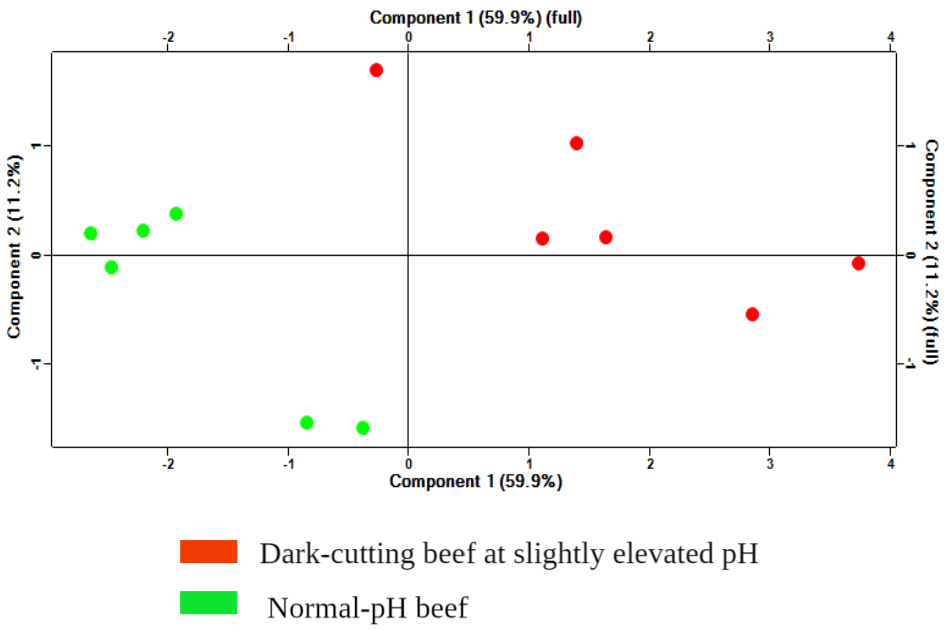

Figure 1: Principal component analysis (PCA) of proteins differentially abundant in dark-colored beef at slightly elevated pH vs. normal-pH beef.

Principal component analysis (PCA) of quantified proteins at the total protein level. Red and green dots represent protein groups from dark-colored beef at slightly elevated pH vs. normal-pH beef, respectively.

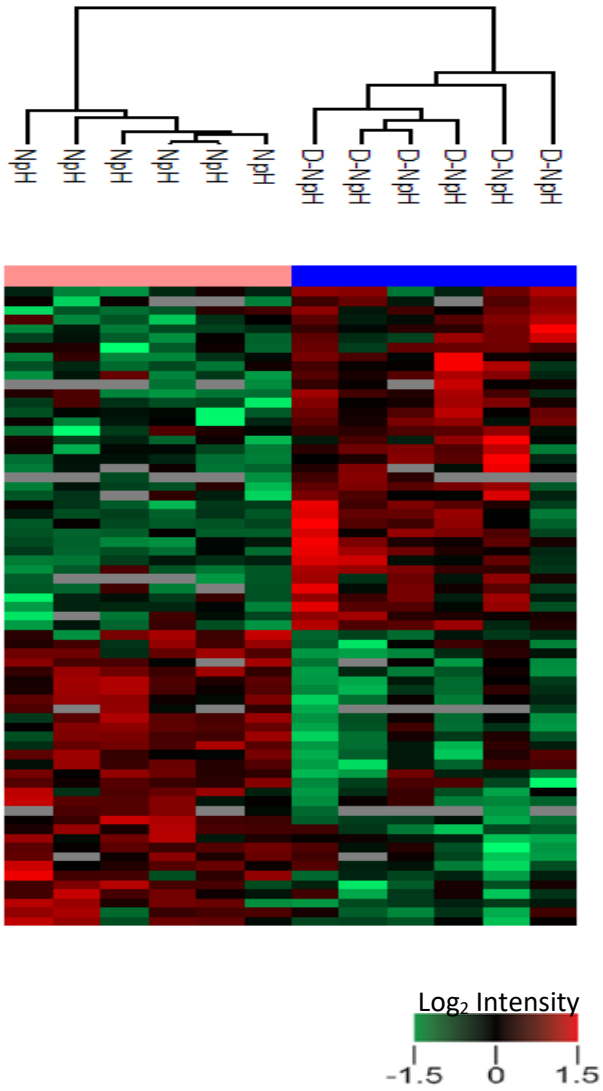

Figure 2: Hierarchical clustering analysis of protein abundance profiles in dark-colored beef at slightly elevated pH vs. normal-pH beef.

Protein abundancechanges in dark-colored beef at slightly elevated pH vs. normal- pH beef.as described in the materials and methods. Red and green colors represent overabundant and less abundant proteins differentially abundant in dark-colored beef at slightly elevated pH compared with normal-pH beef. Heat map color legend represents the $\log_2$ transformed ratio of dark-colored beef at slightly elevated pH vs. normal-pH beef.

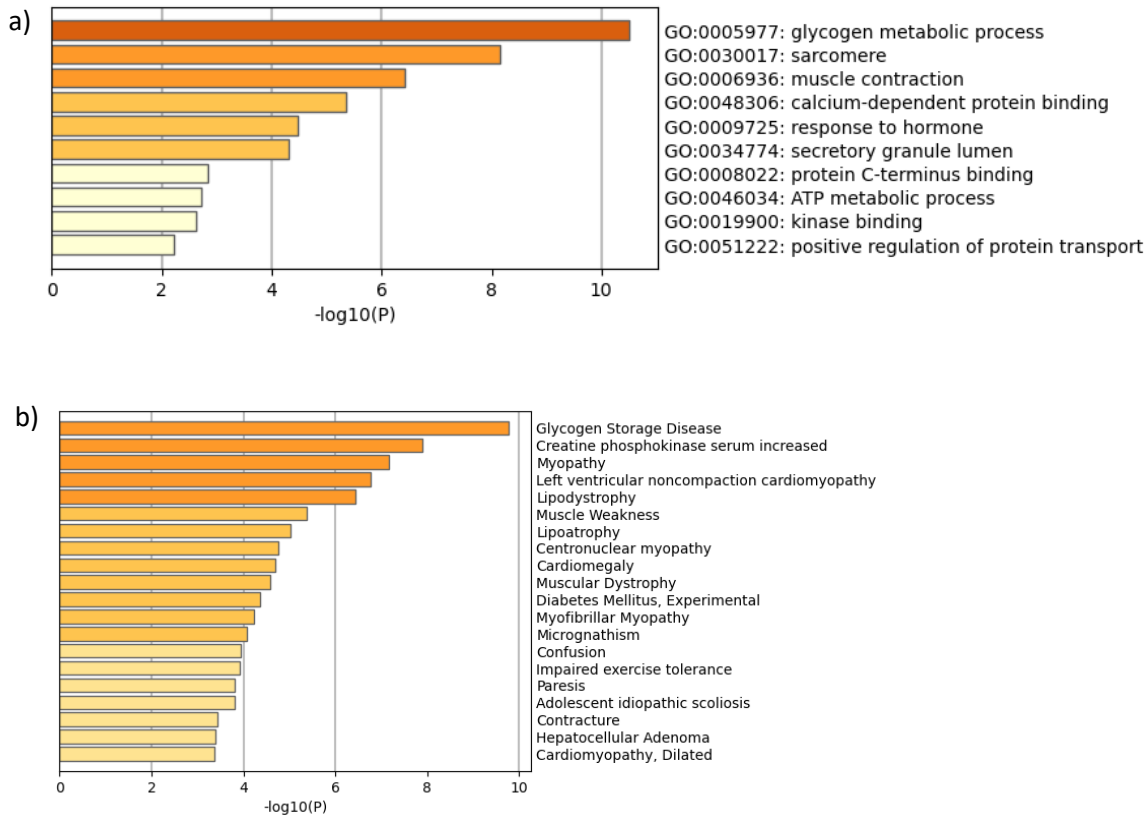

Figure 3: Metascape functional characterization of differentially abundant proteins in dark-colored beef at slightly elevated pH vs. normal-pH beef.

Proteins with significantly altered abundance in dark-colored beef at slightly elevated pH vs. normal-pH beef were analyzed for functional enrichment using Metascape. (a) Statistically enriched biological processes. (b) Statistically enriched terms in the DisGeNET platform of diseases-associated genes and variants. Top clusters with their representative enriched term are shown.

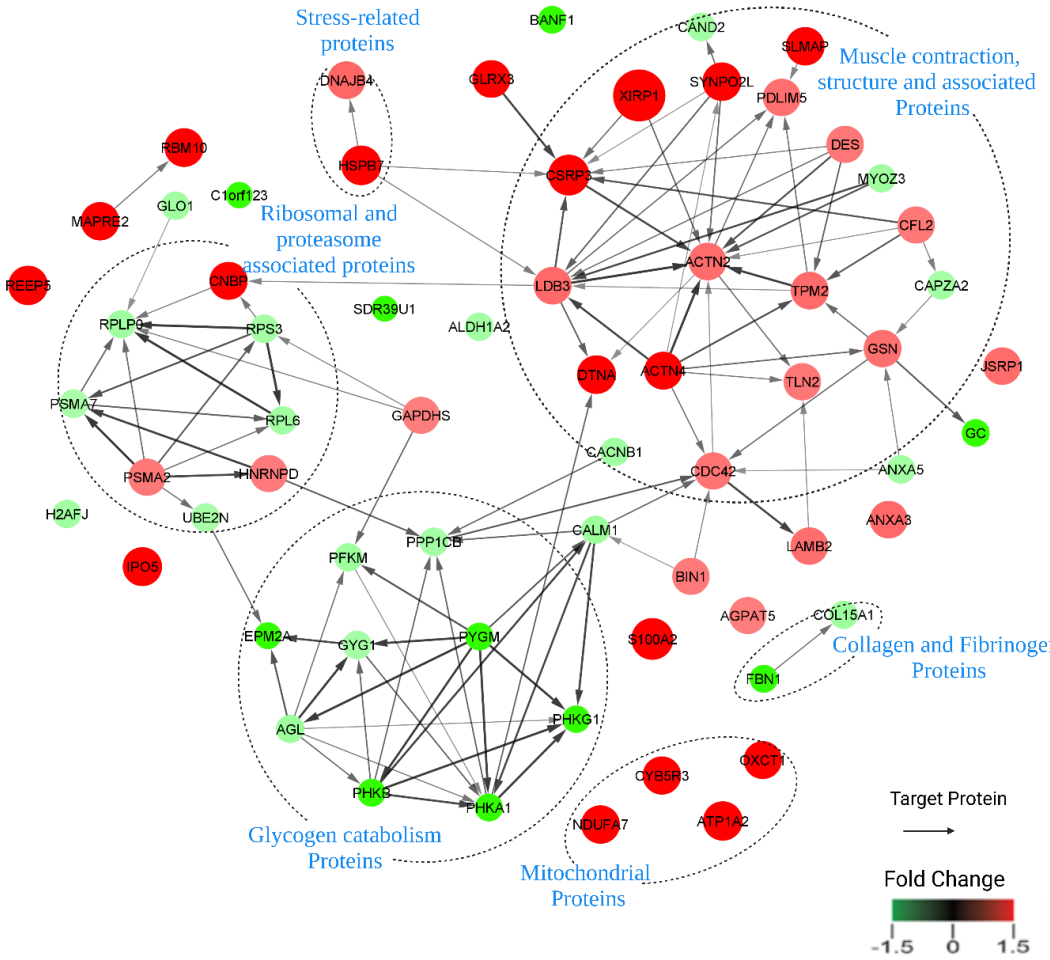

Figure 4: STRING database analysis of proteins up-and down-regulated in dark-colored beef at slightly elevated pH vs. normal-pH beef.

The proteins with significant changes in protein abundance between dark-colored beef at slightly elevated pH vs. normal-pH samples were used to query potential protein-protein interactions in the string database as described in the methods. Protein interactions were confirmed with connections, while non-interacting proteins had no connections between them. The red color represents overabundant proteins and the green color represents less abundant in dark-colored beef at slightly elevated pH vs. normal-pH beef. The size of the circle represents fold change in abundance, while the arrows heads indicate the target of the protein interactions.

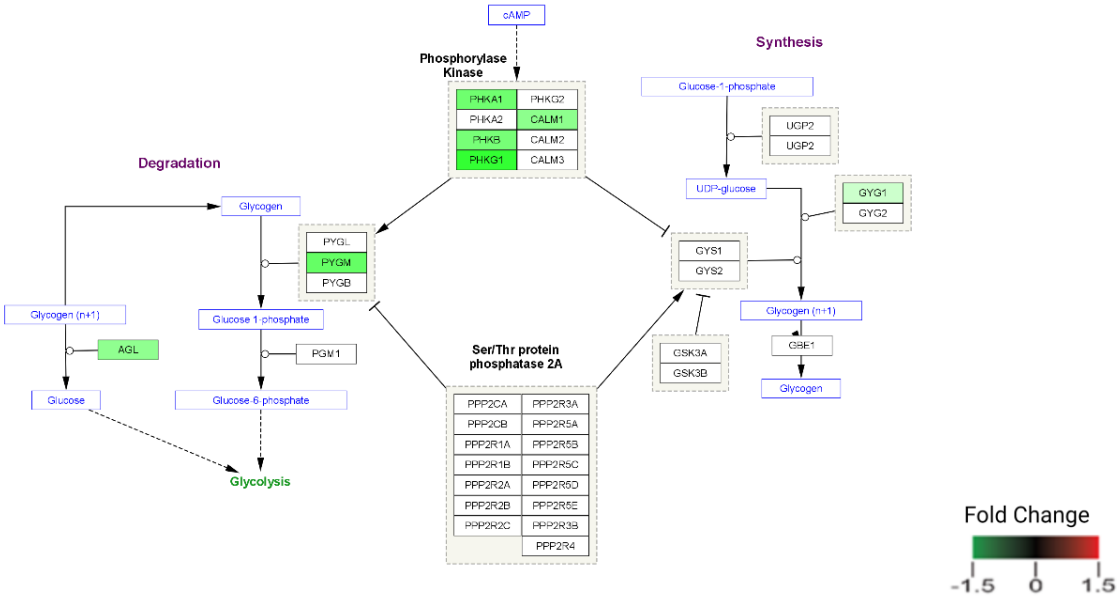

Figure 5: Differentially abundant protein in the dark-colored beef at slightly elevated pH vs. normal-pH beef involved with the glycogen catabolism pathway

The green color represents less abundant proteins in dark-colored beef at slightly elevated pH vs. normal-pH beef. The greater the color intensity, the greater the protein abundance.

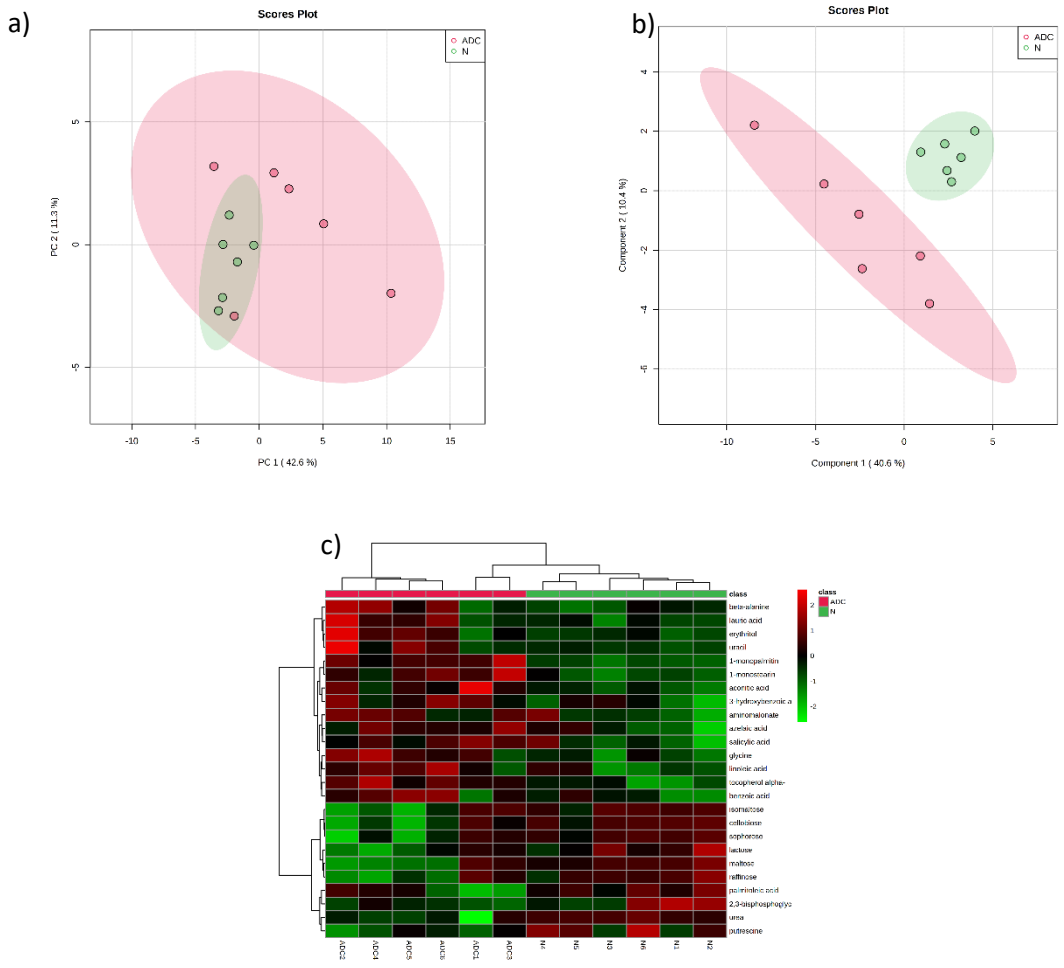

Figure 6: (a-b) Principal component analysis and partial least squares discriminant analysis of metabolite present in dark-cutting beef at slightly elevated muscle pH (ADC; pH =5.70) and normal-pH beef (N; pH = 5.60). (c) Hierarchical cluster analysis of differentially abundant metabolites in dark-colored beef at slightly elevated pH (ADC) relative to normal-pH (N). Heat map color legend represents the $\log_2$ transformed ratio of dark-colored beef at slightly elevated pH color vs. normal-pH beef.

CHAPTER V

PROTEOMICS AND METABOLOMICS SIGNATURES OF DARK-CUTTING BEEF *LONGISSIMUS LUMBORUM* MUSCLES DURING POSTMORTEM WET-AGING

In preparation for submission: Journal of Agricultural and Food Chemistry

Abstract

The protein and metabolite expression profiles of dark-cutting relative to normal-pH beef have been previously examined. However, the effects of postmortem wet-aging on dark-cutting beef degradation profiles is not clear. In this study, we utilized an integrative approach combining proteomics and metabolomics profiling to characterize the degradation behavior as well as define postmortem wet-aging-dependent proteolytic mechanisms in dark-cutting beef *longissimus lumborum* muscles. We show that at day 7 of postmortem wet-aging, dark-cutting beef up-regulates protein categories enriched in response to oxidative stress with down-regulation of carbohydrate-derived biosynthesis and cellular homeostasis processes. Analysis of non-trypsin specific peptide cleavages at day 14 of postmortem wet-aging demonstrated that dark-cutting beef has a greater abundance of peptides associated with muscle structural and mitochondrial proteins. Furthermore, several tri-carboxylic acid (TCA) cycle, free amino acids, and nucleotide metabolites

showed greater abundance in dark-cutting beef on day 7 and 14 of postmortem wet-aging. The results show evidence of enhanced postmortem wet-aging induced muscle proteolysis in dark-cutting compared to normal-pH beef. Thus, a better understanding of postmortem wet-aging-dependent proteolysis in dark-cutting beef may provide novel candidate biomarkers of damage and could provide new insights and strategies to improve quality characteristics of dark-cutting beef.

Keywords: Wet-aging, proteolysis, dark-cutting beef, proteomics, metabolomics

Introduction

The marketability of fresh beef is dependent on the color of meat. Deviations in meat surface color results in discounted meat prices at retail (Suman & Joseph, 2013; Ramanathan et al.,2022; Robbins et al., 2003; Unklesbay & Keller, 1986). An example of a meat color deviation is dark-cutting beef, a quality defect where beef fails to have a characteristic bright cherry-red color typical of normal-pH beef. Several studies utilizing proteomics (Fuente-García et al., 2021; Gagaoua et al., 2021; Kiyimba et al., 2021; Wu et al., 2020) and metabolomics (Cônsolo et al., 2020; Ramanathan et al., 2020b) profiling have demonstrated that muscle darkening in part, is associated with aberrations in muscle glycogen metabolism which in-turn contributes to abnormal muscle pH above 5.8.

Recently, we demonstrated that the greater muscle pH coupled with up-regulation of mitochondrial biogenesis proteins supports enhanced mitochondrial respiration in dark-cutting muscles (Kiyimba et al., 2022). Thus, the amount and activity of mitochondria may contribute to muscle darkening via oxygen consumption. Previous research in our laboratory also showed that postmortem wet-aging can decrease oxygen consumption and improves bloom development in dark-cutting beef (English et al., 2016). However, the impact on muscle protein degradation and the resultant substrate degradome in dark-cutting compared with normal-pH beef remains poorly defined.

During postmortem aging, muscle protein degradation occurs, and the aging process is associated with alterations in muscle structure, decreased anabolic signaling, increased apoptosis, and reduced mitochondrial functionality (Gomes et al., 2017; Huff-Lonergan et al., 1996; Ibebunjo et al., 2013; Rygiel et al., 2016). Thus, the resultant degradation

substrate in aging-induced proteolysis is dependent on processes such as: protease-mediated cleavages (Hipp et al., 2019; Houry, 2014), protein oxidation, and reactive oxygen species-induced oxidative stress (Breusing & Grune, 2008; Szczepanowska et al., 2021).

In aged meat, the endogenous μ-calpain systems are the major contributors to postmortem proteolytic changes (Carlin et al., 2006; Kendall et al., 1993; Koohmaraie, 1992; Lonergan et al., 2001). These systems direct specific cleavages of myofilaments into individual proteins (Goll et al., 1992). However, other pathways, such as the ubiquitin-proteasome systems and lysosomal mediated protease pathways, are also implicated in muscle proteolysis (Anand et al., 2013; Löw, 2011). Although the effects of postmortem aging on muscle proteolysis have been previously examined (Huff-Lonergan et al., 1996; Kim et al., 2016; Lamare et al., 2002; Lonergan et al., 2001; Ma et al., 2017), most meat studies have extensively focused on improving meat tenderness. However, the impact on other meat quality parameters including color more specifically in dark-cutting beef muscles is still not clear.

In this study, we sought to characterize the substrate degradation profiles of wet-aged dark-cutting beef and define which specific mechanism/pathways regulate muscle proteolysis and the effects on meat color. To accomplish this, we used label-free proteomics and non-targeted metabolomics approaches to quantitate the relative changes at various postmortem wet-aging time. Our results suggest enhanced muscle proteolysis and oxidative mechanisms in dark-cutting beef. Thus, a better understanding of the dark-cutting postmortem aging-dependent proteolysis may provide novel candidate biomarkers

of damage and could provide new strategies to improve quality characteristics of dark-cutting beef.

Materials and methods

Sample collection and storage

A total of 12 *longismus lumborum* strip loins (n = 6 no-roll dark-cutting beef and n = 6 normal-pH beef; USDA Choice) were collected within 3 days after harvest from Creekstone Farms, Arkansas City, KS. The collected samples were vacuum packaged and transported on ice to Oklahoma State University's Robert Kerr Food and Agricultural Products Center (FAPC). The loins from normal-pH and dark-cutting beef were fabricated into 3 equal sections and randomly assigned to 1 of 3 aging periods 0, 7, or 14 days (6 × 3 = 18 half loins; 18 half loins ÷ 3 aging periods = 6 replications). Before aging, each section was anaerobically packaged as previously reported by (Wills et al., 2017). The samples were then stored in the dark at 4 ºC.

After each respective postmortem aging time, samples from dark-cutting and normal-pH beef were utilized to measure surface color and biochemical attributes as previously reported (English et al., 2016; Mitacek et al., 2018). The samples for proteomics and metabolomics analysis collected at each postmortem wet-aging time were snap-frozen in liquid nitrogen, pulverized into a powder and stored at -80 ºC until further analysis.

Protein extraction

Proteomics samples were extracted following a method reported by Kiyimba et al. (2021) using n = 6 dark-cutting and n=6 normal-pH beef samples at each aging storage time (0, 7, and 14 days). Briefly, 100 mg of sample from dark-cutting and normal-pH beef was homogenized for 2 min with a small tissue teaser (Model 985,370–395, Biospec product, Inc) in 1mL ice-cold buffer containing (6 M guanidine hydrochloride, 100 mM HEPES, 50 mM chloroacetamide (CCA), 10 mM TRIS (2-carboxyethyl) phosphine TCEP, pH 8.0. The samples were boiled in a water bath for 10 minutes, and sonicated in a Bioruptor sonicating water bath (Diagenode, Denville, NJ) with 30 s and 30 s off cycles for 15 minutes. After, the sample extracts were centrifuged at 10,000 x g for 10 min at 4 ºC and immediately aliquoted and stored at -80 ºC until further analysis.

Protein digestion and profiling

A tryptophan fluorescence assay was used for protein quantification by recording fluorescence in a microplate reader (Spectra MaxM3; Molecular devices, San Jose, CA, USA) at a wavelength of 295 nm/350 nm (excitation /emission). After protein quantification, 20 µg from each treatment group (dark-cutting vs. normal-pH beef) at each respective postmortem wet-aging time (0, 7, and 14 days) were processed using a filter-aided sample preparation (FASP) protocol as previously described by Kiyimba et al. (2021). The resultant dark-cutting and normal-pH beef peptides from each postmortem aging time were extracted and analyzed via LC-MS/MS using fusion Orbitrap mass spectrometer (Thermo Scientific). The collected raw LC-MS/MS data files were searched against a UniProt bovine database concatenated with a reverse decoy database for

evaluating false discovery rate using MaxQuant (V.2.1.4.0; https://www.maxquant.org/). The same search parameters as previously described by Kiyimba et al., (2021) were followed with the addition of a match between runs. The label free quantification (LFQ) data output text files from MaxQuant were imported into Perseus for differential protein expression.

Termini cleavage analysis to reveal aging induced in-situ proteolysis

To access the impact of postmortem wet-aging induced proteolysis in dark-cutting compared with normal-pH beef, we utilized the specific peptides identified by MaxQuant searching to further analyze the non-specific versus trypsin-specific cleavages for evidence of enhanced proteolysis. For this analysis, the same search settings as previously described by Kiyimba et al. (2021) were utilized. Briefly, the text files obtained from MaxQuant searching were analyzed for termini non-specific and specific cleavage using Perseus (https://maxquant.net/perseus/). The individual peptide ratio of the non-specific and trypsin specific peptide LC-MS intensity in dark-cutting versus normal-pH beef at 14 days was calculated and the median intensities were determined. The significant changes in median peptide intensity ratios were validated by a 1-sample t-test of the $\log_2$ expression values at a cutoff of $P \leq 0.05$.

To probe for the specific proteins contributing to the non-specific peptide substrate degrdom in dark-cutting vs normal-pH beef, the differential peptide abundances were determined using FDR permutation-based methods in Perseus and were considered significant at $P < 0.05$. Furthermore, to visualize the 3D structures of the peptides within the specific proteins, protein database (PDB) files were downloaded from UniProt

(https://www.uniport.org) and visualized in PyMoL V.2.5 (https://plymol.org/2; Yuan et al., 2017).

Metabolite extraction and profiling

To determine whether the postmortem wet-aging induced changes in protein profiles reflect in local levels of metabolites, six samples from normal-pH and dark-cutting beef were randomly selected at aging day 7 and 14. The metabolomics samples were analyzed via a non-targeted metabolomics approach conducted at the National Institute of Health West Coast Metabolomics Center, University of California Davis, CA, USA as previously reported by Ramanathan et al. (2020b). The steps in metabolomics profiling such as injector, column, and mass spectrometric settings, were done according to details discussed by (Fiehn, 2016).

Bioinformatics analyses

To determine changes in protein and metabolites profiles of dark-cutting vs normal-pH beef following postmortem wet-aging, the principal component analysis and hierarchical clustering analysis for proteomics data were constructed within the Perseus software (https://maxquant.net/perseus/) and for metabolomics data were constructed using Meta MetaboAnalysit v5.0 (https://www.metaboanalyst.ca). To determine the enriched Gene Ontology terms (GO) of the differentially expressed proteins with more than 1.5 fold change in protein expression, the free web tool Web Gestalt (www.webgestalt.org;Wang et al., 2013) was employed. The background list consisted of all proteins quantified in dark and normal-pH beef proteomes at all aging periods. The

protein-protein interaction networks were constructed using the String app plug-in in Cytoscape (V.3.7.1; https://cytoscape.org).

Statistical analyses

To determine the effects of muscle postmortem wet aging on meat color and biochemical attributes, a completely randomized block design was used. Each loin from normal-pH and dark-cutting beef served as a block. The un-paired two-tailed Student's t-test was used to compare the means of two independent groups. The least square means were separated using the PDIFF option and were considered significant at $P < 0.05$. The multiple comparisons of more than one group were conducted using a one-way ANOVA with Tukey's post hoc test using SAS (SAS Institute, Cary, North Carolina, USA). For the proteomics and metabolomics analyses, the details are included in the previous section.

Results

Changes in muscle surface color properties during postmortem wet-aging

Postmortem wet-aging did not significantly improve surface color characteristics in both dark-cutting and normal-pH beef at 7 and 14 days relative to day 0 (Figure 2a-d). As expected, dark-cutting beef had significantly lower ($P < 0.001$) muscle surface color profiles compared with normal-pH beef (Figure 2a-d). These data showed that both dark and normal muscle respond similarly to postmortem aging conditions.

Postmortem wet aging induces distinct changes in protein and metabolite expression profiles in dark-cutting compared with normal-pH beef

To evaluate the impact of postmortem wet-aging on the substrate degradation profiles in dark-cutting compared with normal-pH beef, we utilized an integrative approach combining proteomics and non-targeted metabolomics profiling. Principal component analysis (PCA) and hierarchical cluster analysis (HCA) of proteomics and metabolomics data revealed distinctive clusters of proteins (Figure 3a-d) and metabolites (Figure 4a-c) co-segregating together in dark-cutting vs. normal-pH beef at each respective postmortem wet-aging period. Furthermore, postmortem muscle aging at day 7, induced an overall up-regulation in protein expression. However, by day14, a decrease in protein expression was observed in dark-cutting compared with normal-pH beef. More specifically, 16 proteins were up-regulated and 6 were down-regulated on day 0 (Figure 3e; Supplemental Table C.1). At 7 days of postmortem wet-aging, 49 proteins were up-regulated and 9 proteins were down-regulated. By 14 days, 28 proteins were found down-regulated and 8 up regulated in dark-cutting beef with more than 1.5-fold (Figure 3e; Supplemental Table C.1).

Metabolomics profiling also yielded a series of differential metabolites in dark-cutting compared to normal-pH beef. Seventy-four metabolites were up-regulated and 6 metabolites down-regulated on day 7 in dark-cutting compared with normal-pH beef. Fifty-three and 30 metabolites were up- and down regulated by day 14 in dark-cutting compared with normal-pH beef, respectively (Figure 4g; Supplemental Table C.3 and C.4). Several of these metabolites were free amino acids, nucleotides, and energy

metabolites involved in the TCA and glycogenolytic/glycolytic pathways (Figure 4d-f and Supplemental Figures C.1-4).

Furthermore, cross-comparison using Ven diagram analysis of the significantly expressed protein and metabolite changes at 0, 7, and 14 days did not yield overlaps in expression (Figure 3e-f; Figure 4g). A total of 16, 31, and 44 proteins were found uniquely abundant at 0, 7, and 14 days of postmortem aging in dark-cutting compared with normal-pH beef. However, metabolites profiles showed 9 uniquely abundant metabolites found only on day 14 in dark-cutting compared with normal-pH beef. Taken together, these results showed that postmortem wet-aging conditions induce differential changes in protein and metabolite profiles of dark-cutting compared with normal-pH beef.

Postmortem wet-aging of dark-cutting beef enhanced proteolytic and oxidative mechanism

To better understand the pathways regulating muscle protein degradation during postmortem wet-aging in dark-cutting compared with normal-pH beef, we explored the functional annotations of the proteins and metabolites within in the distinctive clusters, using Gene Set Enrichment analysis (GSEA). On day 0 of postmortem wet-aging, functional annotations revealed enrichment of several gene categories involved in monocarboxylic acid metabolic process and regulation of proteolysis muscle system process, up-regulated in dark-cutting beef.

The down-regulated categories showed enrichment in negative regulation of transcription by RNA polymerase II (Figure 5a). However, on day 7 of aging, the up-

regulated gene categories were enriched in carbohydrate metabolic process and response to oxidative stress while carbohydrate derived biosynthetic process and cellular homeostasis gene categories were down-regulated (Figure 5b). By 14 days of postmortem wet-aging, the up-regulated differentially expressed proteins in dark-cutting beef were more enriched in gene categories associated with cellular component morphogenesis, generation of precursor metabolites and energy, and protein folding biological processes (Figure 5c). While, the down-regulated proteins were enriched in peptide-, carbohydrate-, purine-containing-, and ribose phosphate- metabolic biological processes (Figure 5c).

Investigations of the protein-protein interaction networks associated with the wet-aging phenotypes in dark-cutting compared with normal-pH beef on day 7 revealed interactions of proteins associated with the proteasome, and glutathione mediated responses to oxygen reactive species proteins, amino acid metabolism, glycolysis, and nucleotide metabolism up-regulated in dark-cutting beef (Figure 5e). However, by day 14 of postmortem wet-aging, the majority of these networks were down-regulated in dark-cutting beef (Figure 5f and Supplemental Figure C.5b).

Analysis of metabolites profiles in wet aged dark-cutting beef revealed greater abundance of free amino acids, TCA, and nucleotide metabolites (Figure 4; Supplemental Table C.4 and Figures C.1-4) in dark-cutting beef compared to normal-pH beef. The majority of the up-regulated metabolites in dark-cutting beef were more abundant at day 14 compared to day 7 of postmortem wet-aging. Among the down-regulated metabolites, several glycolytic metabolites including glucose, fructose, glucose-6-phosphate, glucose-1-phosphate and fructose-6-phoshate were less abundant on 7 vs. 14 days of postmortem wet-aging. The joint protein and metabolite pathway enrichment analysis showed

changes associated with energy metabolism. More specifically, alanine, aspartate and glutamate metabolism, arginine biosynthesis, TCA cycle, glucagon signaling, purine and glutathione metabolism (Figure 4h).

Postmortem wet-aging induced proteolysis in dark-cutting beef is mediated through N-termini cleavages

To further investigate the evidence of enhanced postmortem wet-aging induced proteolytic changes in dark-cutting relative to normal-pH beef, the specific peptides identified by MaxQuant searching were analyzed for the abundance of non-specific vs. trypsin specific cleavages. The non-specific peptide cleavage profiling revealed a greater abundance of N- and C- termini peptides at 14 relative to 0 and 7 days of postmortem wet-aging (Supplemental Figure C.6a). However, the abundance of N-termini cleavage peptides was significantly greater relative to C-termini cleavages ($P < 0.05$, Supplemental Figure C.6a). Furthermore, the up-regulated peptides in dark-cutting beef on day 14 of aging were derived from proteins involved in muscle structure organization and associated proteins. Thus, this suggests enhanced muscle degradation in dark-cutting muscles. However, peptides of proteins involved in energy metabolism more specifically, creatine kinase, glycerol dehyde-3 phosphate, glycogen debranching enzyme, and glycogen phosphorylase showed low abundance in dark-cutting beef (Supplemental Figure C.6 and Table C.2). Additionally, putative cysteine protease (cathepsin k), matrix metallopeptidases (2, 3, and 9) and serine protease cleavage sites (data not shown) were identified in the differentially abundant peptides.

Discussion

Postmortem aging of meat is a strategy widely adopted by the meat industry to improve meat quality characteristics, including; tenderness, flavor, and juiciness. However, the impact of postmortem wet-aging in dark-cutting beef is not well described. In this study, we examined the postmortem wet-aging proteomics and metabolomics profiles of dark-cutting compared with normal-pH beef and defined the mechanism/pathways regulating muscle proteolysis.

Based upon our findings, we conclude that postmortem wet-aging leads to muscle-specific changes in protein and metabolite profiles contributing to enhanced muscle proteolysis in dark-cutting compared with normal-pH beef. This conclusion derives from three lines of evidence. (i) proteomics profiling revealed up-regulation of proteolytic and oxidative proteins in dark-cutting compared with normal-pH beef (Figure 2; Supplemental Table C.1). Of the altered proteins, proteasome proteins (PSMB6, PSA6, PSMA1), mostly members of the 20S core proteasome complex involved in proteolytic degradation of intracellular proteins were up-regulated in dark-cutting beef at day 7 of aging.

The 20 S proteasome complex mediates ubiquitin-independent protein degradation (Ben-Nissan & Sharon, 2014; Kelly et al., 2007; Njomen & Tepe, 2019). Therefore, the greater abundance of these proteins could be attributed to the inherent aberration in postmortem muscle pH reported in dark-cutting beef muscles. A previous study also noted that the postmortem proteasome activities in bovine muscles were stable within the first postmortem hours but increased due to changes in the physiochemical condition of

the muscles (Lamare et al., 2002). Thus, the high muscle pH of dark-cutting beef could in part, be a contributing factor in stabilizing the 20 S proteasome protein complexes. In addition, high muscle pH was shown to increase the activity of neutral muscle proteolytic machinery such as calpains and calcium-dependent proteases (Yu & Lee, 1986). However, these proteolytic systems examined in postmortem aged muscles (Carlin et al., 2006; Kendall et al., 1993; Koohmaraie, 1992; Lonergan et al., 2001) did not show differential changes in protein profiles between dark-cutting and normal-pH beef. The down-regulation of PSMA1, a protein involved in ATP-dependent degradation of ubiquitin proteins in dark-cutting beef could be attributed to fluctuations in ATP levels in the postmortem aging environment. Therefore, our data suggest that postmortem wet-aging dependent muscle degradation in dark-cutting beef could be regulated via ubiquitin-independent protein degradation pathways.

The greater abundance of mitochondrial proteins and respiratory capacity reported in dark-cutting beef (Kiyimba et al., 2022; McKeith et al., 2016) renders the dark-cutting beef muscles more susceptible to oxidative damage. Consistent with this observation, mitochondrial metabolic proteins (Figure 3c-e) and oxidative stress proteins (SOD1, SOD2, RDX2, PRDX6, PARK7, and GSTP1; Figure 4c-e) were up-regulated in dark-cutting beef at day 7 of postmortem wet-aging. The oxidative stress proteins are involved in destroying radicals produced within cells (Kang et al., 1998; MacMillan-Crow & Thompson, 1999). Therefore, up-regulation of these proteins suggests a disproportionate accumulation of damaged and dysfunctional proteins in dark-cutting beef muscles. In support, the levels of heat shock proteins specifically HSPB1, a molecular chaperon involved in maintaining denatured proteins in a folding-competent state was up-regulated

in dark-cutting beef. However, down-regulation of HSPB6 coupled with several other proteins at day 14 (Supplemental Figure C.5b) could be associated with degenerative aging related phenotype resulting from increased oxidative damage. Thus, we speculate that the greater proteolysis and oxidative stress contribute to enhanced muscle proteolysis in dark-cutting beef during postmortem wet-aging.

(ii) Although in the current study we did not quantify the specific activity of proteolytic enzymes driving protein degradation in postmortem skeletal muscles, sequence analysis of generated non-specific cleavage peptides during postmortem wet-aging further provides evidence of markers of protein breakdown in dark-cutting compared with normal-pH beef (Supplemental Figure C.6). More specifically, peptides of structural proteins such as myosin heavy chains, actin, myosin binding protein, nublin, troponin, tropomyosin, and connective tissue-containing proteins (collagen type VI alpha 3 chain) were up-regulated in dark-cutting beef at day 14 of aging (Supplemental Table C.5).

Intriguingly, peptides associated with energy metabolism, specifically peptides of proteins such as creatine kinase, glyceraldehyde-3-phosphate, and phospho-glucomutase were down-regulated at day 14 of aging (Supplemental Table C.4). The disparity in degradation partners of myofibril and energy generating proteins could also be attributed to the influence of muscle pH on the stability of protein complexes. However, degradation of myofibrillar proteins can promote meat tenderness. Previous studies also noted that high pH meats are more tender compared with low pH counterparts (Cônsolo et al., 2020; Huff-Lonergan et al., 1996; Silva et al., 1999; Yu & Lee, 1986). This is attributed to the increased activity of neutral muscle proteolytic machinery such as

calpains and calcium-dependent protease at high muscle pH (Yu & Lee, 1986). However, the implication of aging induced changes in peptide profiles on muscle color in dark-cutting beef are yet to be described.

The evaluation of the generated non-specific peptides suggests that proteolysis in dark-cutting beef could be mainly mediated through N-termini cleavages. Our data showed that the majority of the quantified peptides were derived from the protein N terminus (Supplemental Figure C.6a). A previous study also noted that proteolysis alters the protein sequence resulting in neo-N termini (Lange et al., 2014). However, in some cases several proteins are translated with an N-terminal degradation signal that is stabilized through protein-protein interactions and chaperone mediated folding mechanism (Lange et al., 2014; Varshavsky, 2011). Thus, the greater number of N-termini semi-specific peptides in dark-cutting beef suggests a greater abundance of unstable and misfolded proteins in dark-cutting beef. These, in-turn could display their N-terminus and thus become easily degraded, contributing to more N-termi peptides. This, in part, could explain the greater abundance of heat shock protein HSPB1observed in dark-cutting beef at day 7 of postmortem wet-aging (Supplemental Figure C.5b). However, selective enrichment of N-terminal peptides will be necessary for accurate identification of protein N-termini and proteolytic cleavage sites in aged dark-cutting beef.

(iii) The metabolites profiles observed in dark-cutting compared with normal-pH beef during postmortem wet-aging also support arguments for enhanced proteolytic degradation in dark-cutting beef. Our results showed consistent changes in metabolite profiles reported in postmortem aged meats (Kim et al., 2016; Ma et al., 2017). Among

the differentially abundant metabolites, free amino acids such as valine, threonine, isoleucine, and leucine were up-regulated in dark-cutting beef muscle (Supplemental Figure C.3). Therefore, up-regulation of these metabolites suggests defective down-stream processes of branched-chain amino acid stimulated protein expression (Wang & Guo, 2013). On the other hand, up-regulation of threonine and valine could be associated with aging induced activation of the TOR/S6K signaling (Cao et al., 2019; Kim & Guan, 2019; Saxton & Sabatini, 2017). In addition, the increase in free amino acids concedes with greater expression of amino acid transferases proteins (GOT1, GOT2; Figure 4e).

Although the greater levels of free amino acids in dark-cutting beef might suggest enhanced protein synthetic mechanisms, we speculate that the changes in metabolites expressions during postmortem wet-aging in dark-cutting beef do not result from active gene programming but could rather be due to limitations in the homeostatic balance as well as the aging induced changes in access to substrates.

The down-regulation of glycogenolytic metabolites including glucose, fructose, glucose-1, and 6-phosphate (Figure 3c and Supplemental Figure C.4) coupled with nucleotides such as adenine and cystidine-5-monophosphate (Supplemental Figure C.2) in dark-cutting beef at 7 and 14 days of postmortem wet-aging reflect on the aging induced alterations in the muscle's capacity to generate energy. This can also be attributed to decreased glycogen hydrolysis and low glycogen levels reported in dark-cutting beef muscles (Cônsolo et al., 2021; Gagaoua et al., 2021; Kiyimba et al., 2021; Sentandreu et al., 2021). However, metabolites of the TCA cycle, nucleotide metabolites, and several energy metabolic proteins (Figure 4d and Supplemental Figure C.1-3) were up-regulated in dark-cutting beef muscles during postmortem wet-aging. The exact

explanation for these changes is not clear but we could speculate that the prevalence of oxidative stress in aged dark-cutting muscles could trigger energy adaptation mechanisms necessary to combat the stressors.

Conclusions

In this study, we characterized postmortem wet-aging protein and metabolite profiles of dark-cutting beef and define the mechanism/pathways regulating muscle proteolysis. Our results showed that postmortem wet-aging induce muscle-specific changes in protein and metabolite profiles in dark-cutting relative to normal-pH beef. In addition, dark-cutting beef showed enhanced proteolytic degradation by day 7 mediated by ubiquitin-independent protein degradation via the 20S proteasome complex. Therefore, the alterations in protein and metabolite profiles of dark-cutting beef support the aging induced phenotypic changes, including modifications in energy metabolism and muscle structure. Thus, this study provides molecular-level insights to explain the observed muscle phenotypic changes in postmortem wet-aged dark-cutting beef.

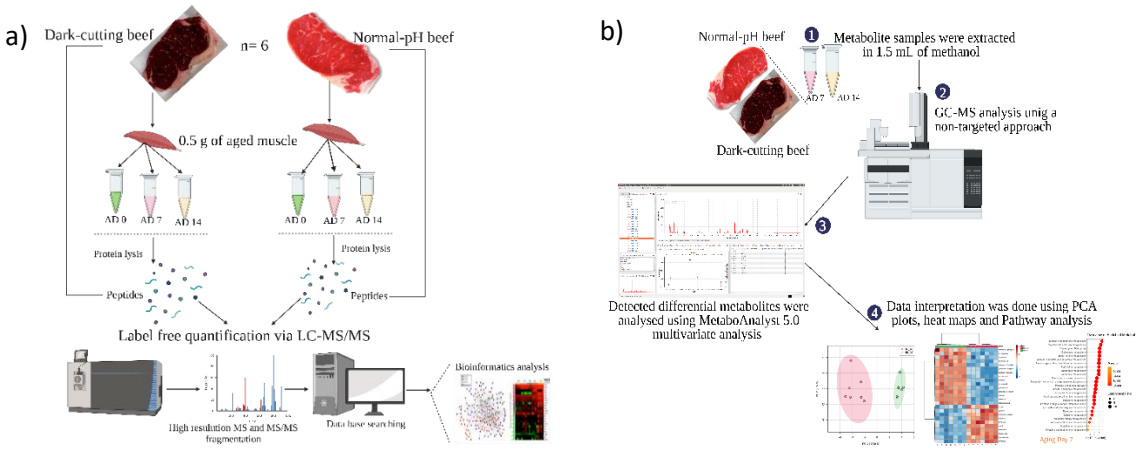

Figure 1: (a) Schematic of proteomics label free LC-MS/MS quantification workflow. (b) Schematic of metabolomics non-targeted GC-MS/MS profiling work flow of postmortem aged dark-cutting and normal-pH beef. The proteomics and metabolomics samples were extracted as described in the methods. 0.5 g *longissimus lumburum* muscle samples from n = 6 dark-cutting and normal-pH beef postmortem aged at 0, 7, and 14 days were utilized for proteomics analysis while samples aged for 7, and 14 days were used for metabolomics analyses.

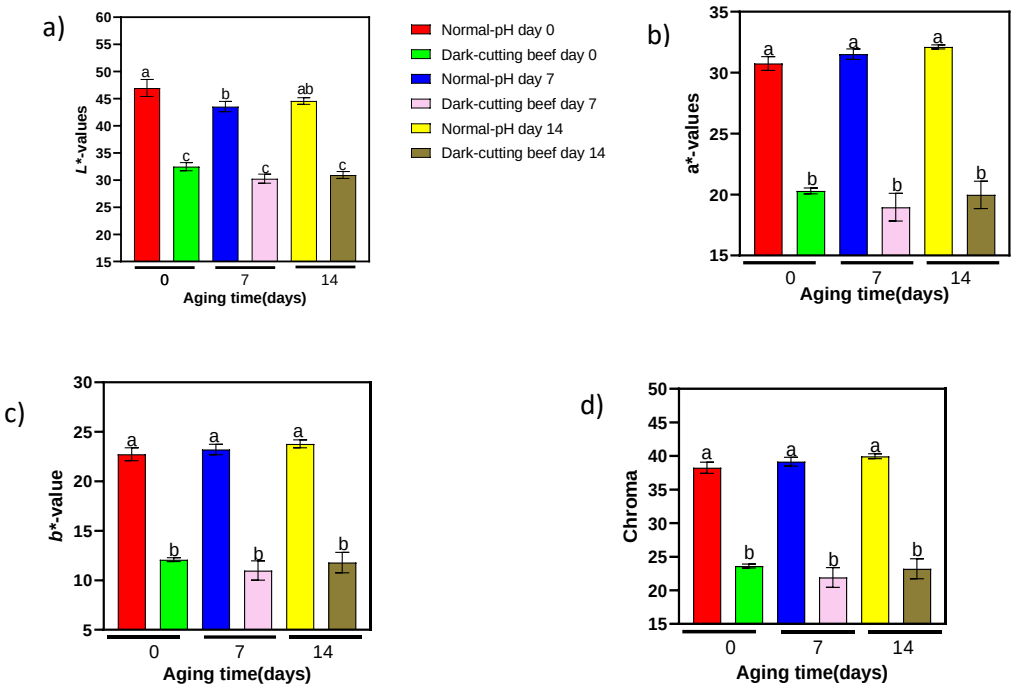

Figure 2: Effects of postmortem wet-aging on surface properties of dark-cutting and normal-pH beef.

Muscle surface color characteristics various at of postmortem aging days (0, 7, and 14 days) were determined by measuring (a-c) *L**-, *a**-, and *b**-values and (d) Chroma-values using a hunter lab mini scan as described in the methods. The error bars represent standard error of mean. The least square means with different letters are significantly different ($P < 0.05$, $n = 6$).

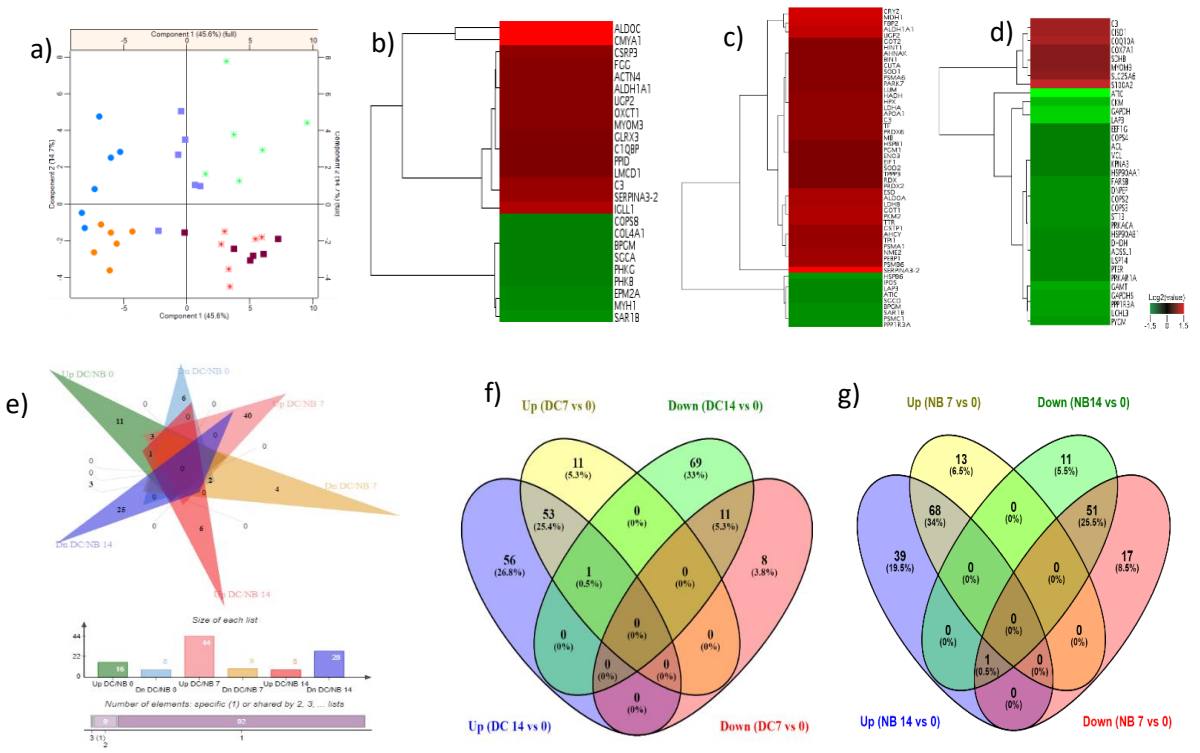

Figure 3: Mapping postmortem aging related changes in protein profiles of dark-cutting and normal-pH beef. (a) Venn diagrams of differentially abundant proteins in dark-cutting and normal-pH beef identified at various aging periods (0, 7, and 14 days of storage). (b) Principal component analysis plot (PCA) of quantified at total protein level in dark-cutting and normal-pH beef. Blue and orange dots represent protein changes at day 0, purple and brown triangles represent protein changes at aging day 7, and green and red stars represent protein changes at aging day 14 in dark-cutting and normal-pH beef respectively. (c) Hierarchical clustering analysis of significantly up-regulated (indicated in red) and down-regulated proteins (indicated in green) with greater than 1.5 fold in dark-cutting and normal-pH beef proteasomes during aging from 0-14 days. Protein expression changes in dark-cutting beef compared to normal-pH beef identified differentially expressed were compared at different aging time in dark-cutting compared with normal-pH beef.

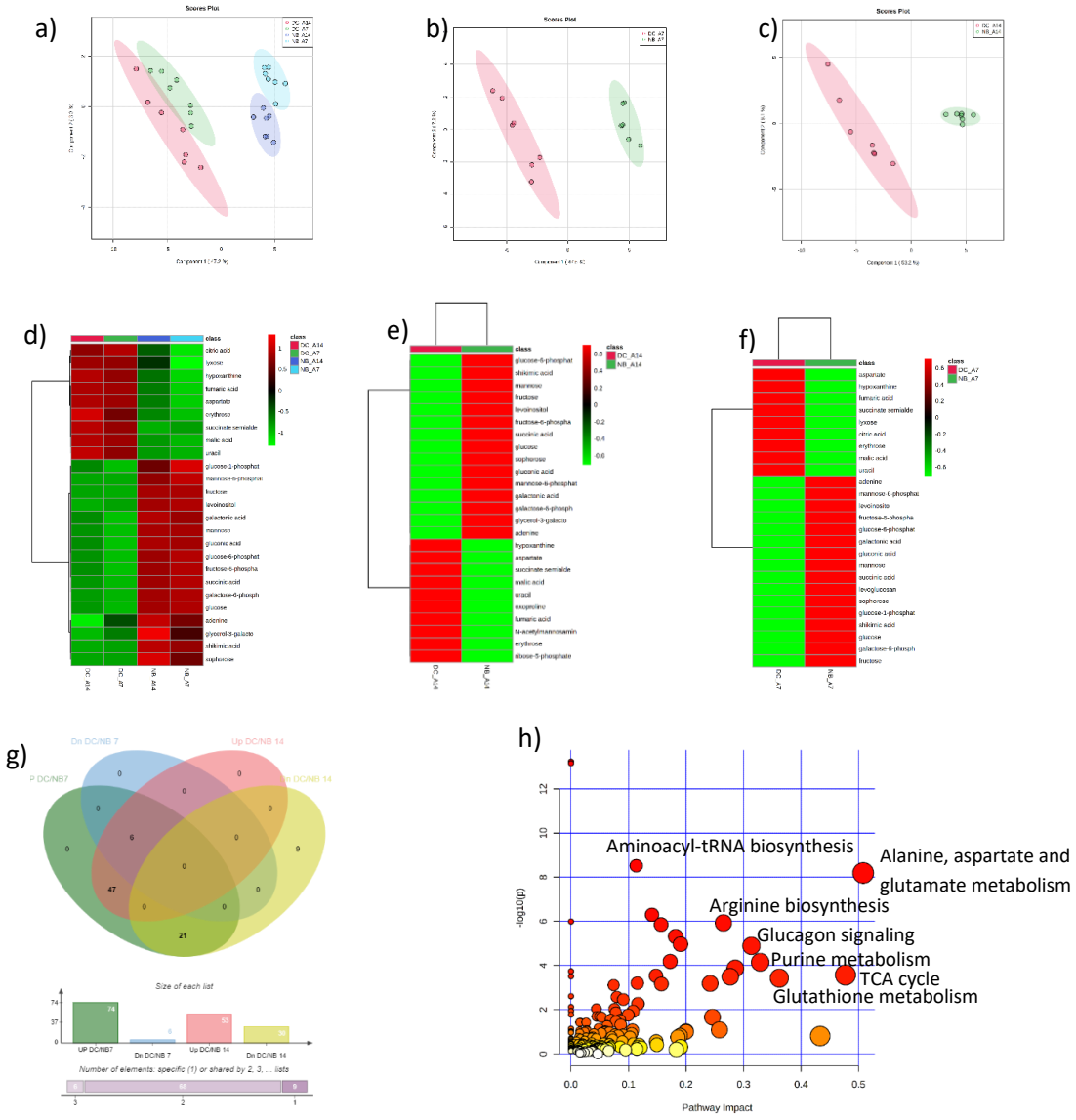

Figure 4: Non-targeted metabolomics profiling under postmortem wet ageing reveals distict aging induced metabolite signatures in dark-cutting compared with normal-pH beef. (a-c) Partial least squares-discrimianative anlysis (PLS-DA) of (a) all samples in dark-cutting and normal-pH beef at day 7 and 14 of postmortem storage, (b-c) samples for only 7 and 14 days of storage, respectively. (d-f) Heatmaps of significantly differentially abundant metabolites ($p < 0.05$) with greater than 1.5 fold change in dark-cutting and normal-pH beef at each respective postmortme aging period. (g) Venn diagram analysis showing the distribution of the significantly up- and down-regulated metabolites at each respective postmortem aging period. (h) Joint pathway enrichment analysis of proteins and metabolites at aging day 14.

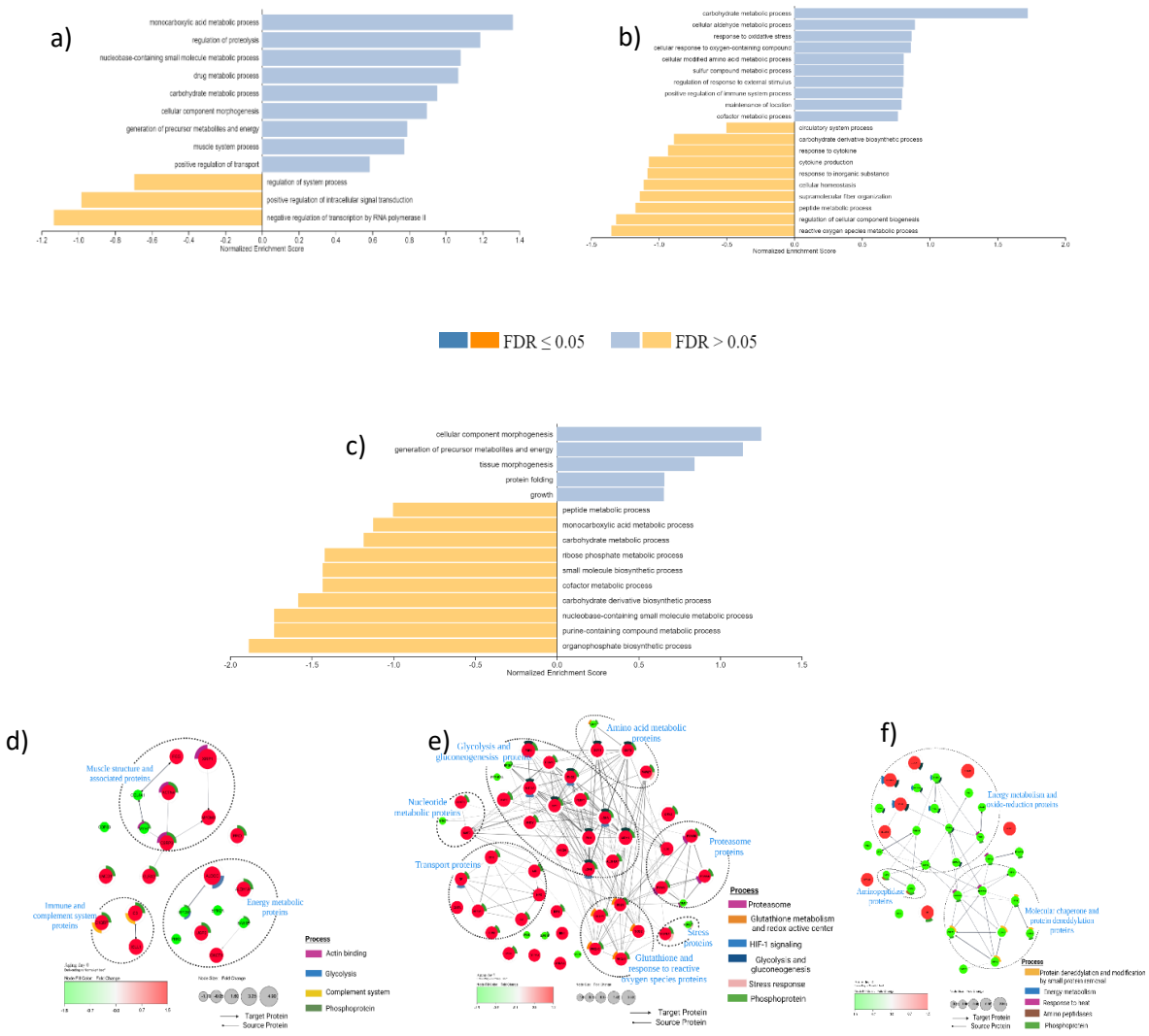

Figure 5: Functional characterization and protein-protein interaction networks networks of differentially abundant proteins in dark-cutting and normal-pH beef during postmortem aging at 0, 7, and 14 days. (a-c) Gene Set Enrichment analysis of differentially expressed proteins in dark-cutting vs normal-pH beef at 0, 7, and 14 days of postmortem aging. (d-f) Protein-protein interaction networks of differentially expressed proteins in dark-cutting vs normal-pH beef at 0, 7, and 14 days of postmortem aging analyzed by String-DB plug-in in Cytoscape The strong protein interactions are indicated by thicker lines. The arrows show the source and target of interaction. Green color represents down-regulation and red color represents up-regulation.

CHAPTER VI

EFFECTS OF GLYCOGEN SUPPLEMENTATION ON MUSCLE pH DECLINE, MYOGLOBIN OXIDATION, AND ENZYME ACTIVITIES IN DARK-CUTTING BEEF *LONGISSIMUS LUMBURUM* MUSCLES

In preparation for submission: Meat and Muscle Biology

Abstract

Glycogen metabolism is important in postmortem muscle acidification, mainly through the production of lactic acid. The occurrence of dark-cutting phenotypes in beef is associated with depleted muscle glycogen pre-slaughter. Previous research investigated the effects of supplementing excess glycogen to pork, lamb, chicken, and turkey normal-pH muscles. However, limited studies have evaluated the impact of supplementing glycogen to dark-cutting beef muscles. Therefore, the effects of low glycogen (2.5-, 5-, and 10- mM) supplementation on muscle pH decline, glycogenolytic and energy-sensing enzyme activities, and myoglobin oxidation were monitored at 1 and 24 h. One gram of (n = 6) normal-pH and one gram of (n = 6) dark-cutting beef *longissimus lumborum* muscles were incubated separately in 1 mL of an anaerobic glycolysis buffer at room temperature with or without 10 mM glycogen. Furthermore, muscle pH decline and myoglobin oxidation were monitored with

the addition of mitochondrial inhibitors at complex I, IV, and V. The results showed that supplementing glycogen reduced muscle pH ($P = 0.001$) in treated samples compared with control groups but had no effect on myoglobin oxidation after 1 and 24 h of incubation ($P > 0.05$). Glycogen phosphorylase and lactate dehydrogenase activity were increased ($P < 0.05$) by glycogen supplementation. Furthermore, addition of mitochondrial inhibitors to 10 mM glycogen-supplemented dark-cutting beef muscles significantly lowered pH values by 24 h similar to values observed in intact normal-pH beef muscles. These results showed that in-vitro glycogen supplementation at lower concentration can restore postmortem pH decline in dark-cutting muscles. Hence, the inherently low substrate levels in dark-cutting beef can regulate pH decline.

Key words: Dark-cutting beef, Glycogen metabolism, Muscle pH decline, mitochondria

Introduction

Consumers perception of meat and meat products is a key determinant of meat value. Meat consumers consider the bright-red color of beef as an indicator of freshness and wholesomeness (Boykin et al., 2017; Ramanathanet al., 2020a; Salim et al., 2019; Sammel & Claus, 2003; Troy & Kerry, 2010). However, in cases of a color deviation, packers discount beef during grading. While the occurrence of dark-cutting beef has decreased through improved farm management practices, the molecular and mechanistic basis for the occurrence is still unknown.

The development of color in beef is regulated by the rate and extent of postmortem pH decline. Thus, the current biochemical evidence suggests that insufficient glycogen levels due to pre-slaughter stress in dark-cutting beef muscles contribute to abnormal postmortem muscle pH in excess of 5.8 (Fuente-García et al., 2021; Holdstock et al., 2014; Kiyimba et al., 2021; Mahmood et al., 2018; Poleti et al., 2018; Roy et al., 2022). The high postmortem muscle pH contributes to muscle darkening via (i) sustaining mitochondrial respiration postmortem, which increases the muscles' oxygen consumption while decreasing oxygen available to bind myoglobin (Ashmore et al., 1972; Mancini et al., 2018; McKeith et al., 2016; Ramanathan et al., 2009; Tang, et al., 2005); (ii) the greater than normal muscle pH also influences myofibril shrinkage by affecting the water held within the muscle reducing the capacity of the muscles to reflect light (AMSA, 2012; Apple et al., 2011; Sawyer et al., 2009) therefore, dark-cutting beef appears dark.

Glycogen is a branched polymer of glucosyl residues which is rapidly degraded to generate glucose-1-phosphate during glycolysis (Roach, 2013). In postmortem muscles,

glycogen is mobilized into ATP and lactate, ultimately increasing H^+ ions that drive postmortem pH decline. Therefore, the amount of glycogen at slaughter regulates postmortem skeletal muscle metabolism mainly through the production of lactate (Chauhan et al., 2019; Immonen et al., 2000; Scheffler et al., 2011). However, there is a lack of a linear relationship between muscle glycogen content and ultimate muscle pH (England et al., 2016) suggesting that other energy pathways could be involved in muscle pH decline.

The effects of glycogen on postmortem muscle metabolism have been previously examined in-vitro by supplementing excess glycogen (at 30 mM) in pork (England et al., 2016) lamb, chicken, and turkey normal-pH muscles (Chauhan et al., 2019). Additionally, the impact of feeding high starch diets to increase glycogen content was evaluated (Rosenvold et al., 2001). However, there is a gap in our understanding of how glycogen contributes to muscle darkening in beef. Also, how the path of energy production from glycogen is initiated and maintained in dark-cutting beef is incompletely understood. In this study, we tested a model in which substrate inhibition mechanisms pre-slaughter regulate glycogen metabolism, and the impact on postmortem muscle metabolism in dark-cutting beef muscles. Our results show that in-vitro supplementation of low glycogen concentrations to dark-cutting muscles restores pH decline and increases the activity of enzymes involved in glycogen degradation and lactate formation.

Materials and methods

Samples collection and preparation

Longissimus lumborum muscles from six bright red normal-pH and six dark-cutting beef loins (Institutional Meat Purchasing Specification #180, NAMP, 2002; grain-finished, spray chilled) from A maturity carcasses were procured from a local facility at CreekStone Farms, Arkansa City, KS. Samples were transported to Oklahoma State University Food and Agricultural Product Center and fabricated into steaks 2.54 cm thick. The first half of the loin was used in measuring color and muscle biochemical properties. The last half of the loin was powdered in liquid nitrogen and immediately stored at -80 ^{o}C until further analyses.

Muscle color attributes and biochemical properties were determined following methods described by (English et al., 2016). Briefly, muscle color characteristics (*L**-, *a**-, *b**, chroma, and hue-values) were determined using a HunterLab MiniScan spectrophotometer. Muscle pH was determined using an Accumet 50 pH meter (Fisher Scientific, Fairlawn, NJ). The pH meter was calibrated with standard buffers at pH 4.0 and 7.0 and inserted into the meat at three different locations. The average pH of the steaks was measured and recorded.

Experimental setup

To simulate muscle glycolysis: 100 mg powdered *longissimus lumborum* muscles from 12 samples (n = 6 dark-cutting and n = 6 normal-pH beef) were homogenized and incubated in 1 mL of an anaerobic buffer (10 mM Na_2HPO_4, 5 mM $MgCl_2$, 60 mM KCl, 5 mM ATP, 0.5 mM ADP, 0.5 mM NAD +, 25 mM carnosine, 30 mM creatine and

10 mM sodium acetate; pH 7.4 with or without glycogen) according to England et al. (2016). Glycogen was supplemented at 0, 2.5 mM, 5 mM, and 10 mM. The controls consisted of normal-pH beef without glycogen as a negative control while dark-cutting beef without glycogen supplementation was used as a positive control. The treatments consisted of dark-cutting beef supplemented with glycogen at 2.5 mM, 5 mM, and 10 mM and normal-pH beef supplemented with 10 mM glycogen. The control and treated samples were incubated in separate vessels of 50 mL Corning Falcon canonical centrifuge tubes (Catlog No: 1443222 Fisher Scientific, PA) at room temperature (25 ºC). The tubes were closed with lids to simulate anaerobic conditions. Decline in pH, myoglobin oxidation, and enzyme activities were monitored at 1, 12, and 24 h of incubation.

Measurement of pH decline following glycogen supplementation

To determine the effect of glycogen supplementation on pH decline in dark-cutting muscle, samples were collected from the incubation vessel at 1, 12, and 24 h. Muscle homogenate were then diluted with buffer (25 mM sodium iodoacetate, 750 Mm KCl, pH 7.0) in a 4:1 dilution according to England et al., (2016). Samples were centrifuged at 13,000 x g for 5 min and the pH of the muscle homogenate was determined using an Acument 50 pH meter.

Determination of myoglobin oxidation

To determine the effect of glycogen supplementation on myoglobin stability, we measured the percentage of metmyoglobin formed following glycogen supplementation in treated compared with the control groups. Metmyoglobin was measured using a

spectrophotometric method by scanning absorption from 450 to 650 nm using a microplate reader (Spectra Max M3, Molecular Devices, San Jose, CA). Myoglobin oxidation after 1, 12, and 24 h of incubation in a glycolysis buffer was determined by measuring the wavelength maxima at 503, 557, and 582 nm, according to Tang et al. (2005).

Analysis of enzyme activities

To determine the effects of glycogen supplementation on activity of enzymes modulating energy metabolism and glycolysis, the activities of enzymes glycogen phosphorylase, lactate dehydrogenase, and adenosine monophosphate activated protein kinase (AMPK and phosphorylated AMPK, pAMPK) were determined using standard enzyme assay kits obtained from Abcam (Boston, MA). Aliquots of sample homogenates from controls (normal-pH beef and dark-cutting beef without glycogen supplementation) and treated samples (dark-cutting beef with 10 mM glycogen) at 1 and 24 h of incubation was used for this analysis.

Glycogen phosphorylase activity was determined using a colorimetric assay kit (Abcam, ab273271) following release of glucose-1-phosphate from glycogen. The optical density (OD) of the generated colored product was determined spectrophotometrically at 450 nm using a microplate reader (Spectra Max M3, Molecular Devices, San Jose, CA) according to the enzyme assay kit protocols. The slope of increase in OD at 450 nm of the standard curve was determined and used to determine glycogen phosphorylase activity. Lactate dehydrogenase activity was determined using a fluorometric assay kit (Abcam, ab197000) by monitoring fluorescence spectrophotometrically at Excitation

/Emission wavelengths of 535 and 587 nm, respectively, using (Spectra Max M3, Molecular Devices, San Jose, CA) according to the enzyme assay kit protocols.

The AMPK and pAMPK activity were determined using a sandwich in vitro enzyme-linked immunosorbent assay ELISA kit (Abcam, ab279734-phospho-AMPK alpha 1(S487) and total AMPK alpha 1). Control samples (normal-pH and dark-cutting beef) and dark-cutting beef treated with 10 mM glycogen at 1 and 24 h incubation were pipetted into a 96 well plate coated with anti-pan AMPK alpha 1 antibody. In selected wells, 100 µL of rabbit anti-phospho-AMPK alpha 1 (S487) antibody was added to detect phosphorylated AMPK alpha 1. The remaining wells were treated with 100 µL biotinylated anti-pan-AMPK alpha 1 antibody to detect pan AMPK alpha 1. The samples were then incubated for 2.5 h at room temperature. After, unbound antibody was washed away with 1X was buffer. 100 µL of HRP-conjugate anti-rabbit IgG or HRP-Streptavidin was pipetted to corresponding wells, incubated for 1 h and washed. After, 100 µL of TMB substrate solution was added and the samples were incubated for 30 min at room temperature in the dark with gentle shaking. Finally, 50 µL stop solution was added, and the intensity of the color was measured spectrophotometrically at 450 nm using a microplate reader (Spectra Max M3, Molecular device, San Jose, CA).

Effect of mitochondrial inhibitors on muscle glycolysis

In a separate experiment, the impact of mitochondrial respiratory capacity on muscle glycolysis and pH decline was evaluated. Mitochondrial inhibitors at complex I (2 µM rotenone), Complex IV (2 µM oligomycin), and complex V (1 mM potassium cyanide) was added to vessel of dark-cutting beef supplemented with 10 mM glycogen.

Muscle pH decline and metmyoglobin oxidation were monitored at 1, 12, and 24 h of incubation.

Statistical analysis

A completely randomized design with a factorial arrangement was used to evaluate the combined effects of glycogen supplementation on muscle pH decline, myoglobin oxidation and enzyme activities. The fixed effects/factors included glycogen, muscle type (dark-cutting vs normal-pH beef), incubation time, and their interactions. Overall, the experiment was replicated 6 times (n = 6). The enzyme activity experiment was replicated 5 times (n = 5), while AMPK and pAMPK activity study was replicated 3 times (n = 3). The data were analyzed using the Mixed Procedure of SAS (version 9.4, SAS Inst. Inc., Cary, NC). Least square means were separated using a pairwise t-test and were considered significant at $\alpha = 0.05$.

Results

Muscle biochemical and color characteristics

The results for muscle biochemical and color characteristics are presented in Figure 1. As expected, dark-cutting beef samples used in this study had lower *L**-, *a**-, and *b** values compared to normal-pH beef (Figure 1 a-c, $P < 0.05$). Our results are consistent with previous reports that found lower values in dark-cutting beef compared to normal-pH beef (Mahmood et al., 2017; Wills et al., 2017; Wulf et al., 2002). The *L**- values represent muscle lightness while low *a** values show that dark-cutting beef has low red intensity. Measurement of muscle pH also indicated that dark-cutting beef had a significantly greater muscle pH compared with normal-pH beef (Figure 1d). Thus, our

results confirmed that the dark-cutting muscles used in the current study met the benchmark characteristics of dark-cutting phenotypes reported in beef (Cônsolo et al., 2021; Fuente-Garcia et al., 2020; Ramanathan et al., 2020b).

Glycogen content drives postmortem muscle pH decline

To evaluate whether muscle glycogen is the limiting factor in driving postmortem pH decline in dark-cutting beef muscle, different levels of glycogen at 0, 2.5, 5, and 10 mM were supplemented to dark-cutting beef muscles homogenates using an in-vitro anaerobic glycolysis vessel. Compared to normal-pH beef (negative) and dark-cutting beef (positive) controls, in vitro glycogen supplementation at 2.5-, 5-, and 10 mM decreased ($P < 0.05$,) muscle pH (~ 10 %, Figure 2a) by 1 h of incubation. However, at 24 h of incubation, samples supplemented with 10 mM glycogen had the greatest decrease ($P < 0.05$) in muscle pH relative to 2.5 and 5 mM glycogen concentrations. Thus, these results suggest that in-vitro supplementation of glycogen at 10 mM restores pH decline in dark-cutting muscles.

To further evaluate the impact of mitochondrial capacity on glycolysis and muscle pH decline, mitochondrial inhibitors were added at different complexes (Complex I, IV, and V). The results revealed that inhibition of mitochondrial complexes led to an increase ($P < 0.05$) in pH decline (~ 15 %, Figure 2b) by 1 h of incubation. At 24 h of incubation, inhibition of Complex V with potassium cyanide (1 mM) decreased ($P< 0.05$) pH of the homogenate similar to values observed in intact normal-pH beef muscles (Figure 1d). Thus, these results suggest that inhibition of mitochondria limits the transport of

glycolytic end product pyruvate into the mitochondria for oxidation. Therefore, much of the pyruvate could be converted into lactate which results in greater pH decline.

Glycogen supplementation does not alter myoglobin oxidation

The effects of in-vitro glycogen supplementation on myoglobin oxidation was evaluated by measuring the percentage metmyoglobin formed in muscle homogenates collected from the chambers at 1, 12, and 24 h of incubation. As shown in Figure 3, compared with control groups, glycogen supplementation did not alter myoglobin oxidation ($P > 0.05$). However, as incubation time increased, samples incubated with glycogen showed a tendency for increased metmyoglobin formation compared to normal-pH beef controls. Accordingly, samples incubated in presence of mitochondrial inhibitors at complex V showed reduction in myoglobin oxidation ($P < 0.001$) at 1 h of incubation. However, as incubation time increased, metmyoglobin formation also increased.

Glycogen supplementation increases activity of enzymes involved in glycolysis but suppresses activity of energy sensing enzyme

Glycogen phosphorylase, an enzyme involved in glycogen mobilization and utilization showed greater activity in both dark-cutting beef control and muscle homogenates supplemented with 10 mM glycogen compared to normal-pH beef (Figure 4a). In addition, lactate dehydrogenase (LDH), an enzyme required for conversion of the glycolytic product pyruvate also showed more activity in dark-cutting beef supplemented with 10 mM glycogen compared to the positive and negative control groups (Figure 4b). These results are consistent with known role of LDH in diverting carbohydrate metabolites away from mitochondrial import and oxidation as part of glycolysis.

To evaluate the impact of glycogen supplementation on energy balance, we measured the adenosine monophosphate activated protein kinase (AMPK), and phosphorylated adenosine monophosphate activated protein kinase (pAMPK) activities using an ELISA assay. The results showed that the activity of AMPK was decreased ($P < 0.05$, Figure 4c) following glycogen supplementation and with increasing incubation time from 1 to 24 h. However, dark-cutting control group without glycogen had slightly greater AMPK activity compared with normal-pH beef at 1 and 24 h of incubation (Figure 4c). The activity of the phosphorylated form of the enzyme (pAMPK) did not show difference between glycogen supplemented dark-cutting muscles compared with control groups (Figure 4d).

Discussion

During postmortem glycolysis, skeletal muscles mobilize glycogen into ATP and lactate ultimately increasing H^+ ions that drive postmortem pH decline. However, in dark-cutting beef, chronic stress before slaughter reduces muscle glycogen and the capacity to accumulate lactic acid contributing to greater than normal-muscle pH in excess of 5.8 (Fuente-García et al., 2021; Kiyimba et al., 2021; Mahmood et al., 2018; Poleti et al., 2018; Ponnampalam et al., 2017). In this study, we proposed a model that substrate inhibition mechanisms regulate muscle pH decline and overall postmortem metabolism in dark-cutting beef muscles. In support of this model, we show that dark-cutting beef muscle homogenates supplemented with 10 mM glycogen (Figure 2a) in an anaerobic glycolysis buffer restores muscle decline in dark-cutting beef.

The decline in pH after glycogen supplementation suggest that glycogen is a limiting factor in dark-cutting beef postmortem pH decline. Consistent with this observation, muscle pH decline increased with increase in glycogen concentrations (Figure 2a). Therefore, the low abundance of several enzymes involved in glycogen mobilization and utilization (Kiyimba et al., 2021; Fuente-García et al., 2021; Mahmood et al., 2018) in dark-cutting beef could be associated with limited substarte levels. However, our finding is inconsistent with previous studies in pork, lamb, and chicken normal-pH skeletal muscles where glycolysis, glycogenosis, and pH decline was stopped prematurely in oxidative muscles. Thus, this suggests that glycogen was not the limiting factor but rather some other factors limited pH decline (Chauhan et al., 2019; England et al., 2016). The discrepancy in the results between studies could be also associated with difference in glycogen concentrations used in the studies. In the current study, low glycogen levels at 2.5-, 5-, and 10 mM were used compared with 30 mM glycogen in previous studies. We speculate that excess glycogen supplemented in previous studies could have contributed to more substrate availability inhibiting the activity of enzymes involved in glycolysis, glycogenosis, and pH decline.

The increase in glycogen phosphorylase activity after glycogen supplementation in dark-cutting beef support arguments for presence of substrate inhibition mechanisms in dark-cutting beef. Glycogen phosphorylase catalyzes the rate-limiting step in glycogen degradation pathways by creating phosphoroelastic cleavages in glycogen to produce glucose-1-phosphate (Hespel & Richter, 1992; Jensen & Richter, 2012; Komoda & Matsunaga, 2015; Roach, 2005). Therefore, the high glycogen concentration following supplementation in dark-cutting muscles arguments net glycogen breakdown resulting

from glycogen phosphorylase activation by glycogen (Figure 4a). Thus, the increased glycogen breakdown might stimulate more glycolysis leading to a greater pH decline in supplemented dark-cutting muscles compared to controls.

Glycolyis and mitochondrial respiration are tightly coupled processes. Therefore we proposed that inhibition of mitochondrial at complex I, IV, and V could arrest glycolysis and terminated pH decline. However, dark-cutting beef muscles suplemented with glycogen and mitochondrial inhibitors decreased muscle pH (Figure 2b). Although we did not measure the mitochondrial pyruvate carirrier protein activities, our results show that the decrease in muscle pH following mitochondria ihibition could be associated with decrease in transport of glycolysis end product pyruvate into the mitochondrial for oxidation. Thus, this increased the abundance of pyruvate available for conversion into lactate. Consistent with this observation, lactate dehydrogenase activity, an enzyme involved in diverting carbohydrate metabolites away from mitochondrial import and oxidation as part of glycolysis (Feron, 2009; Souto-Carneiro et al., 2020), was increased with glycogen supplementation (Figure 4b). Therefore, our data shows that limiting the mitochondrial activity coupled with glycogen supplementation in-vitro is sufficient to stimulate lactate dehydrogenase activity and might drive muscle pH decline in dark-cutting beef muscles. Therefore, the greater mitochondrial respiratory capacity in dark-cutting beef (Ashmore et al., 1972; Kiyimba et al., 2022; McKeith et al., 2016) coupled with the low glycogen abundance in-vivo limits the capacity of the muscle to accumulate lactate contributing to greater than normal muscle pH.

Although muscle pH decline follows glycolysis and lactic acid accumulation, postmortem metabolism utilizes other energy pathways mediated by adenylate kinases

(Scheffler et al., 2011). Therefore, we hypothesized that in an attempt to regulate energy balance, dark-cutting beef muscles might respond by activating the adenylate kinase catalyzed reaction networks. However, evaluation of AMPK activity showed that AMPK activity was slightly increased in dark-cutting compared to normal-pH beef muscles while the phosphorylated AMPK (pAMPK) did not show any difference in activity in dark-cutting muscles compared with normal-pH beef muscles (Figure 4a and 4d). Additionally, supplementation of glycogen reduced AMPK activity but not the phosphorylated AMPK (Figure 4 c and d). AMPK is a regulator of energy balance and is activated by metabolic processes that inhibit ATP synthesis or accelerates ATP consumption (Hardie, 2007; Kahn et al., 2005; McBride et al., 2009). Therefore, the difference in activity of AMPK could be associated differences in substrate sensitivity between normal-pH and dark-cutting beef muscles. Dark-cutting muscles have greater abundance of oxidative fibers (Ramanathan et al., 2020b; Roy et al., 2022). Thus, the distinct muscle fibers types between normal-pH and dark-cutting beef muscles markedly might contribute to different sensitivity to energy balance.

The decrease in AMPK activity following glycogen supplementation could be attributed to the inhibition of AMPK enzyme by glycogen. Glycogen is a known inhibitor of AMPK and glycogen loading in skeletal muscle was shown to suppress activation of AMPK when glycogen binds at the β subunit of the glycogen binding domain (Derave et al., 2000; Polekhina et al., 2003; Wojtaszewski et al., 2003). Therefore, the increase in glycogen abundance in supplemented dark-cutting muscles could have resulted into glycogen binding at the AMPK glycogen binding domain.

Alternatively, glycogen supplementation might have increased ATP levels due to enhanced glycolysis. The increase in ATP levels inhibits AMPK activity while high levels of AMP stimulates AMPK activity allosterically (Derave et al., 2000; Kahn et al., 2005; Wojtaszewski et al., 2003). Therefore, this would suggest that fuel-dependent mechanisms independent of energy status in dark-cutting beef may regulate AMPK signaling. Hence, the idea that fluctuations in energy levels pre-slaughter might contribute to the activation of the adenylate kinase catalyzed reaction networks was not supported by our findings.

Conclusion

In this study, we demonstrated that low substrate levels regulate dark-cutting beef muscle metabolism. Our results showed that supplementing dark-cutting beef with 10 mM glycogen in-vitro restores muscle pH decline through increased activity of enzymes involved in glycogen breakdown and lactate formation. However, glycogen supplementation had no effect on myoglobin oxidation after 1 and 24 h of incubation. We further showed that inhibiting the mitochondrial respiratory capacity at complex I, IV, and V increased pH decline in dark-cutting muscles and this is attributed to accumulation of the glycolytic substrate pyruvate available for conversion into lactate. Additionally, our data suggest that fluctuations in energy levels pre-slaughter might contribute less to the activation of the adenylate kinase catalyzed reaction networks in dark-cutting muscles.

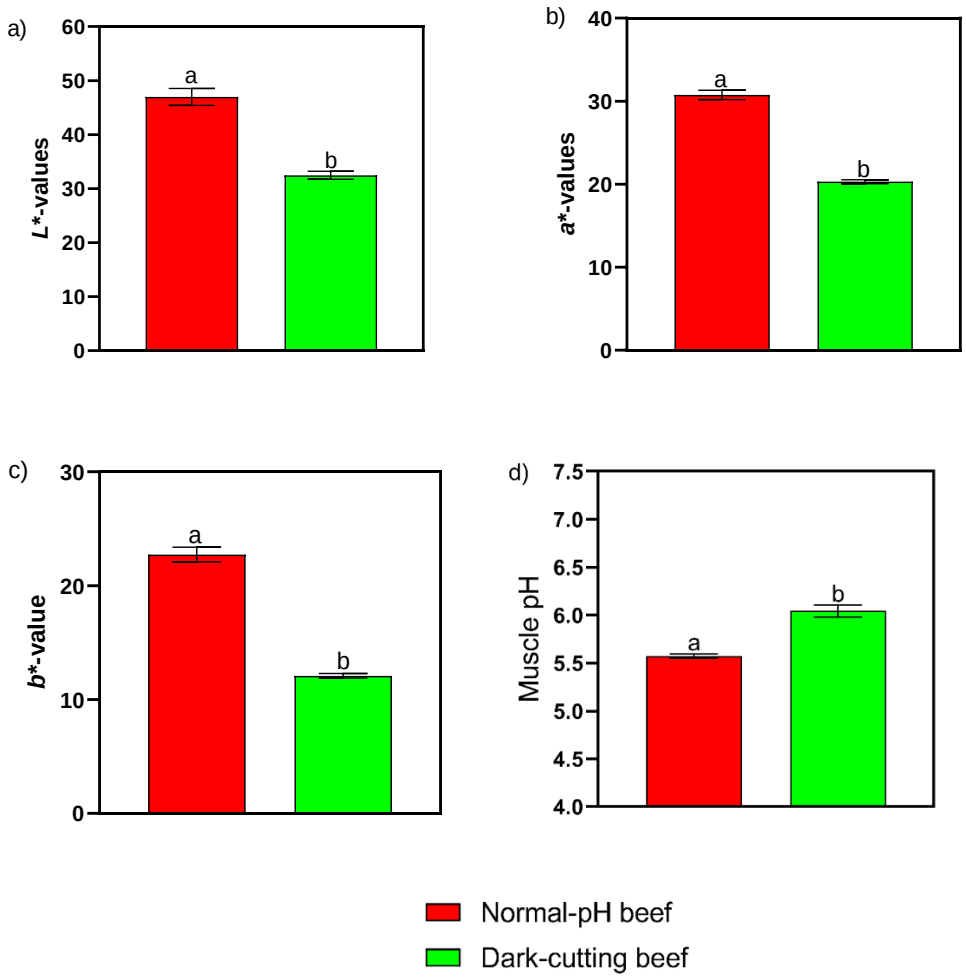

Figure 1: Muscle surface color characteristics and muscle pH values of dark-cutting and normal-pH beef. (a-c) *L**-, *a**, and *b**-values, (d) muscle pH values of dark-cutting compared with normal-pH beef were quantified as described in the Methods. The error bars represent standard error of mean (n = 6). The bars with different letters represents least square means that are different at $P < 0.05$.

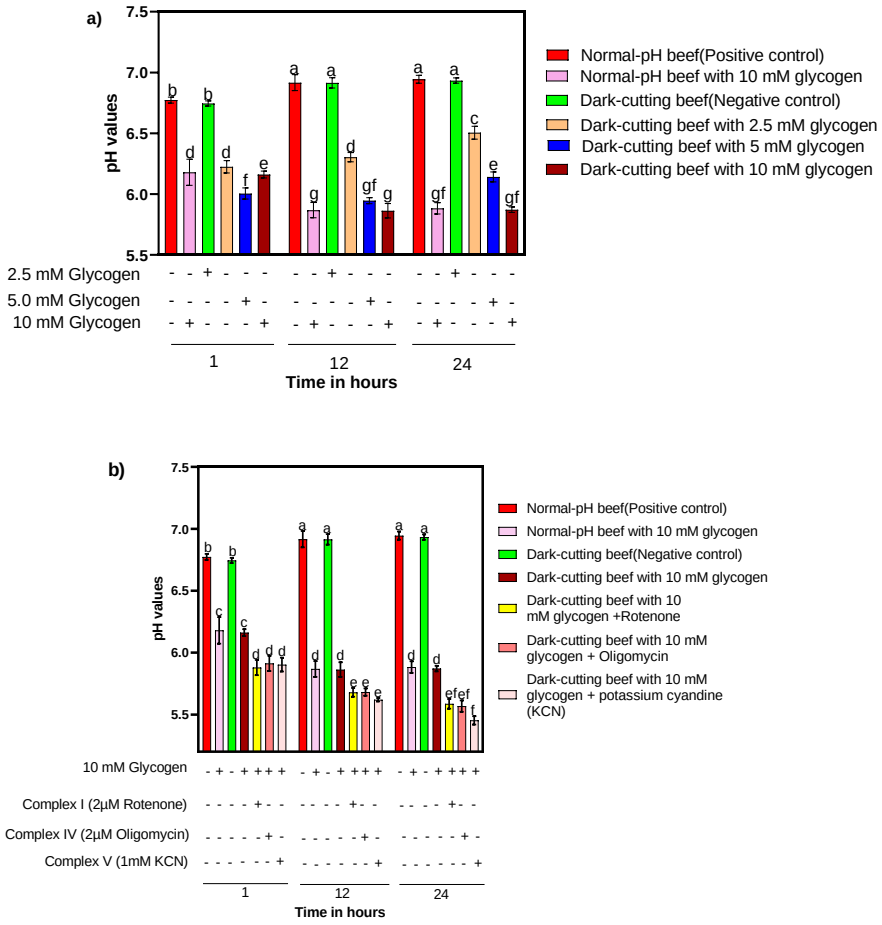

Figure 2: Effect of in-vitro glycogen supplementation on muscle pH levels in dark-cutting beef muscle homogenate. (a) Changes in muscle pH levels following addition of glycogen at 2.5 mM, 5.0 mM, and 10 mM glycogen. (b) Effect of mitochondrial inhibitors on muscle homogenate pH decline in-vitro. Inhibition of the mitochondria was archived by adding 2 µM Rotenone (Complex I), 2 µM Oligomycin (IV) and 1mM potassium cyanide (Complex V). Muscle homogenate pH decline was monitored as described in the Methods. The error bars represent standard error of mean (n = 6). The bars with different letters represents least square means that are different at $P < 0.05$.

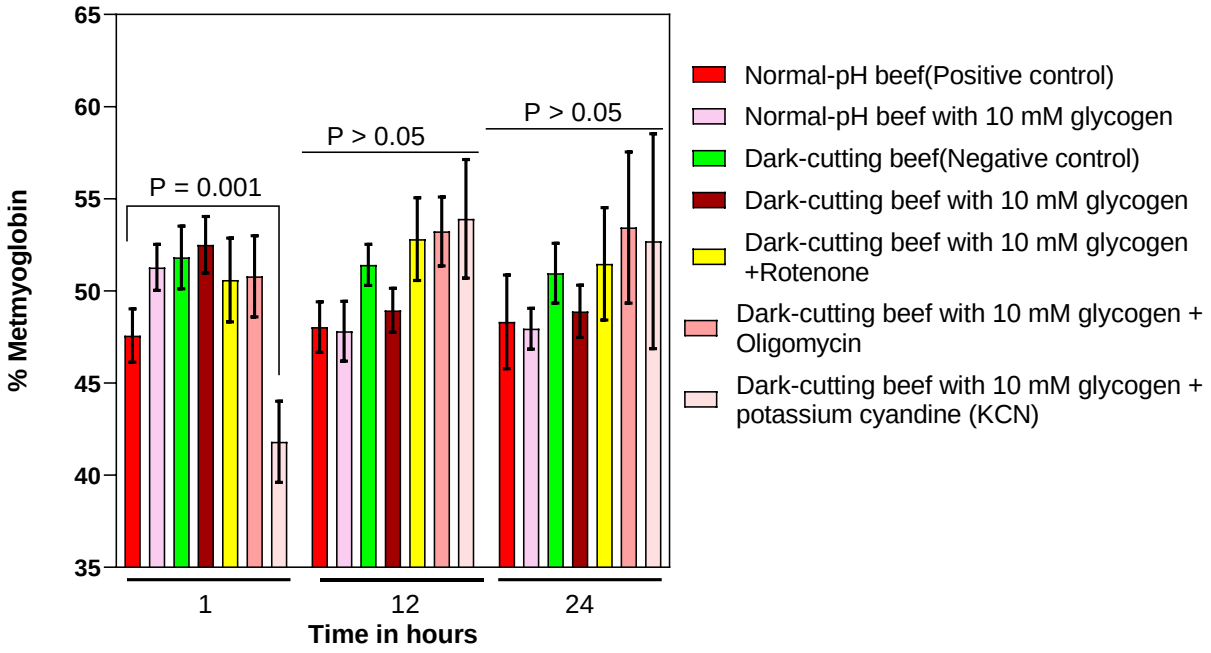

Figure 3: Effect of glycogen supplementation and mitochondria inhibition on myoglobin oxidation.

The rate of myoglobin oxidation was determined as percentage metmyoglobin formed after 1, 12, and 24 h of incubation in an aerobic glycolysis buffer. Myoglobin oxidation was determined by measuring the wavelength maxima at 503, 557, and 582 nm as described in the Methods.

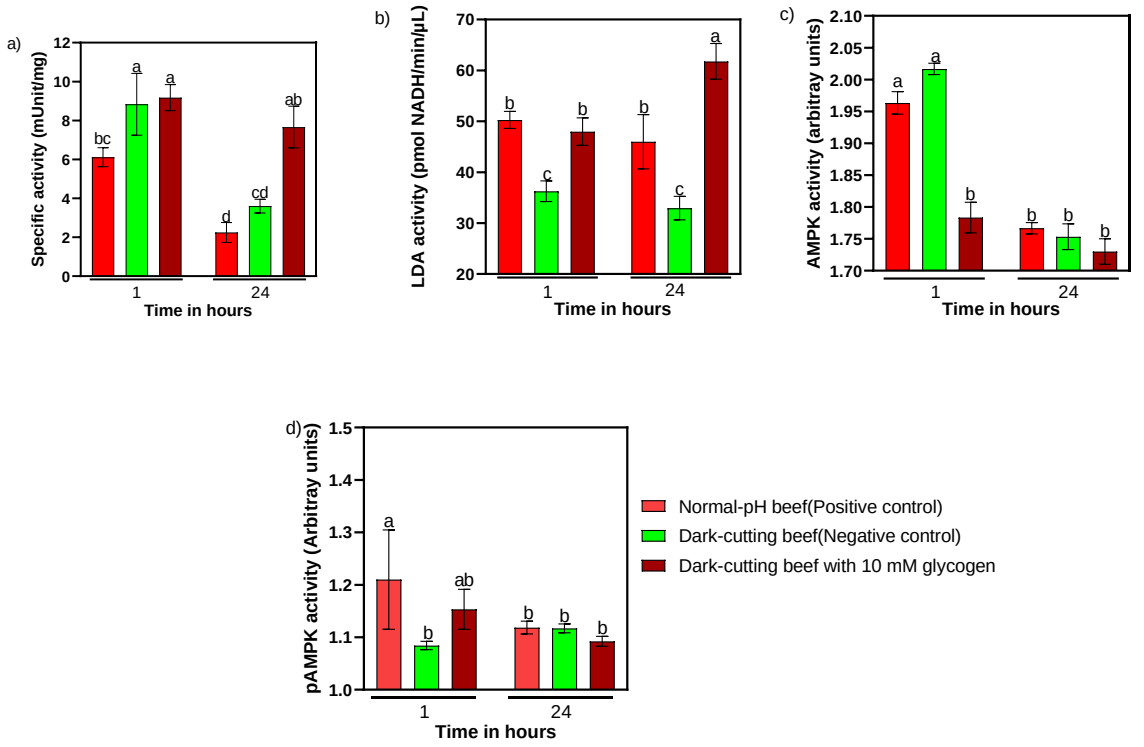

Figure 4: Effect of glycogen supplementation on activity of enzymes involved in glycolysis and energy metabolism. (a) glycogen phosphorylase activity, (b) lactate dehydrogenase activity, (c) adenosine monophosphate protein kinase activity (AMPK), and (d) phosphorylated adenosine monophosphate protein kinase activity (pAMPK). The enzyme activities were measured using standard assay kits as described in the methods. The bars with different letters represents least square means that are different at $P < 0.05$.

REFERENCES

Abdelnour, S. A., Abd El-Hack, M. E., Khafaga, A. F., Arif, M., Taha, A. E., & Noreldin, A. E. (2019). Stress biomarkers and proteomics alteration to thermal stress in ruminants: A review. *Journal of Thermal Biology*, *79*, 120–134. https://doi.org/10.1016/J.JTHERBIO.2018.12.013

AMSA. (2012). Meat color measurement guidelines. In American Meat Science Association (Ed.), *American Meat Science Association*. https://doi.org/10.1007/s11786-018-0341-9

Anand, R., Langer, T., & Baker, M. J. (2013). Proteolytic control of mitochondrial function and morphogenesis. *Biochimica et Biophysica Acta (BBA) - Molecular Cell Research*, *1833*(1), 195–204. https://doi.org/10.1016/J.BBAMCR.2012.06.025

Anderson, S., Collaborators:, Aldana, S., Beggs, M., Birkey, J., Conquest, A., Conway, R., Hemminger, T., Herrick, J., Hurley, C., Ionita, C., Longbind, J., McMaignal, S., Milu, A., Mitchell, T., Nanke, K., Perez, A., Phelps, M., Reitz, J., Zerr, S. (2007). Determination of Fat,Moisture, and Protein in Meat and Meat Products by Using the FOSS FoodScan Near-Infrared Spectrophotometer with FOSS Artificial Neural Network Calibration Model and Associated Database: Collaborative Study. *Journal of AOAC international*, *90*(4), 1073–1083. https://doi.org/10.1093/JAOAC/90.4.1073

Apaoblaza, A., Gerrard, S. D., Matarneh, S. K., Wicks, J. C., Kirkpatrick, L., England, E. M., Scheffler, T. L., Duckett, S. K., Shi, H., Silva, S. L., Grant, A. L., & Gerrard, D. E. (2020). Muscle from grass- and grain-fed cattle differs energetically. *Meat Science*, *161*, 107996. https://doi.org/10.1016/J.MEATSCI.2019.107996 .

Apple, J. K., Sawyer, J. T., Meullenet, J. F., Yancey, J. W. S., & Wharton, M. D. (2011). Lactic acid enhancement can improve the fresh and cooked color of dark-cutting beef. *Journal of Animal Science*, *89*(12), 4207–4220. https://doi.org/10.2527/jas.2011-4147

Ashmore, C. R., Doerr, L., Foster, G., & Carroll, F. (1971). Respiration of mitochondria isolated from dark-cutting beef. *Journal of Animal Science*, *33*(3), 574–577. https://doi.org/10.2527/jas1971.333574x

Ashmore, C. R., Parker, W., & Doerr, L. (1972). Respiration of Mitochondria Isolated from Dark-Cutting Beef: Postmortem Changes. *Journal of Animal Science*, *34*(1), 46–48. https://doi.org/10.2527/jas1972.34146x

Baker, E. C., Cilkiz, K. Z., Riggs, P. K., Littlejohn, B. P., Long, C. R., Welsh, T. H., Randel, R. D., & Riley, D. G. (2020). Effect of prenatal transportation stress on DNA methylation in Brahman heifers. *Livestock Science*, *240*, 104116. https://doi.org/10.1016/j.livsci.2020.104116

Barrès, R., Osler, M. E., Yan, J., Rune, A., Fritz, T., Caidahl, K., Krook, A., & Zierath, J. R. (2009). Non-CpG Methylation of the PGC-1α Promoter through DNMT3B Controls Mitochondrial Density. *Cell Metabolism*, *10*(3), 189–198. https://doi.org/10.1016/J.CMET.2009.07.011

Baughman, J. M., Perocchi, F., Girgis, H. S., Plovanich, M., Belcher-Timme, C. A., Sancak, Y., Bao, X. R., Strittmatter, L., Goldberger, O., Bogorad, R. L., Koteliansky, V., & Mootha, V. K. (2011). Integrative genomics identifies MCU as an essential component of the mitochondrial calcium uniporter. *Nature 2011 476:7360*, *476*(7360), 341–345. https://doi.org/10.1038/nature10234

Baumgard, L. H., & Rhoads, R. P. (2013). Effects of Heat Stress on Postabsorptive Metabolism and Energetics. *Https://Doi.Org/10.1146/Annurev-Animal-031412-103644*, *1*, 311–337. https://doi.org/10.1146/ANNUREV-ANIMAL-031412-103644

Bell, E. L., Emerling, B. M., & Chandel, N. S. (2005). Mitochondrial regulation of oxygen sensing. In *Mitochondrion* (Vol. 5, Issue 5, pp. 322–332). https://doi.org/10.1016/j.mito.2005.06.005

Bendall, J. R. (1979). Relations between muscle pH and important biochemical parameters during the postmortem changes in mammalian muscles. *Meat Science*, *3*(2), 143–157. https://doi.org/10.1016/0309-1740(79)90016-0

Bereiter-Hahn, J. (1990). Behavior of Mitochondria in the Living Cell. *International Review of Cytology*, *122*(C), 1–63. https://doi.org/10.1016/S0074-7696(08)61205-X

Bernardi, P., & Di Lisa, F. (2015). The mitochondrial permeability transition pore: Molecular nature and role as a target in cardioprotection. In *Journal of Molecular and Cellular Cardiology* (Vol. 78, pp. 100–106). https://doi.org/10.1016/j.yjmcc.2014.09.023

Boykin, C. A., Eastwood, L. C., Harris, M. K., Hale, D. S., Kerth, C. R., Griffin, D. B., Arnold, A. N., Hasty, J. D., Belk, K. E., Woerner, D. R., Delmore, R. J., Martin, J. N., VanOverbeke, D. L., Mafi, G. G., Pfeiffer, M. M., Lawrence, T. E., McEvers, T. J., Schmidt, T. B., Maddock, R. J., Savell, J. W. (2017). National Beef Quality Audit-2016: In-plant survey of carcass characteristics related to quality, quantity, and value of fed steers and heifers. *Journal of Animal Science*, *95*(7), 2993–3002. https://doi.org/10.2527/jas.2017.1543

Breusing, N., & Grune, T. (2008). Regulation of proteasome-mediated protein degradation during oxidative stress and aging. *Biological Chemistry*, *389*(3), 203–209. https://doi.org/10.1515/BC.2008.029/machinereadablecitation/RIS

Brookes, P. S., Yoon, Y., Robotham, J. L., Anders, M. W., & Sheu, S. S. (2004). Calcium, ATP, and ROS: A mitochondrial love-hate triangle. *American Journal of Physiology - Cell Physiology*, *287*(4 56-4). https://doi.org/10.1152/AJPCELL.00139.2004/ASSET/IMAGES/LARGE/ZH00100421350009.JPEG

Butcher, S. K., & Lord, J. M. (2004). Stress responses and innate immunity: Aging as a contributory factor. In *Aging Cell* (Vol. 3, Issue 4, pp. 151–160). John Wiley & Sons, Ltd. https://doi.org/10.1111/j.1474-9728.2004.00103.x

Cao, P., Kim, S. J., Xing, A., Schenck, C. A., Liu, L., Jiang, N., Wang, J., Last, R. L., & Brandizzi, F. (2019). Homeostasis of branched-chain amino acids is critical for the activity of TOR signaling in Arabidopsis. *ELife*, *8*. https://doi.org/10.7554/ELIFE.50747

Cao, Y. L., Meng, S., Chen, Y., Feng, J. X., Gu, D. D., Yu, B., Li, Y. J., Yang, J. Y., Liao, S., Chan, D. C., & Gao, S. (2017). MFN1 structures reveal nucleotide-triggered dimerization critical for mitochondrial fusion. *Nature*, *542*(7641), 372–376. https://doi.org/10.1038/nature21077

Carlin, K. R. M., Huff-Lonergan, E., Rowe, L. J., & Lonergan, S. M. (2006). Effect of oxidation, pH, and ionic strength on calpastatin inhibition of μ- and m-calpain. *Journal of Animal Science*, *84*(4), 925–937. https://doi.org/10.2527/2006.844925X

Cartoni, R., Léger, B., Hock, M. B., Praz, M., Crettenand, A., Pich, S., Ziltener, J. L., Luthi, F., Dériaz, O., Zorzano, A., Gobelet, C., Kralli, A., & Russell, A. P. (2005). Mitofusins 1/2 and ERRα expression are increased in human skeletal muscle after physical exercise. *Journal of Physiology*, *567*(1), 349–358. https://doi.org/10.1113/JPHYSIOL.2005.092031

Calvo, J. A., Daniels, T. G., Wang, X., Paul, A., Lin, J., Spiegelman, B. M., Stevenson, S. C., & Rangwala, S. M. (2008). Muscle-specific expression of PPARγ coactivator-1α improves exercise performance and increases peak oxygen uptake. *Journal of Applied Physiology*, *104*(5), 1304–1312. https://doi.org/10.1152/japplphysiol.01231.2007

Chauhan, S. S., LeMaster, M. N., Clark, D. L., Foster, M. K., Miller, C. E., England, E. M., Chauhan, S. S., LeMaster, M. N., Clark, D. L., Foster, M. K., Miller, C. E., & England, E. M. (2019). Glycolysis and pH Decline Terminate Prematurely in Oxidative Muscles despite the Presence of Excess Glycogen. *Meat and Muscle Biology*, *3*(1). https://doi.org/10.22175/MMB2019.02.0006

Chen, C., Zhang, J., Guo, Z., Shi, X., Zhang, Y., Zhang, L., Yu, Q., & Han, L. (2020). Effect of oxidative stress on AIF-mediated apoptosis and bovine muscle tenderness during postmortem aging. *Journal of Food Science*, *85*(1), 77–85. https://doi.org/10.1111/1750-3841.14969

Chin, E. R. (2004). The role of calcium and calcium/calmodulin-dependent kinases in skeletal muscle plasticity and mitochondrial biogenesis. *Proceedings of the Nutrition Society*, *63*(2), 279–286. https://doi.org/10.1079/PNS2004335

Cônsolo, N. R. B., Rosa, A. F., Barbosa, L. C. G. S., Maclean, P. H., Higuera-Padilla, A., Colnago, L. A., & Titto, E. A. L. (2021). Preliminary study on the characterization of Longissimus lumborum dark cutting meat in Angus × Nellore crossbreed cattle using NMR-based metabolomics. *Meat Science*, *172*, 108350. https://doi.org/10.1016/j.meatsci.2020.108350

Crick, F. (1970). Central Dogma of Molecular Biology. *Nature 1970 227:5258*, *227*(5258), 561–563. https://doi.org/10.1038/227561a0

Denzer, M. L., Mafi, G. G., VanOverebeke, D. L., & Ramanathan, R. (2022). Effects of glucono delta-lactone enhancement and nitrite-embedded packaging on fresh color, cooked color, and sensory attributes of dark-cutting beef. *Applied Food Research*, *2*(2), 100189. https://doi.org/10.1016/J.AFRES.2022.100189

Derave, W., Ai, H., Ihlemann, J., Witters, L. A., Kristiansen, S., Richter, E. A., & Ploug, T. (2000). Dissociation of AMP-activated protein kinase activation and glucose transport in contracting slow-twitch muscle. *Diabetes*, *49*(8), 1281–1287. https://doi.org/10.2337/DIABETES.49.8.1281

Dong, Z., Shanmughapriya, S., Tomar, D., Siddiqui, N., Lynch, S., Nemani, N., Breves, S. L., Zhang, X., Tripathi, A., Palaniappan, P., Riitano, M. F., Worth, A. M., Seelam, A., Carvalho, E., Subbiah, R., Jaña, F., Soboloff, J., Peng, Y., Cheung, J. Y., Madesh, M. (2017). Mitochondrial Ca2+ Uniporter Is a Mitochondrial Luminal Redox Sensor that Augments MCU Channel Activity. *Molecular Cell*, *65*(6), 1014-1028.e7. https://doi.org/10.1016/J.MOLCEL.2017.01.032

Egbert, W. R., & Cornforth, D. P. (1986). Factors Influencing Color of Dark Cutting Beef Muscle. *Journal of Food Science*, *51*(1), 57–59. https://doi.org/10.1111/j.1365-2621.1986.tb10835.x

Elkhalifa, E. A., Anglemier, A. F., Kennick, W. H., & Elgasim, E. A. (1984). Effect of Prerigor Pressurization on Postmortem Bovine Muscle Lactate Dehydrogenase Activity and Glycogen Degradation. *Journal of Food Science*, *49*(2), 593–594. https://doi.org/10.1111/J.1365-2621.1984.TB12476.X

England, E. M., Matarneh, S. K., Oliver, E. M., Apaoblaza, A., Scheffler, T. L., Shi, H., & Gerrard, D. E. (2016). Excess glycogen does not resolve high ultimate pH of oxidative muscle. *Meat Science*, *114*, 95–102. https://doi.org/10.1016/j.meatsci.2015.10.010

Engler, D., Pham, T., Fullerton, M. J., Ooi, G., Funder, J. W., & Clarke, I. J. (1989). Studies of the secretion of corticotropin-releasing factor and arginine vasopressin into the hypophysial-portal circulation of the conscious sheep: I. effect of an audiovisual stimulus and insulin-induced hypoglycemia. *Neuroendocrinology*, *49*(4), 367–381. https://doi.org/10.1159/000125141

English, A. R., Mafi, G. G., VanOverbeke, D. L., & Ramanathan, R. (2016). Effects of extended aging and modified atmospheric packaging on beef top loin steak color. *Journal of Animal Science*, *94*(4), 1727–1737. https://doi.org/10.2527/jas.2015-0149

Erlich, A. T., Tryon, L. D., Crilly, M. J., Memme, J. M., Moosavi, Z. S. M., Oliveira, A. N., Beyfuss, K., & Hood, D. A. (2016). Function of specialized regulatory proteins and signaling pathways in exercise-induced muscle mitochondrial biogenesis. *Integrative Medicine Research*, *5*(3), 187–197. https://doi.org/10.1016/j.imr.2016.05.003

Estabrook, R. W. (1967). Mitochondrial respiratory control and the polarographic measurement of ADP : O ratios. *Methods in Enzymology*, *10*(C), 41–47. https://doi.org/10.1016/0076-6879(67)10010-4

Farouk, M. M., & Lovatt, S. J. (2000). Initial chilling rate of pre-rigor beef muscles as an indicator of colour of thawed meat. *Meat Science*, *56*(2), 139–144. https://doi.org/10.1016/S0309-1740(00)00031-0

Faustman, C., & Cassens, R. G. (1990). The biochemical basis for discoloration in fresh meat: A review. *Journal of Muscle Foods*, *1*(3), 217–243. https://doi.org/10.1111/j.1745-4573.1990.tb00366.x

Fawcett, E. M., Johnson, J. K., Braden, C., Garcia, E. M., & Miller, D. L. (2019). Epigenetic bookmarking of H2S exposure in Caenorhabditis elegans. *BioRxiv*, 619734. https://doi.org/10.1101/619734

Feron, O. (2009). Pyruvate into lactate and back: From the Warburg effect to symbiotic energy fuel exchange in cancer cells. *Radiotherapy and Oncology*, *92*(3), 329–333. https://doi.org/10.1016/J.RADONC.2009.06.025

Fiehn, O. (2016). Metabolomics by Gas Chromatography-Mass Spectrometry: the combination of targeted and untargeted profiling. *Current Protocols in Molecular Biology / Edited by Frederick M. Ausubel ... [et Al.]*, *114*, 30.4.1. https://doi.org/10.1002/0471142727.MB3004S114

Field, R. A. (1971). Effect of castration on meat quality and quantity. *Journal of Animal Science*, *32*(5), 849–858. https://doi.org/10.2527/jas1971.325849x

Fuente-García, C., Aldai, N., Sentandreu, E., Oliván, M., Franco, D., García-Torres, S., & Sentandreu, M. Á. (2022). Assessment of caspase activity in post mortem muscle as a way to explain characteristics of DFD beef. *Journal of Food Composition and Analysis*, *111*, 104599. https://doi.org/10.1016/J.JFCA.2022.104599

Fuente-García, C., Sentandreu, M. A., Aldai, N., Oliván, M., & Sentandreu, E. (2021). Proteomic pipeline for biomarker hunting of defective bovine meat assisted by liquid chromatography-mass spectrometry analysis and chemometrics. *Journal of Proteomics*, *238*, 104153. https://doi.org/10.1016/j.jprot.2021.104153

Fuente-Garcia, C., Sentandreu, E., Aldai, N., Oliván, M., & Sentandreu, M. Á. (2020). Characterization of the Myofibrillar Proteome as a Way to Better Understand Differences in Bovine Meats Having Different Ultimate pH Values. *Proteomics*, *20*(12), 2000012. https://doi.org/10.1002/pmic.202000012

Gagaoua, M., Warner, R. D., Purslow, P., Ramanathan, R., Mullen, A. M., López-Pedrouso, M., Franco, D., Lorenzo, J. M., Tomasevic, I., Picard, B., Troy, D., & Terlouw, E. M. C. (2021). Dark-cutting beef: A brief review and an integromics meta-analysis at the proteome level to decipher the underlying pathways. *Meat Science*, *181*, 108611. https://doi.org/10.1016/J.MEATSCI.2021.108611

Gallo, C., Lizondo, G., & Knowles, T. G. (2003). Effects of journey and lairage time on steers transported to slaughter in Chile. *Veterinary Record*, *152*(12), 361–364. https://doi.org/10.1136/vr.152.12.361

García-Bermúdez, J., & Cuezva, J. M. (2016). The ATPase Inhibitory Factor 1 (IF1): A master regulator of energy metabolism and of cell survival. *Biochimica et Biophysica Acta - Bioenergetics*, *1857*(8), 1167–1182. https://doi.org/10.1016/j.bbabio.2016.02.004

Gidalevitz, T., Prahlad, V., Morimoto, R. I., Morimoto, R., Selkoe, D., & Kelly, J. (2011). The Stress of Protein Misfolding: From Single Cells to Multicellular Organisms. *Cold Spring Harbor Perspectives in Biology*, *3*(6), a009704. https://doi.org/10.1101/CSHPERSPECT.A009704

Gill, J. A., & La Merrill, M. A. (2017). An emerging role for epigenetic regulation of Pgc-1α expression in environmentally stimulated brown adipose thermogenesis. *Environmental Epigenetics*, *3*(2). https://doi.org/10.1093/eep/dvx009

Goll, D. E., Thompson, V. F., Taylor, R. G., & Christiansen, J. A. (1992). Role of the calpain system in muscle growth. *Biochimie*, *74*(3), 225–237. https://doi.org/10.1016/0300-9084(92)90121-T

Gomes, M. J., Martinez, P. F., Pagan, L. U., Damatto, R. L., Cezar, M. D. M., Lima, A. R. R., Okoshi, K., & Okoshi, M. P. (2017). Skeletal muscle aging: influence of oxidative stress and physical exercise. *Oncotarget*, *8*(12), 20428. https://doi.org/10.18632/ONCOTARGET.14670

González-Cabo, P., Vázquez-Manrique, R. P., García-Gimeno, M. A., Sanz, P., & Palau, F. (2005). Frataxin interacts functionally with mitochondrial electron transport chain proteins. *Human Molecular Genetics*, *14*(15), 2091–2098. https://doi.org/10.1093/hmg/ddi214

Gottlieb, E., Armour, S. M., & Thompson, C. B. (2002). Mitochondrial respiratory control is lost during growth factor deprivation. *Proceedings of the National Academy of Sciences of the United States of America*, *99*(20), 12801–12806. https://doi.org/10.1073/pnas.202477599

Gurd, B. J. (2011). Deacetylation of PGC-1a by SIRT1: Importance for skeletal muscle function andexercise-induced mitochondrial biogenesis. *Applied Physiology, Nutrition and Metabolism*, *36*(5), 589–597. https://doi.org/10.1139/H11-070/ASSET/IMAGES/LARGE/H11-070F2.JPEG

Han, H., Hemp, J., Pace, L. A., Ouyang, H., Ganesan, K., Roh, J. H., Daldal, F., Blanke, S. R., & Gennis, R. B. (2011). Adaptation of aerobic respiration to low O2 environments. *Proceedings of the National Academy of Sciences of the United States of America*, *108*(34), 14109–14114. https://doi.org/10.1073/pnas.1018958108

Hardie, D. G. (2007). AMP-activated/SNF1 protein kinases: conserved guardians of cellular energy. *Nature Reviews Molecular Cell Biology 2007 8:10*, *8*(10), 774–785. https://doi.org/10.1038/nrm2249

Hespel, P., & Richter, E. A. (1992). Mechanism linking glycogen concentration and glycogenolytic rate in perfused contracting rat skeletal muscle. *Biochemical Journal*, *284*(3), 777–780. https://doi.org/10.1042/BJ2840777

Hipp, M. S., Kasturi, P., & Hartl, F. U. (2019). The proteostasis network and its decline in ageing. *Nature Reviews Molecular Cell Biology 2019 20:7*, *20*(7), 421–435. https://doi.org/10.1038/s41580-019-0101-y

Holdstock, J., Aalhus, J. L., Uttaro, B. A., López-Campos, Ó., Larsen, I. L., & Bruce, H. L. (2014). The impact of ultimate pH on muscle characteristics and sensory attributes of the longissimus thoracis within the dark cutting (Canada B4) beef carcass grade. *Meat Science*, *98*(4), 842–849. https://doi.org/10.1016/j.meatsci.2014.07.029

Holloszy, J. 0. (1967). Biochemical Adaptations in Muscle effects of exercise on mitochondrial oxygen uptake and respiratory enzyme activity in skeletal muscle*. In *The journal of biological chemistry* (Vol. 242, Issue 9). http://www.jbc.org/

Honda, S., Aihara, T., Hontani, M., Okubo, K., & Hirose, S. (2005). Mutational analysis of action of mitochondrial fusion factor mitofusin-2. *Journal of Cell Science*, *118*(14), 3153–3161. https://doi.org/10.1242/jcs.02449

Houry, W. A. (2014). The molecular chaperones interaction networks in protein folding and degradation. In *The Molecular Chaperones Interaction Networks in Protein Folding and Degradation*. Springer New York. https://doi.org/10.1007/978-1-4939-1130-1

Huang, Y. L., Shen, Z. Q., Wu, C. Y., Teng, Y. C., Liao, C. C., Kao, C. H., Chen, L. K., Lin, C. H., & Tsai, T. F. (2018). Comparative proteomic profiling reveals a role for Cisd2 in skeletal muscle aging. *Aging Cell*, *17*(1). https://doi.org/10.1111/acel.12705

Huff-Lonergan, E., Mitsuhashi, T., Beekman, D. D., Parrish, F. C., Olson, D. G., & Robson, R. M. (1996). Proteolysis of Specific Muscle Structural Proteins by μ-Calpain at Low pH and Temperature is Similar to Degradation in Postmortem Bovine Muscle. *Journal of Animal Science*, *74*(5), 993–1008. https://doi.org/10.2527/1996.745993X

Ibebunjo, C., Chick, J. M., Kendall, T., Eash, J. K., Li, C., Zhang, Y., Vickers, C., Wu, Z., Clarke, B. A., Shi, J., Cruz, J., Fournier, B., Brachat, S., Gutzwiller, S., Ma, Q., Markovits, J., Broome, M., Steinkrauss, M., Skuba, E., Glass, D. J. (2013). Genomic and Proteomic Profiling Reveals Reduced Mitochondrial Function and Disruption of the Neuromuscular Junction Driving Rat Sarcopenia. *Molecular and Cellular Biology*, *33*(2), 194–212. https://doi.org/10.1128/MCB.01036-12/SUPPL_FILE/ZMB999109802SO1.PDF

Ijaz, M., Zhang, D., Hou, C., Mahmood, M., Hussain, Z., Zheng, X., & Li, X. (2022). Changes in postmortem metabolites profile of atypical and typical DFD beef. *Meat Science*, *193*, 108922. https://doi.org/10.1016/J.MEATSCI.2022.108922

Immonen, K., Ruusunen, M., Hissa, K., & Puolanne, E. (2000). Bovine muscle glycogen concentration in relation to finishing diet, slaughter and ultimate pH. *Meat Science*, *55*(1), 25–31. https://doi.org/10.1016/S0309-1740(99)00121-7

Ishihara, N., Eura, Y., & Mihara, K. (2004). Mitofusin 1 and 2 play distinct roles in mitochondrial fusion reactions via GTPase activity. *Journal of Cell Science*, *117*(26), 6535–6546. https://doi.org/10.1242/jcs.01565

Jain, S. S., Paglialunga, S., Vigna, C., Ludzki, A., Herbst, E. A., Lally, J. S., Schrauwen, P., Hoeks, J., Tupling, A. R., Bonen, A., & Holloway, G. P. (2014). High-Fat Diet–Induced Mitochondrial Biogenesis Is Regulated by Mitochondrial-Derived Reactive Oxygen Species Activation of CaMKII. *Diabetes*, *63*(6), 1907–1913. https://doi.org/10.2337/db13-0816

Jensen, T. E., & Richter, E. A. (2012). Regulation of glucose and glycogen metabolism during and after exercise. *The Journal of Physiology*, *590*(Pt 5), 1069. https://doi.org/10.1113/JPHYSIOL.2011.224972

Ježek, P., & Hlavatá, L. (2005). Mitochondria in homeostasis of reactive oxygen species in cell, tissues, and organism. In *International Journal of Biochemistry and Cell Biology* (Vol. 37, Issue 12, pp. 2478–2503). Pergamon. https://doi.org/10.1016/j.biocel.2005.05.013

Jouaville, L. S., Pinton, P., Bastianutto, C., Rutter, G. A., & Rizzuto, R. (1999). Regulation of mitochondrial ATP synthesis by calcium: Evidence for a long-term metabolic priming. *Proceedings of the National Academy of Sciences of the United States of America*, *96*(24), 13807–13812. https://doi.org/10.1073/pnas.96.24.13807

Jung, C., Higgins, C. M. J., & Xu, Z. (2002). Mitochondrial electron transport chain complex dysfunction in a transgenic mouse model for amyotrophic lateral sclerosis. *Journal of Neurochemistry*, *83*(3), 535–545. https://doi.org/10.1046/j.1471-4159.2002.01112.x

Kadim, I. T., Mahgoub, O., Al-Ajmi, D. S., Al-Maqbaly, R. S., Al-Mugheiry, S. M., & Bartolome, D. Y. (2004). The influence of season on quality characteristics of hot-boned beef m. longissimus thoracis. *Meat Science*, *66*(4), 831–836. https://doi.org/10.1016/j.meatsci.2003.08.001

Kahn, B. B., Alquier, T., Carling, D., & Hardie, D. G. (2005). AMP-activated protein kinase: Ancient energy gauge provides clues to modern understanding of metabolism. *Cell Metabolism*, *1*(1), 15–25. https://doi.org/10.1016/J.CMET.2004.12.003

Kang, S. W., Baines, I. C., & Rhee, S. G. (1998). Characterization of a mammalian peroxiredoxin that contains one conserved cysteine. *Journal of Biological Chemistry*, *273*(11), 6303–6311. https://doi.org/10.1074/jbc.273.11.6303

Karlsson, L., Barbaro, M., Ewing, E., Gomez-Cabrero, D., & Lajic, S. (2019). Epigenetic Alterations Associated With Early Prenatal Dexamethasone Treatment. *Journal of the Endocrine Society*, *3*(1), 250–263. https://doi.org/10.1210/js.2018-00377

Kawalec, M., Boratyńska-Jasińska, A., Beresewicz, M., Dymkowska, D., Zabłocki, K., & Zabłocka, B. (2015). Mitofusin 2 Deficiency Affects Energy Metabolism and Mitochondrial Biogenesis in MEF Cells. *PLOS ONE*, *10*(7), e0134162. https://doi.org/10.1371/JOURNAL.PONE.0134162

Kelly, D. P., & Scarpulla, R. C. (2004). Transcriptional regulatory circuits controlling mitochondrial biogenesis and function. *Genes & Development*, *18*(4), 357–368. https://doi.org/10.1101/gad.1177604

Kelly, S. M., VanSlyke, J. K., & Musil, L. S. (2007). Regulation of ubiquitin-proteasome system-mediated degradation by cytosolic stress. *Molecular Biology of the Cell*, *18*(11),4279–4291. https://doi.org/10.1091/MBC.E07-05-0487/ASSET/IMAGES/LARGE/ZMK0110782670009.JPEG

Kendall, T. L., Koohmaraie, M., Arbona, J. R., Williams, S. E., & Young, L. L. (1993). Effect of pH and ionic strength on bovine m-calpain and calpastatin activity. *Journal of Animal Science*, *71*(1), 96–104. https://doi.org/10.2527/1993.71196X

Kim, J., & Guan, K. L. (2019). mTOR as a central hub of nutrient signalling and cell growth. *Nature Cell Biology 2019 21:1*, *21*(1), 63–71. https://doi.org/10.1038/s41556-018-0205-1

Kim, K. H., Rodriguez, A. M., Carrico, P. M., & Melendez, J. A. (2001). Potential mechanisms for the inhibition of tumor cell growth by manganese superoxide dismutase. *Antioxidants and Redox Signaling*, *3*(3), 361–373. https://doi.org/10.1089/15230860152409013

Kim, Y. H. B., Kemp, R., & Samuelsson, L. M. (2016). Effects of dry-aging on meat quality attributes and metabolite profiles of beef loins. *Meat Science*, *111*, 168–176. https://doi.org/10.1016/j.meatsci.2015.09.008

Kim, Y. S., Yoon, S. K., Song, Y. H., & Lee, S. K. (2003). Effect of season on color of Hanwoo (Korean native cattle) beef. *Meat Science*, *63*(4), 509–513. https://doi.org/10.1016/S0309-1740(02)00112-2

Kiyimba, F., Hartson, S. D., Rogers, J., VanOverbeke, D. L., Mafi, G. G., & Ramanathan, R. (2021). Changes in glycolytic and mitochondrial protein profiles regulates postmortem muscle acidification and oxygen consumption in dark-cutting beef. *Journal of Proteomics*, *232*, 104016. https://doi.org/10.1016/j.jprot.2020.104016

Kiyimba, F., Hartson, S. D., Rogers, J., VanOverbeke, D. L., Mafi, G. G., & Ramanathan, R. (2022). Dark-cutting beef mitochondrial proteomic signatures reveal increased biogenesis proteins and bioenergetics capabilities. *Journal of Proteomics*, *265*, 104637. https://doi.org/10.1016/J.JPROT.2022.104637

Knee, B. W., Cummins, L. J., Walker, P. J., Kearney, G. A., Warner, R. D., Knee, B. W., Cummins, L. J., Walker, P. J., Kearney, G. A., & Warner, R. D. (2007). Reducing dark-cutting in pasture-fed beef steers by high-energy supplementation. *Australian Journal of Experimental Agriculture*, *47*(11), 1277–1283. https://doi.org/10.1071/EA05362

Komoda, T., & Matsunaga, T. (2015). Metabolic Pathways in the Human Body. In *Biochemistry for Medical Professionals* (pp. 25–63). Elsevier. https://doi.org/10.1016/b978-0-12-801918-4.00004-9

Koohmaraie, M. (1992). The role of $Ca2^{+}$-dependent proteases (calpains) in post mortem proteolysis and meat tenderness. *Biochimie*, *74*(3), 239–245. https://doi.org/10.1016/0300-9084(92)90122-U

Kucera, M., Isserlin, R., Arkhangorodsky, A., & Bader, G. D. (2016). AutoAnnotate: A Cytoscape app for summarizing networks with semantic annotations. *F1000Research*, *5*. https://doi.org/10.12688/F1000RESEARCH.9090.1

Lamare, M., Taylor, R. G., Farout, L., Briand, Y., & Briand, M. (2002). Changes in proteasome activity during postmortem aging of bovine muscle. *Meat Science*, *61*(2), 199–204. https://doi.org/10.1016/S0309-1740(01)00187-5

Lanari, M. C., & Cassens, R. G. (1991). Mitochondrial Activity and Beef Muscle Color Stability. *Journal of Food Science*, *56*(6), 1476–1479. https://doi.org/10.1111/j.1365-2621.1991.tb08619.x

Lange, P. F., Huesgen, P. F., Nguyen, K., & Overall, C. M. (2014). Annotating N termini for the human proteome project: N termini and Nα-acetylation status differentiate stable cleaved protein species from degradation remnants in the human erythrocyte proteome. *Journal of Proteome Research*, *13*(4), 2028–2044. https://doi.org/10.1021/PR401191W/SUPPL_FILE/PR401191W_SI_003.PDF

Lawrie, R. A. (1958). Physiological stress in relation to dark-cutting beef. *Journal of the Science of Food and Agriculture*, *9*(11), 721–727. https://doi.org/10.1002/jsfa.2740091106

Lee, H. C., & Wei, Y. H. (2005). Mitochondrial biogenesis and mitochondrial DNA maintenance of mammalian cells under oxidative stress. *International Journal of Biochemistry and Cell Biology*. 37(4), 822-834. https://doi.org/10.1016/j.biocel.2004.09.010

Lei, H., Yang, T., Mahmood, S., Abo-Ismail, M., Roy, B. C., Li, C., Plastow, G. S., & Bruce, H. L. (2020). *A genome-wide case-control association study of dark cutting in beef cattle*. Canadian Journal of Animal Science. 101(1),158-167. https://doi.org/10.1139/cjas-2019-0039

Ling, C., Del Guerra, S., Lupi, R., Rönn, T., Granhall, C., Luthman, H., Masiello, P., Marchetti, P., Groop, L., & Del Prato, S. (2008). Epigenetic regulation of PPARGC1A in human type 2 diabetic islets and effect on insulin secretion. *Diabetologia*, *51*(4), 615–622. https://doi.org/10.1007/S00125-007-0916-5/FIGURES/3

Liu, Y., Jin, M., Wang, Y., Zhu, J., Tan, R., Zhao, J., Ji, X., Jin, C., Jia, Y., Ren, T., & Xing, J. (2020). MCU-induced mitochondrial calcium uptake promotes mitochondrial biogenesis and colorectal cancer growth. *Signal Transduction and Targeted Therapy 2020 5:1*, *5*(1), 1–13. https://doi.org/10.1038/s41392-020-0155-5

Lonergan, S. M., Huff-Lonergan, E., Wiegand, B. R., & Kriese-Anderson, L. A. (2001). Postmortem proteolysis and tenderization of top loin steaks from Brangus cattle 1. *Journal of Muscle Foods*, *12*(2), 121–136. https://doi.org/10.1111/J.1745-4573.2001.TB00304.X

Löw, P. (2011). The role of ubiquitin–proteasome system in ageing. *General and Comparative Endocrinology*, *172*(1), 39–43. https://doi.org/10.1016/J.YGCEN.2011.02.005

Lu, X., Cornforth, D. P., Carpenter, C. E., Zhu, L., & Luo, X. (2020). Effect of oxygen concentration in modified atmosphere packaging on color changes of the M. longissimus thoraces et lumborum from dark cutting beef carcasses. *Meat Science*, *161*, 107999. https://doi.org/10.1016/J.MEATSCI.2019.107999

Ma, D., Kim, Y. H. B., Cooper, B., Oh, J. H., Chun, H., Choe, J. H., Schoonmaker, J. P., Ajuwon, K., & Min, B. (2017). Metabolomics Profiling to Determine the Effect of Postmortem Aging on Color and Lipid Oxidative Stabilities of Different Bovine Muscles. *Journal of Agricultural and Food Chemistry*, *65*(31), 6708–6716. https://doi.org/10.1021/acs.jafc.7b02175

MacDougall, D. B. (1982). Changes in the colour and opacity of meat. *Food Chemistry*. 9(1), 75-88. https://doi.org/10.1016/0308-8146(82)90070-X

MacMillan-Crow, L. A., & Thompson, J. A. (1999). Tyrosine Modifications and Inactivation of Active Site Manganese Superoxide Dismutase Mutant (Y34F) by Peroxynitrite. *Archives of Biochemistry and Biophysics*, *366*(1), 82–88. https://doi.org/10.1006/ABBI.1999.1202

Mahmood, S., Roy, B. C., Larsen, I. L., Aalhus, J. L., Dixon, W. T., & Bruce, H. L. (2017). Understanding the quality of typical and atypical dark cutting beef from heifers and steers. *Meat Science*, *133*, 75–85. https://doi.org/10.1016/J.MEATSCI.2017.06.010

Mahmood, Shahid, Turchinsky, N., Paradis, F., Dixon, W. T., & Bruce, H. L. (2018). Proteomics of dark cutting longissimus thoracis muscle from heifer and steer carcasses. *Meat Science*, *137*(August 2017), 47–57. https://doi.org/10.1016/j.meatsci.2017.11.014

Mancini, R. A., Seyfert, M., & Hunt, M. C. (2008). Effects of data expression, sample location, and oxygen partial pressure on initial nitric oxide metmyoglobin formation and metmyoglobin-reducing-activity measurement in beef muscle. *Meat Science*, *79*(2), 244–251. https://doi.org/10.1016/J.MEATSCI.2007.09.008

Mancini, R. A., Belskie, K., Suman, S. P., & Ramanathan, R. (2018). Muscle-Specific Mitochondrial Functionality and Its Influence on Fresh Beef Color Stability. *Journal of Food Science*, *83*(8), 2077–2082. https://doi.org/10.1111/1750-3841.14219

Marcinko, K., & Steinberg, G. R. (2014). The role of AMPK in controlling metabolism and mitochondrial biogenesis during exercise. *Experimental Physiology*, *99*(12), 1581–1585. https://doi.org/10.1113/EXPPHYSIOL.2014.082255

Marin, T. L., Gongol, B., Zhang, F., Martin, M., Johnson, D. A., Xiao, H., Wang, Y., Subramaniam, S., Chien, S., & Shyy, J. Y. J. (2017). AMPK promotes mitochondrial biogenesis and function by phosphorylating the epigenetic factors DNMT1, RBBP7, and HAT1. *Science Signaling*, *10*(464). https://doi.org/10.1126/SCISIGNAL.AAF7478/SUPPL_FILE/AAF7478_SM.PDF

Matilainen, O., Quirós, P. M., & Auwerx, J. (2017). Mitochondria and Epigenetics – Crosstalk in Homeostasis and Stress. In *Trends in Cell Biology* 27, (6), pp. 453–463. Elsevier Ltd. https://doi.org/10.1016/j.tcb.2017.02.004

McBride, A., Ghilagaber, S., Nikolaev, A., & Hardie, D. G. (2009). The Glycogen-Binding Domain on the AMPK β Subunit Allows the Kinase to Act as a Glycogen Sensor. *Cell Metabolism*, *9*(1), 23–34. https://doi.org/10.1016/J.CMET.2008.11.008

McCommis, K. S., & Finck, B. N. (2015). Mitochondrial pyruvate transport: a historical perspective and future research directions. *Biochemical Journal*, *466*(3), 443–454. https://doi.org/10.1042/BJ20141171

McKeith, R. O., King, D. A., Grayson, A. L., Shackelford, S. D., Gehring, K. B., Savell, J. W., & Wheeler, T. L. (2016). Mitochondrial abundance and efficiency contribute to lean color of dark cutting beef. *Meat Science*, *116*, 165–173. https://doi.org/10.1016/j.meatsci.2016.01.016

Menzies, K. J., Singh, K., Saleem, A., & Hood, D. A. (2013). Sirtuin 1-mediated effects of exercise and resveratrol on mitochondrial biogenesis. *Journal of Biological Chemistry*, *288*(10), 6968–6979. https://doi.org/10.1074/jbc.M112.431155

Mitacek, R. M., English, A. R., Mafi, G. G., VanOverbeke, D. L., & Ramanathan, R. (2018). Modified Atmosphere Packaging Improves Surface Color of Dark-Cutting Beef. *Meat and Muscle Biology*, *2*(1), 57. https://doi.org/10.22175/mmb2017.04.0023

Mitacek, R. M., Ke, Y., Prenni, J. E., Jadeja, R., VanOverbeke, D. L., Mafi, G. G., & Ramanathan, R. (2019). Mitochondrial Degeneration, Depletion of NADH, and Oxidative Stress Decrease Color Stability of Wet-Aged Beef Longissimus Steaks. *Journal of Food Science*, *84*(1), 38–50. https://doi.org/10.1111/1750-3841.14396

Namba, T. (2019). BAP31 regulates mitochondrial function via interaction with Tom40 within ER-mitochondria contact sites. *Science Advances*, *5*(6). https://doi.org/10.1126/sciadv.aaw1386

Neutzner, A., Benard, G., Youle, R. J., & Karbowski, M. (2008). Role of the Ubiquitin Conjugation System in the Maintenance of Mitochondrial Homeostasis. *Annals of the New York Academy of Sciences*, *1147*(1), 242–253. https://doi.org/10.1196/annals.1427.012

Njomen, E., & Tepe, J. J. (2019). Regulation of Autophagic Flux by the 20S Proteasome. *Cell Chemical Biology*, *26*(9), 1283-1294.e5. https://doi.org/10.1016/J.CHEMBIOL.2019.07.002

O'Keeffe, M., & Hood, D. E. (1982). Biochemical factors influencing metmyoglobin formation on beef from muscles of differing colour stability. *Meat Science*, *7*(3), 209–228. https://doi.org/10.1016/0309-1740(82)90087-0

Orrenius, S., Gogvadze, V., & Zhivotovsky, B. (2007). Mitochondrial Oxidative Stress: Implications for Cell Death. *Annu. Rev. Pharmacol. Toxicol*, *47*, 143–183. https://doi.org/10.1146/annurev.pharmtox.47.120505.105122

Osellame, L. D., Blacker, T. S., & Duchen, M. R. (2012). Cellular and molecular mechanisms of mitochondrial function. In *Best Practice and Research: Clinical Endocrinology and Metabolism* 26, (6), 711–723. Bailliere Tindall Ltd. https://doi.org/10.1016/j.beem.2012.05.003

Palikaras, K., Lionaki, E., & Tavernarakis, N. (2015). Balancing mitochondrial biogenesis and mitophagy to maintain energy metabolism homeostasis. In *Cell Death and Differentiation* 22, (9), 1399–1401. Nature Publishing Group. https://doi.org/10.1038/cdd.2015.86

Palmer, C. S., Osellame, L. D., Stojanovski, D., & Ryan, M. T. (2011). The regulation of mitochondrial morphology: Intricate mechanisms and dynamic machinery. In *Cellular Signalling* 23, (10), 1534–1545. https://doi.org/10.1016/j.cellsig.2011.05.021

Patron, M., Raffaello, A., Granatiero, V., Tosatto, A., Merli, G., Stefani, D. De, Wright, L., Pallafacchina, G., Terrin, A., Mammucari, C., & Rizzuto, R. (2013). The mitochondrial calcium uniporter (MCU): Molecular identity and physiological roles. *Journal of Biological Chemistry*, *288*(15), 10750–10758. https://doi.org/10.1074/jbc.R112.420752

Petracci, M., Fletcher, D. L., & Northcutt, J. K. (2001). The effect of holding temperature on live shrink, processing yield, and breast meat quality of broiler chickens. *Poultry Science*, *80*(5), 670–675. https://doi.org/10.1093/ps/80.5.670

Picard, M., McEwen, B. S., Epel, E. S., & Sandi, C. (2018). An energetic view of stress: Focus on mitochondria. In *Frontiers in Neuroendocrinology*. 49, 72–85. Academic Press Inc. https://doi.org/10.1016/j.yfrne.2018.01.001

Pirola, C. J., Fernández Gianotti, T., Burgueño, A. L., Rey-Funes, M., Loidl, C. F., Mallardi, P., Martino, J. S., Castaño, G. O., & Sookoian, S. (2013). Epigenetic modification of liver mitochondrial DNA is associated with histological severity of nonalcoholic fatty liver disease. *Gut*, *62*(9), 1356–1363. https://doi.org/10.1136/GUTJNL-2012-302962

Pohjoismäki, J. L. O., Boettger, T., Liu, Z., Goffart, S., Szibor, M., & Braun, T. (2012). Oxidative stress during mitochondrial biogenesis compromises mtDNA integrity in growing hearts and induces a global DNA repair response. *Nucleic Acids Research*, *40*(14), 6595–6607. https://doi.org/10.1093/nar/gks301

Polekhina, G., Gupta, A., Michell, B. J., Van Denderen, B., Murthy, S., Feil, S. C., Jennings, I. G., Campbell, D. J., Witters, L. A., Parker, M. W., Kemp, B. E., & Stapleton, D. (2003). AMPK β Subunit Targets Metabolic Stress Sensing to Glycogen. *Current Biology*, *13*(10), 867–871. https://doi.org/10.1016/S0960-9822(03)00292-6

Poleti, M. D., Moncau, C. T., Silva-Vignato, B., Rosa, A. F., Lobo, A. R., Cataldi, T. R., Negrão, J. A., Silva, S. L., Eler, J. P., & de Carvalho Balieiro, J. C. (2018). Label-free quantitative proteomic analysis reveals muscle contraction and metabolism proteins linked to ultimate pH in bovine skeletal muscle. *Meat Science*, *145*, 209–219. https://doi.org/10.1016/j.meatsci.2018.06.041

Ponnampalam, E. N., Hopkins, D. L., Bruce, H., Li, D., Baldi, G., & Bekhit, A. E. din. (2017). Causes and Contributing Factors to "Dark Cutting" Meat: Current Trends and Future Directions: A Review. In *Comprehensive Reviews in Food Science and Food Safety*. 16, (3), 400–430. Blackwell Publishing Inc. https://doi.org/10.1111/1541-4337.12258

Postnikova, G. B., Tselikova, S. V., & Shekhovtsova, E. A. (2009). Myoglobin and mitochondria: Oxymyoglobin interacts with mitochondrial membrane during deoxygenation. *Biochemistry*, *74*(11),1211–1218. https://doi.org/10.1134/S0006297909110054

Powers, S. K., Criswell, D., Lawler, J., Li Li Ji, Martin, D., Herb, R. A., & Dudley, G. (1994). Influence of exercise and fiber type on antioxidant enzyme activity in rat skeletal muscle. *Https://Doi.Org/10.1152/Ajpregu.1994.266.2.R375*, *266*(2 35-2). https://doi.org/10.1152/AJPREGU.1994.266.2.R375

Priolo, A., Micol, D., & Agabriel, J. (2001). Effects of grass feeding systems on ruminant meat colour and flavour. A review. *Animal Research*, *50*(3), 185–200. https://doi.org/10.1051/ANIMRES:2001125

Ramanathan, R., Hunt, M. C., English, A. R., Mafi, G. G., & VanOverbeke, D. L. (2019). Effects of Aging, Modified Atmospheric Packaging, and Display Time on Metmyoglobin Reducing Activity and Oxygen Consumption of High-pH Beef. *Meat and Muscle Biology*, *3*(1), 276. https://doi.org/10.22175/mmb2019.05.0017

Ramanathan, R., Mancini, R. A., Naveena, B. M., & Konda, M. K. R. (2010). Effects of lactate-enhancement on surface reflectance and absorbance properties of beef longissimus steaks. *Meat Science*, *84*(1), 219–226. https://doi.org/10.1016/j.meatsci.2009.08.027

Ramanathan, R., Nair, M. N., Hunt, M. C., & Suman, S. P. (2019). Mitochondrial functionality and beef colour: A review of recent research. *South African Journal of Animal Science*, *49*(1), 9. https://doi.org/10.4314/sajas.v49i1.2

Ramanathan, R., Hunt, M. C., Mancini, R. A., Nair, M. N., Denzer, M. L., Suman, S. P., & Mafi, G. G. (2020a). Recent Updates in Meat Color Research: Integrating Traditional and High-Throughput Approaches. *Meat and Muscle Biology*, *4*(2), 1–24. https://doi.org/10.22175/MMB.9598

Ramanathan, R., Kiyimba, F., Gonzalez, J. M., Mafi, G. G., & DeSilva, U. (2020b). Impact of up- and down-regulation of metabolites and mitochondrial properties on pH and color of longissimus muscle from normal-pH and dark-cutting beef. *Journal of Agricultural and Food Chemistry*. 68(27), 7194-7203 https://doi.org/10.1021/acs.jafc.0c01884

Ramanathan, R., Lambert, L. H., Nair, M. N., Morgan, B., Feuz, R., Mafi, G., & Pfeiffer, M. (2022). Economic Loss, Amount of Beef Discarded, Natural Resources Wastage, and Environmental Impact Due to Beef Discoloration. *Meat and Muscle Biology*, *6*(1), 13218–13219. https://doi.org/10.22175/MMB.13218

Ramanathan, R., & Mancini, R. A. (2018). Role of Mitochondria in Beef Color: A Review. *Meat and Muscle Biology*, *2*(1), 309. https://doi.org/10.22175/mmb2018.05.0013

Ramanathan, R., Mancini, R. A., & Konda, M. R. (2009). Effects of lactate on beef heart mitochondrial oxygen consumption and muscle darkening. *Journal of Agricultural and Food Chemistry*, *57*(4), 1550–1555. https://doi.org/10.1021/jf802933p

Ramanathan, R., Suman, S. P., & Faustman, C. (2020). Biomolecular Interactions Governing Fresh Meat Color in Post-mortem Skeletal Muscle: A Review. *Journal of Agricultural and Food Chemistry*. https://doi.org/10.1021/acs.jafc.9b08098

Remels, A. H. V. V., Langen, R. C. J. J., Schrauwen, P., Schaart, G., Schols, A. M. W. J. W. J., & Gosker, H. R. (2010). Regulation of mitochondrial biogenesis during myogenesis. *Molecular and Cellular Endocrinology*, *315*(1–2), 113–120. https://doi.org/10.1016/j.mce.2009.09.029

Roach, P. (2005). Glycogen and its Metabolism. *Current Molecular Medicine*, *2*(2), 101–120. https://doi.org/10.2174/1566524024605761

Roach, P. J. (2013). Glycogen Metabolism. *Encyclopedia of Biological Chemistry: Second Edition*, 425–427. https://doi.org/10.1016/B978-0-12-378630-2.00042-6

Robbins, K., Jensen, J., Ryan, K. J., Homco-Ryan, C., McKeith, F. K., & Brewer, M. S. (2003). Consumer attitudes towards beef and acceptability of enhanced beef. *Meat Science*, *65*(2), 721–729. https://doi.org/10.1016/S0309-1740(02)00274-7

Robergs, R. A., Ghiasvand, F., & Parker, D. (2004). Biochemistry of exercise-induced metabolic acidosis. *American Journal of Physiology-Regulatory, Integrative and Comparative Physiology*, *287*(3), R502–R516. https://doi.org/10.1152/ajpregu.00114.2004

Romanello, V., & Sandri, M. (2010). Mitochondrial biogenesis and fragmentation as regulators of muscle protein degradation. *Current Hypertension Reports*, *12*(6), 433–439. https://doi.org/10.1007/S11906-010-0157-8/FIGURES/1

Rosa, A. F., Ventura, R., Oliveira, G., Perez, B. C., Mattos, E. C., Carvalho, M. E., & Ferraz, J. B. E. (2017, August). Can genetics be associated with the high frequency of dark, firm and dry meat in Brazilian Nellore beef cattle?. In 63rd International Congress of Meat Sciecnce and Technology:Nurturing locally, growing globally. Academic Publishers,. 2017.

Rosenvold, K., Petersen, J. S., Lærke, H. N., Jensen, S. K., Therkildsen, M., Karlsson, A. H., Møller, H. S., & Andersen, H. J. (2001). Muscle glycogen stores and meat quality as affected by strategic finishing feeding of slaughter pigs. *Journal of Animal Science*, *79*(2), 382–391. https://doi.org/10.2527/2001.792382X

Roy, D. B., Mahmood, M. S., & Bruce, D. H. L. (2022). Are muscle fiber types different between normal and dark-cutting beef? Canadian Journal of Animal Science. 102(2), 274-288. https://doi.org/10.1139/CJAS-2021-0085

Rutter, J., & Hughes, A. L. (2015). Power^2: The power of yeast genetics applied to the powerhouse of the cell. In *Trends in Endocrinology and Metabolism*. 26(2), 59–68. Elsevier Inc. https://doi.org/10.1016/j.tem.2014.12.002

Rygiel, K. A., Picard, M., & Turnbull, D. M. (2016). The ageing neuromuscular system and sarcopenia: a mitochondrial perspective. *The Journal of Physiology*, *594*(16), 4499–4512. https://doi.org/10.1113/JP271212

Saeki, K., Suzuki, H., Tsuneoka, M., Maeda, M., Iwamoto, R., Hasuwa, H., Shida, S., Takahashi, T., Sakaguchi, M., Endo, T., Miura, Y., Mekada, E., & Mihara, K. (2000). *Identification of Mammalian TOM22 as a Subunit of the Preprotein Translocase of the Mitochondrial Outer Membrane*. Journal of Biochemical Chemistry. 275(41), 1996-32002. https://doi.org/10.1074/jbc.M004794200

Sakellariou, G. K., Pearson, T., Lightfoot, A. P., Nye, G. A., Wells, N., Giakoumaki, I. I., Vasilaki, A., Griffiths, R. D., Jackson, M. J., & McArdle, A. (2016). Mitochondrial ROS regulate oxidative damage and mitophagy but not age-related muscle fiber atrophy. *Scientific Reports*, *6, 33955(2016)*. https://doi.org/10.1038/srep33944

Salim, A. P. A. A., Suman, S. P., Canto, A. C. V. C. S., Costa-Lima, B. R. C., Viana, F. M., Monteiro, M. L. G., Silva, T. J. P., & Conte-Junior, C. A. (2019). Muscle-specific color stability in fresh beef from grain-finished Bos indicus cattle. *Asian-Australasian Journal of Animal Sciences*, *32*(7), 1036–1043. https://doi.org/10.5713/ajas.18.0531

Sammel, L. M., & Claus, J. R. (2003). Citric Acid and Sodium Citrate Effects on Reducing Pink Color Defect of Cooked Intact Turkey Breasts and Ground Turkey Rolls. *Journal of Food Science*, *68*(3), 874–878. https://doi.org/10.1111/j.1365-2621.2003.tb08259.x

Sammel, L. M., Hunt, M. C., Kropf, D. H., Hachmeister, K. A., Kastner, C. L., & Johnson, D. E. (2002). Influence of chemical characteristics of beef inside and outside semimembranosus on color traits. *Journal of Food Science*, *67*(4), 1323–1330. https://doi.org/10.1111/j.1365-2621.2002.tb10282.x

Sanders .W. R., Garcia-Moll, M., Mellor, J., Salmons, S., & Harlan, W. (1987). *The journal of biological chemistry Adaptation of Skeletal Muscle to Increased Contractile activity expression of nuclear genes encoding mitochondrial proteins.* Journal of Biochemical Chemistry. 262(6), 2764-2767. https://doi.org/10.1016/S0021-9258(18)61572-8

Santetl, A., Frank, S., Gaume, B., Herrler, M., Youle, R. J., & Fuller, M. T. (2003). Mitofusin-1 protein is a generally expressed mediator of mitochondrial fusion in mammalian cells. *Journal of Cell Science*, *116*(13), 2763–2774. https://doi.org/10.1242/jcs.00479

Sawyer, J. T., Apple, J. K., Johnson, Z. B., Baublits, R. T., & Yancey, J. W. S. (2009). Fresh and cooked color of dark-cutting beef can be altered by post-rigor enhancement with lactic acid. *Meat Science*, *83*(2), 263–270. https://doi.org/10.1016/j.meatsci.2009.05.008

Saxton, R. A., & Sabatini, D. M. (2017). mTOR Signaling in Growth, Metabolism, and Disease. *Cell*, *168*(6), 960–976. https://doi.org/10.1016/J.CELL.2017.02.004

Scheffler, T. L., Park, S., & Gerrard, D. E. (2011). Lessons to learn about postmortem metabolism using the AMPKγ3R200Q mutation in the pig. *Meat Science*, *89*(3), 244–250. https://doi.org/10.1016/J.MEATSCI.2011.04.030

Scheinman, R. I., Gualberto, A., Jewell, C. M., Cidlowski, J. A., & Baldwin, A. S. (1997). Characterization of mechanisms involved in transrepression of NF-κB by activated glucocorticoid receptors. *Pneumologie*, *51*(2), 152. https://doi.org/10.1128/mcb.15.2.943

Schrepfer, E., & Scorrano, L. (2016). Mitofusins, from Mitochondria to Metabolism. *Molecular Cell*, *61*(5), 683–694. https://doi.org/10.1016/J.MOLCEL.2016.02.022

Sejian, V., Bhatta, R., Gaughan, J. B., Dunshea, F. R., & Lacetera, N. (2018). Review: Adaptation of animals to heat stress. *Animal*, *12*(2), 431–s444. https://doi.org/10.1017/S1751731118001945

Sentandreu, E., Fuente-García, C., Pardo, O., Oliván, M., León, N., Aldai, N., Yusà, V., & Sentandreu, M. A. (2021). Protein Biomarkers of Bovine Defective Meats at a Glance: Gel-Free Hybrid Quadrupole-Orbitrap Analysis for Rapid Screening. *Journal of Agricultural and Food Chemistry*, *69*(26), 7478–7487. https://doi.org/10.1021/acs.jafc.1c02016

Shapiro, J. A. (2009). Revisiting the Central Dogma in the 21st Century. *Annals of the New York Academy of Sciences*, *1178*(1), 6–28. https://doi.org/10.1111/J.1749-6632.2009.04990.X

Sidell, B. D. (1998). Intracellular oxygen diffusion: the roles of myoglobin and lipid at cold body temperature. *Journal of Experimental Biology*, *201*(8), 119-1128. https://doi.org/10.1242/jeb.201.8.1119

Silva, J. A., Patarata, L., & Martins, C. (1999). Influence of ultimate pH on bovine meat tenderness during ageing. *Meat Science*, *52*(4), 453–459. https://doi.org/10.1016/S0309-1740(99)00029-7

Skibiel, A. L., Zachut, M., do Amaral, B. C., Levin, Y., & Dahl, G. E. (2018). Liver proteomic analysis of postpartum Holstein cows exposed to heat stress or cooling conditions during the dry period. *Journal of Dairy Science*, *101*(1), 705–716. https://doi.org/10.3168/JDS.2017-13258

Skogerson, K., Wohlgemuth, G., Barupal, D. K., & Fiehn, O. (2011). The volatile compound BinBase mass spectral database. *BMC Bioinformatics*, *12*(1), 1–15. https://doi.org/10.1186/1471-2105-12-321/Figures/7

Smith, A. L. (1967). Preparation, properties, and conditions for assay of mitochondria: Slaughterhouse material, small-scale. *Methods in Enzymology*, *10*(C), 81–86. https://doi.org/10.1016/0076-6879(67)10016-5

Sokolova, I. M., Sokolov, E. P., & Haider, F. (2019). *Mitochondrial Mechanisms Underlying Tolerance to Fluctuating Oxygen Conditions: Lessons from Hypoxia-Tolerant Organisms*. Integrative and Comparative Biology. 59(4), 938-952. https://doi.org/10.1093/icb/icz047

Souto-Carneiro, M. M., Klika, K. D., Abreu, M. T., Meyer, A. P., Saffrich, R., Sandhoff, R., Jennemann, R., Kraus, F. V., Tykocinski, L., Eckstein, V., Carvalho, L., Kriegsmann, M., Giese, T., Lorenz, H. M., & Carvalho, R. A. (2020). Effect of Increased Lactate Dehydrogenase A Activity and Aerobic Glycolysis on the Proinflammatory Profile of Autoimmune CD8+ T Cells in Rheumatoid Arthritis. *Arthritis and Rheumatology*, *72*(12), 2050–2064. https://doi.org/10.1002/ART.41420/ABSTRACT

Steel, C., Mcgilchrist, P., Rivas, P. G., Warner, R., & Tarr, G. (2018). *Effect of weather conditions ante-mortem on the incidence of dark cutting in feedlot finished cattle-A retrospective analysis*.

Steiner, J. L., Murphy, E. A., McClellan, J. L., Carmichael, M. D., & Davis, J. M. (2011). Exercise training increases mitochondrial biogenesis in the brain. *Journal of Applied Physiology*, *111*(4), 1066–1071. https://doi.org/10.1152/japplphysiol.00343.2011

Studham, M. E., Tjärnberg, A., Nordling, T. E. M., Nelander, S., & Sonnhammer, E. L. L. (2014). Functional association networks as priors for gene regulatory network inference. *Bioinformatics*, *30*(12). https://doi.org/10.1093/Bioinformatics/BTU285

Suman, S. P., & Joseph, P. (2013). Myoglobin Chemistry and Meat Color. *Annual Review of Food Science and Technology*, *4*(1), 79–99. https://doi.org/10.1146/annurev-food-030212-182623

Szczepanowska, K., Trifunovic, A., Trifunovic, C. A., & Szczepanowska, K. (2021). Mitochondrial matrix proteases: quality control and beyond. *The FEBS Journal*. 289(22), 7128-7146. https://doi.org/10.1111/FEBS.15964

Szklarczyk, D., Morris, J. H., Cook, H., Kuhn, M., Wyder, S., Simonovic, M., Santos, A., Doncheva, N. T., Roth, A., Bork, P., Jensen, L. J., & von Mering, C. (2017). The STRING database in 2017: quality-controlled protein–protein association networks, made broadly accessible. *Nucleic Acids Research*, *45*(1), 362–368. https://doi.org/10.1093/NAR/GKW937

Tachibana, K., Takayanagi, K., Akimoto, A., Ueda, K., Shinkai, Y., Umezawa, M., & Takeda, K. (2015). Prenatal diesel exhaust exposure disrupts the DNA methylation profile in the brain of mouse offspring. *The Journal of Toxicological Sciences*, *40*(1), 1–11. https://doi.org/10.2131/jts.40.1

Tang, J., Faustman, C., Mancini, R. A., Seyfert, M., & Hunt, M. C. (2005). Mitochondrial reduction of metmyoglobin: dependence on the electron transport chain. *Journal of Agricultural and Food Chemistry*, *53*(13), 5449–5455. https://doi.org/10.1021/jf050092h

Tomar, D., Dong, Z., Shanmughapriya, S., Koch, D. A., Thomas, T., Hoffman, N. E., Timbalia, S. A., Goldman, S. J., Breves, S. L., Corbally, D. P., Nemani, N., Fairweather, J. P., Cutri, A. R., Zhang, X., Song, J., Jaña, F., Huang, J., Barrero, C., Rabinowitz, J. E., Madesh, M. (2016). MCUR1 Is a Scaffold Factor for the MCU Complex Function and Promotes Mitochondrial Bioenergetics. *Cell Reports*, *15*(8), 1673–1685. https://doi.org/10.1016/J.CELREP.2016.04.050

Troy, D. J., & Kerry, J. P. (2010). Consumer perception and the role of science in the meat industry. *Meat Science*, *86*(1), 214–226. https://doi.org/10.1016/J.MEATSCI.2010.05.009

Tsigos, C., & Chrousos, G. P. (2002). Hypothalamic-pituitary-adrenal axis, neuroendocrine factors and stress. *Journal of Psychosomatic Research*, *53*(4), 865–871. https://doi.org/10.1016/S0022-3999(02)00429-4

Ulrich-Lai, Y. M., & Herman, J. P. (2009). Neural regulation of endocrine and autonomic stress responses. In *Nature Reviews Neuroscience* 10 (6), 397–409. https://doi.org/10.1038/nrn2647

Unklesbay, K., & Keller, N. (1986). Determination of Internal Color of Beef Ribeye Steaks Using Digital Image Analysis. *Food Structure*, *5*(2), 227–231. https://digitalcommons.usu.edu/foodmicrostructureAvailableat:https://digitalcommons.usu.edu/foodmicrostructure/vol5/iss2/6

Varshavsky, A. (2011). The N-end rule pathway and regulation by proteolysis. *Protein Science*, *20*(8), 1298–1345. https://doi.org/10.1002/PRO.666

Vega, R. B., Huss, J. M., & Kelly, D. P. (2000). The Coactivator PGC-1 Cooperates with Peroxisome Proliferator-Activated Receptor α in Transcriptional Control of Nuclear Genes Encoding Mitochondrial Fatty Acid Oxidation Enzymes. *Molecular and Cellular Biology*, *20*(5), 1868–1876. https://doi.org/10.1128/MCB.20.5.1868-1876.2000/ASSET/A5A82AE2-50FC-4DA1-9B99-D928F0D143F9/ASSETS/GRAPHIC/MB0501309006.JPEG

Wang, C. X., & Guo, F. F. (2013). Branched chain amino acids and metabolic regulation. *Chinese Science Bulletin. 58*(11), 1228–1235. https://doi.org/10.1007/S11434-013-5681-X

Wang, J., Duncan, D., Shi, Z., & Zhang, B. (2013). WEB-based GEne SeT AnaLysis Toolkit (WebGestalt): update 2013. *Nucleic Acids Research*, *41*(1), 77–83. https://doi.org/10.1093/NAR/GKT439

Węglarz, A. (2018). Meat quality defined based on pH and colour depending on cattle category and slaughter season. colour and pH as determinants of meat quality dependent on cattle category and slaughter season. *Czech Journal of Animal Science*, *55*(12), 548–556. https://doi.org/10.17221/2520-cjas

Wenz, T. (2013). Regulation of mitochondrial biogenesis and PGC-1α under cellular stress. In *Mitochondrion* 13(2), 134–142). https://doi.org/10.1016/j.mito.2013.01.006

Westermann, B. (2010). Mitochondrial fusion and fission in cell life and death. In *Nature Reviews Molecular Cell Biology*. 11(12), 872–884. https://doi.org/10.1038/nrm3013

Wills, K. M., Mitacek, R. M., Mafi, G. G., Vanoverbeke, D. L., Jaroni, D., Jadeja, R., & Ramanathan, R. (2017). Improving the lean muscle color of dark-cutting beef by aging, antioxidant-enhancement, and modified atmospheric packaging. *Journal of Animal Science*, *95*(12), 5378–5387. https://doi.org/10.2527/jas2017.1967

Wišniewski, J. R., & Gaugaz, F. Z. (2015). Fast and sensitive total protein and peptide assays for proteomic analysis. *Analytical Chemistry*, *87*(8), 4110–4116. https://doi.org/10.1021/ac504689z

Wojtaszewski, J. F. P., MacDonald, C., Nielsen, J. N., Hellsten, Y., Grahame Hardie, D., Kemp, B. E., Kiens, B., & Richter, E. A. (2003). Regulation of 5′-AMP-activated protein kinase activity and substrate utilization in exercising human skeletal muscle. *American Journal of Physiology - Endocrinology and Metabolism*, *284*(4 47-4), 813–822. https://doi.org/10.1152/AJPENDO.00436.2002/ASSET/IMAGES/LARGE/H10431237006.JPEG

Wright, D. C. (2007). Mechanisms of calcium-induced mitochondrial biogenesis and GLUT4 synthesis. *Applied Physiology, Nutrition and Metabolism*, *32*(5), 840–845. https://doi.org/10.1139/H07-062/ASSET/IMAGES/LARGE/H07-062F1.JPEG

Wu, H., Kanatous, S. B., Thurmond, F. A., Gallardo, T., Isotani, E., Bassel-Duby, R., & Williams, R. S. (2002). Regulation of mitochondrial biogenesis in skeletal muscle by caMK. *Science*, *296*(5566), 349–352. https://doi.org/10.1126/SCIENCE.1071163

Wu, S., Luo, X., Yang, X., Hopkins, D. L., Mao, Y., & Zhang, Y. (2020). Understanding the development of color and color stability of dark cutting beef based on mitochondrial proteomics. *Meat Science*, *163*, 108046. https://doi.org/10.1016/j.meatsci.2020.108046

Wu, Z., Puigserver, P., Andersson, U., Zhang, C., Adelmant, G., Mootha, V., Troy, A., Cinti, S., Lowell, B., Scarpulla, R. C., & Spiegelman, B. M. (1999). Mechanisms controlling mitochondrial biogenesis and respiration through the thermogenic coactivator PGC-1. *Cell*, *98*(1), 115–124. https://doi.org/10.1016/S0092-8674(00)80611-X

Wulf, D. M., Emnett, R. S., Leheska, J. M., & Moeller, S. J. (2002). Relationships among glycolytic potential, dark cutting (dark, firm, and dry) beef, and cooked beef palatability. *Journal of Animal Science*, *80*(7), 1895–1903. https://doi.org/10.2527/2002.8071895x

Young, B. A., Walker, B., Dixon, A. E., & Walker, V. A. (1989). Physiological Adaptation to the Environment. *Journal of Animal Science*, *67*(9), 2426–2432. https://doi.org/10.2527/JAS1989.6792426X

Yu, L. P., & Lee, Y. B. (1986). Effects of Postmortem pH and Temperature Muscle Structure and Meat Tenderness. *Journal of Food Science*, *51*(3), 774–780. https://doi.org/10.1111/J.1365-2621.1986.TB13931.X

Yu, Q., Tian, X., Shao, L., Xu, L., Dai, R., & Li, X. (2018). Label-free proteomic strategy to compare the proteome differences between longissimus lumborum and psoas major muscles during early postmortem periods. *Food Chemistry*, *269*, 427–435. https://doi.org/10.1016/j.foodchem.2018.07.040

Yuan, S., Chan, H. C. S., & Hu, Z. (2017). Using PyMOL as a platform for computational drug design. *Wiley Interdisciplinary Reviews: Computational Molecular Science*, *7*(2), e1298. https://doi.org/10.1002/WCMS.1298

Yuan, Y., Cruzat, V. F., Newshome, P., Cheng, J., Chen, Y., & Lu, Y. (2016). Regulation of SIRT1 in aging: Roles in mitochondrial function and biogenesis. *Mechanisms of Ageing and Development*, *155*, 10–21. https://doi.org/10.1016/J.MAD.2016.02.003

Yun, J., & Finkel, T. (2014). Mitohormesis. In *Cell Metabolism*. 19(5), 757–766. https://doi.org/10.1016/j.cmet.2014.01.011

Zhai, C., Djimsa, B. A., Prenni, J. E., Woerner, D. R., Belk, K. E., & Nair, M. N. (2020). Tandem mass tag labeling to characterize muscle-specific proteome changes in beef during early postmortem period. *Journal of Proteomics*, *222*, 103794. https://doi.org/10.1016/j.jprot.2020.103794

Zhang, H., Bosch-Marce, M., Shimoda, L. A., Yee, S. T., Jin, H. B., Wesley, J. B., Gonzalez, F. J., & Semenza, G. L. (2008). Mitochondrial autophagy is an HIF-1-dependent adaptive metabolic response to hypoxia. *Journal of Biological Chemistry*, *283*(16), 10892–10903. https://doi.org/10.1074/jbc.M800102200

Zhang, J., Ma, G., Guo, Z., Yu, Q., Han, L., Han, M., & Zhu, Y. (2018). Study on the apoptosis mediated by apoptosis-inducing-factor and influencing factors of bovine muscle during postmortem aging. *Food Chemistry*, *266*, 359–367. https://doi.org/10.1016/j.foodchem.2018.06.032

Zhang, Z. Y., Jia, G. Q., Zuo, J. J., Zhang, Y., Lei, J., Ren, L., & Feng, D. Y. (2012). Effects of constant and cyclic heat stress on muscle metabolism and meat quality of broiler breast fillet and thigh meat. *Poultry Science*, *91*(11), 2931–2937. https://doi.org/10.3382/ps.2012-02255

Zhou, Y., Zhou, B., Pache, L., Chang, M., Khodabakhshi, A. H., Tanaseichuk, O., Benner, C., & Chanda, S. K. (2019). Metascape provides a biologist-oriented resource for the analysis of systems-level datasets. *Nature Communications*, *10*(1523). https://doi.org/10.1038/S41467-019-09234-6

Zong, H., Ren, J. M., Young, L. H., Pypaert, M., Mu, J., Birnbaum, M. J., & Shulman, G. I. (2002). AMP kinase is required for mitochondrial biogenesis in skeletal muscle in response to chronic energy deprivation. *Proceedings of the National Academy of Sciences of the United States of America*. 99(25), 15983-15987. https://doi.org/10.1073/pnas.252625599

Zorov, D. B., Juhaszova, M., & Sollott, S. J. (2014). Mitochondrial Reactive Oxygen Species (ROS) and ROS-Induced ROS Release. *Physiol Rev*, *94*, 909–950. https://doi.org/10.1152/physrev.00026.2013.-Byproducts

APPENDICES

APPENDIX A: CHAPTER III SUPPLEMENTAL FILES

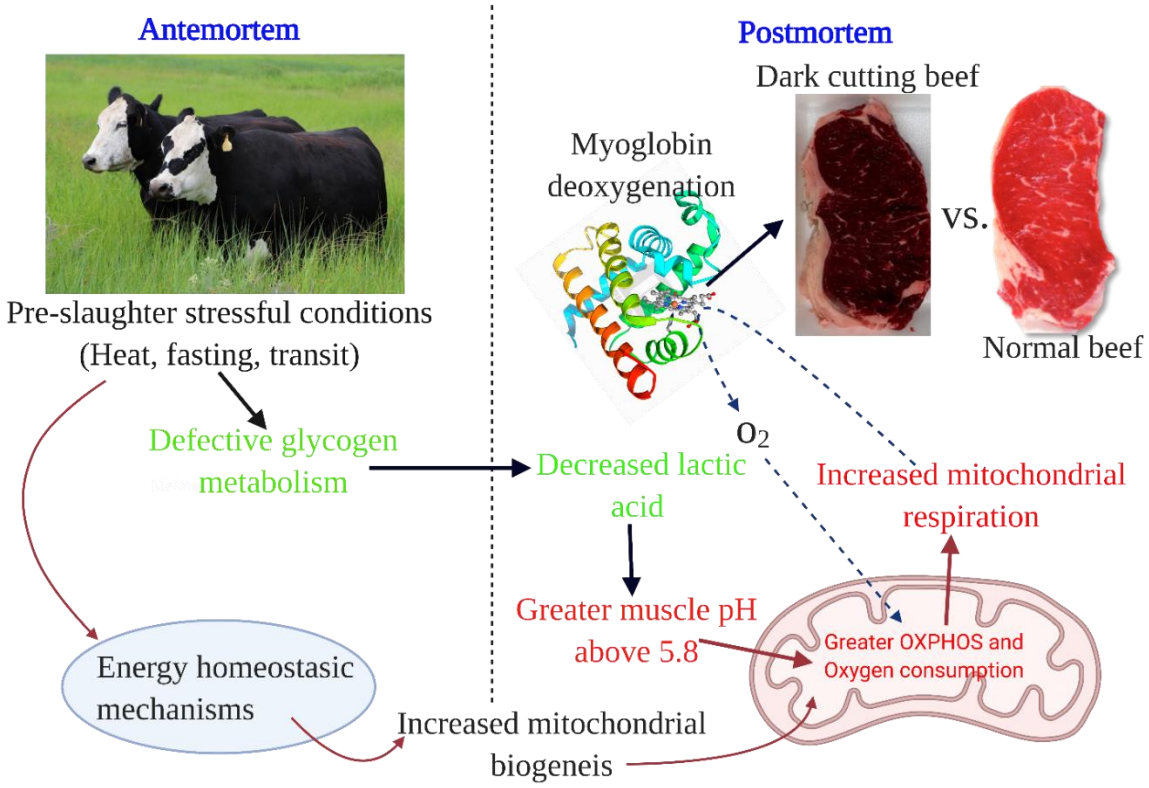

Figure A.1: Graphical abstract

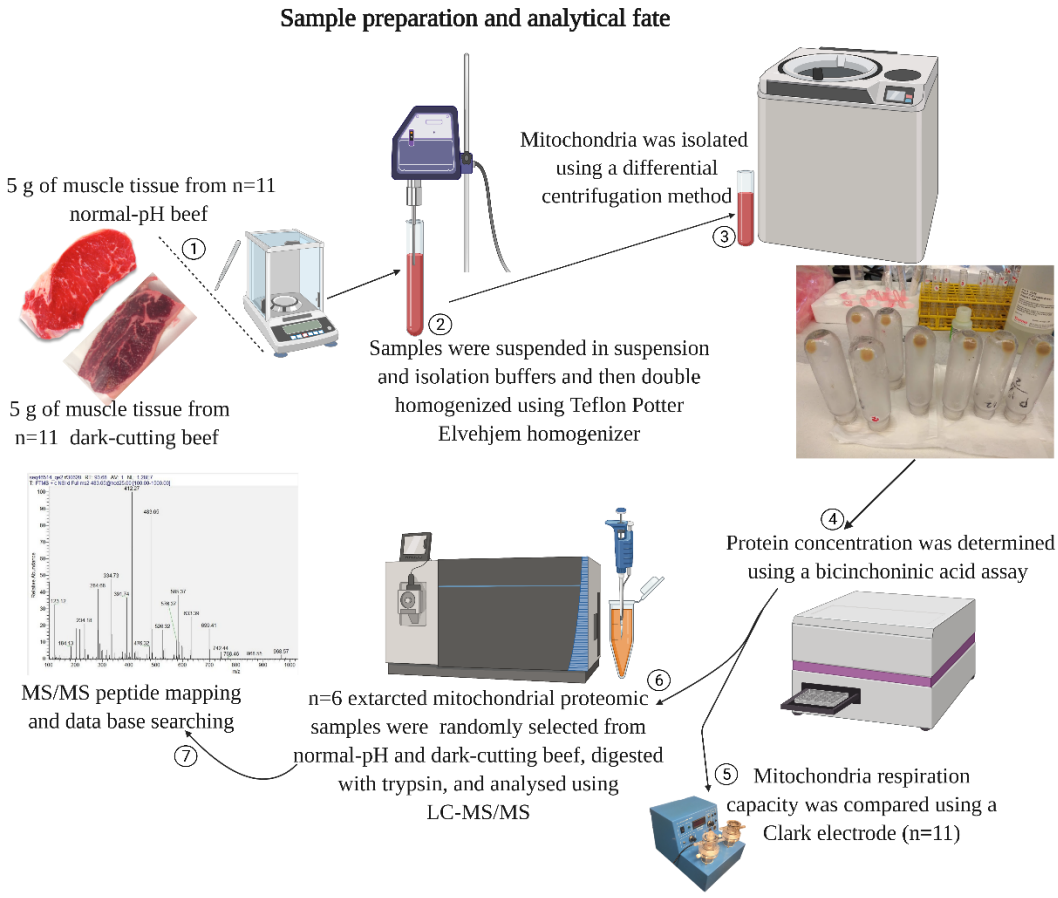

Figure A.2: Flow diagram visualizing sample preparation and analytical fate of normal and dark-cutting beef longissimus muscle. Skeletal muscle tissues from normal-pH and dark-cutting beef collected from a local slaughter facility were utilized in this study. The Mitochondria was isolated and used to compare mitochondrial respiration and proteomic expression profiles quantified according to the flow diagram as described in the Methods.

Table A.1: Containing list of differentially expressed proteins up-regulated in mitochondrial proteome of dark-cutting vs normal-pH beef.

Group	Protein name	Fold Change	Protein profile in DC/NB	Protein id	Gene name
Mitochondrial biogenesis and translation mechanisms	Mitofusion 2	2.4	↑DC	E1BKT8	MFN2
	PGC-1 and ERR-induced regulator in muscle protein 1	2.1	↑DC	A5D7L8	PERM1
	Mitochondrial fission 1 protein	1.7	↑DC	Q3T0I5	FIS1
	Mitochondrial fission process protein 1	2.0	↑DC	Q0VCJ0	MTFP1
	Ring-type E3 ubiquitin transferase (MUL1 protein)	1.8	↑DC	E1BGD5	MUL1
	Eukaryotic translation initiation factor 1	1.7	↑DC	Q5E938	EIF1
	Eukaryotic translation initiation factor 3 subunit I	2.9	↑DC	Q5E966	EIF3I
	Y-box-ninding protein 1(Nuclease-sensitive element-binding protein 1)	1.8	↑DC	P67808	YBX1
Mitochondrial transmembrane and transport proteins	Transmebrane protein 109 (TMEM109 protein)	2.3	↑DC	Q29RH9	TMEM109
	Mitochondrial import receptor subunit TOM40 homolog	1.5	↑DC	Q1LZB5	TOMM40
	Transmembrane protein 43	1.5	↑DC	A6QQR5	TMEM43

	Mitochondrial import receptor subunit TOM22 homolog	1.6	↑DC	A6QPI6	TOMM22
	Transmembrane emp24 domain-containing protein 9	1.5	↑DC	Q3T133	TMED9
	Monocarboxylate transporter 1	1.7	↑DC	Q3MHW6	SLC16A1
	ATPase family AAA domain-containing protein 1	1.9	↑DC	F6QV99	ATAD1
Calcium binding and transport proteins	Calcium-transporting ATPase	1.8	↑DC	Q0VCY0	ATP2A1
	Calcium-transporting ATPase	1.7	↑DC	F1MPR3	ATP2A2
	Calcium-transporting ATPase	2.1	↑DC	E1BMQ6	ATP2A3
	Stromal interaction molecule 1	1.7	↑DC	Q58CP9	STIM1
	Cardiac phospholamban	2.5	↑DC	F2Z4I4	PLN
	Calreticulin	1.7	↑DC	P52193	CALR
	Calnexin	1.6	↑DC	A7Z066	CANX
	Ryanodine receptor 1	2.1	↑DC	E1BDQ4	RYR1
	Trimeric intracellular cation channel type A	2.0	↑DC	A4FV75	TMEM38A
	Annexin A2	1.4	↑DC	P04272	ANXA2

	Calsequestrin	2.6	↑DC	Q05JF3	CAQS1
	Calcium/calmodulindependant protein kinase (CAMK2A protein)	2.1	↑DC	Q08E45	CAMK2A
	Sarcalumenin	1.8	↑DC	F1MJW7	SRL
Fatty acid metabolism	Acyl-CoA synthatase long-chain family member 1(ACSL1 protein)	1.9		Q0VCZ8	ACSL1
	Long-chain fatty acid transport protein 1	2.2	↑DC	A4IFM2	SLC27A1
	Fat storage-inducing transmembrane protein 1	2.0	↑DC	A7YWN2	FITM1
	Carboxylic ester hydrolase	3.0	↑DC	Q3SZM8	BREH1
	Very-long-chain enoyl-CoA reductase	2.6	↑DC	Q3ZCD7	TECR
	Carnitine O-palmitoyltransferase 1, muscle isoform	1.8	↑DC	Q58DK1	CPT1B
	Phospholipase B-like 1	2.0	↑DC	Q9GL30	PLBD1
	Adiponectin	2.2	↑DC	Q3Y5Z3	ADIPOQ
Mitochondrial electron transport and oxidation -reduction proteins	ATP synthase subunit a	1.5	↑DC	P00847	MT-ATP6
	Cytochrome c oxidase subunit 1	1.7	↑DC	P00396	COX1
	Cytochrome c oxidase subunit 3	2.0	↑DC	Q6QTG5	COX3

	Cytochrome b-c1 complex subunit 11	1.3	↑DC	P13272	UQCRFS1
	Aconitate hydratase, mitochondrial	1.4	↑DC	P20004	ACO2
	Cytochrom b5 type B protein	1.7	↑DC	Q0P5F6	CYB5B
	Adenylate kinase 4, mitochondrial	1.6	↑DC	Q0VCP1	AK4
	Kynurenine--oxoglutarate transaminase 3	5.3	↑DC	Q0P5G4	CCBL2
	Peroxiredoxin-4	1.9	↑DC	Q9BGI2	PRDX4
	4-aminobutyrate aminotransferase, mitochondrial	1.6	↑DC	Q9BGI0	ABAT
	Catalase	4.1	↑DC	P00432	CAT
	Enoyl-CoA hydratase and 3-hydroxyacyl CoA dehydrogenase	2.0	↑DC	E1BMH4	EHHADH
	Dehydrogenase/reductase SDR family member 7B	2.5	↑DC	Q3T0R4	DHRS7B
	Pyridine nucleotide-disulfide oxidoreductase domain-containing protein 2	2.6	↑DC	Q3MHH6	PYROXD2
	Prenylcysteine oxidase 1(PCYOX1 protein)	1.7	↑DC	F1N2K1	PCYOX1
	Dehydrogenase/reductase SDR family member 7C	3.2	↑DC	Q1RMJ5	DHRS7C
	Dolichyl-diphosphooligosaccharide--protein glycosyltransferase subunit 1	1.6	↑DC	A3KN04	RPN1

Alpha-soluble NSF attachment protein	1.6	↑DC	A5D7S0	NAPA
PGRMC2 protein	1.5	↑DC	A5PJQ6	PGRMC2
Protein disulfide-isomerase	2.2	↑DC	P05307	P4HB
PDIA6 protein	2.0	↑DC	A6QNL5	PDIA6
TPSB1 protein	2.4	↑DC	A6QPI9	TPSB1
Dolichyl-diphosphooligosaccharide--protein glycosyltransferase 48 kDa subunit	1.6	↑DC	A6QPY0	DDOST
HRC protein	2.3	↑DC	A6QQD7	HRC
Catechol O-methyltransferase	1.7	↑DC	A7MBI7	COMT
SYPL1 protein	2.0	↑DC	A8PVV5	SYPL1
TRIM72 protein(misugumin-53)	1.7	↑DC	E1BE77	TRIM72
Heterogenous nuclear ribonucleoprotein A3	1.5	↑DC	E1BEG2	HNRNPA3
Prolactin regulatory element binding	1.8	↑DC	E1BL12	PREB
Sarcolemma associated protein (SLMAP protein)	2.5	↑DC	E1BMC6	SLMAP
KRAS proto-oncogen, GTPase(KRAS protein)	1.4	↑DC	E1BMX0	KRAS
RAB39A, member RAS oncogen family	1.8	↑DC	G3X7D3	RAB39A

	Protein disulfide-isomerase A4	1.9	↑DC	Q29RV1	PDIA4
	Alpha-amylase	2.0	↑DC	F1MJQ3	AMY2B
	Hedgehog acyltransferase-like	1.9	↑DC	F1MK91	HHATL
	Cathepsin D	1.8	↑DC	P80209	CTSD
	STXBP3 protein	2.6	↑DC	F1MXB4	STXBP3
	NAD(P)(+)--arginine ADP-ribosyltransferase	2.0	↑DC	F6RR68	ART1
	Hras proto-oncogen, Gtpase (HRAS protein0	1.7	↑DC	G3MXH2	HRAS
	Beta-2-microglobulin	3.0	↑DC	P01888	B2M
	Guanine nucleotide-binding protein G(I)/G(S)/G(T) subunit beta-2	1.7	↑DC	P11017	GNB2
	BOLA class I histocompatibility antigen, alpha chain BL3-7	3.4	↑DC	P13753	HLA-B
	BolA-like protein 1	1.6	↑DC	Q3T138	BOLA1
	CHMP4B protein	2.8	↑DC	Q08E32	CHMP4B
	Charged multivesicular body protein 6 (CHMP6 protein)	1.8	↑DC	Q148L0	CHMP6
	1-acylglycerol-3-phosphate O-acycltransferase 5(AGPAT5 protein)	2.0	↑DC	Q0IID8	AGPAT5

	Peptidyl-prolyl cis-trans isomerase B	1.9	↑DC	P80311	PPIB
	Endoplasmic reticulum resident protein 29	2.5	↑DC	P81623	ERP29
	Endoplasmic reticulum chaperon BiP (78 kDa glucose-regulated protein)	1.8	↑DC	Q0VCX2	HSPA5
	PA2G4 protein	1.8	↑DC	Q3ZBH5	PA2G4
	PRA1 family protein 3	1.9	↑DC	Q5E9M1	ARL6IP5
	Cellular nucleic acid-binding protein	2.0	↑DC	Q3T0Q6	CNBP
	GTP-binding protein SAR1b	1.7	↑DC	Q3T0T7	SAR1B
	Dolichyl-diphosphooligosaccharide--protein glycosyltransferase subunit 2	1.5	↑DC	Q3SZI6	RPN2
	Serine protease 23	2.8	↑DC	Q1LZE9	PRSS23
	ADP-ribose glycohydrolase MACROD1	1.5	↑DC	Q2KHU5	MACROD1
	Alpha-1B-glycoprotein	2.9	↑DC	Q2KJF1	A1BG

Table A.2: Containing list of differentially expressed proteins down-regulated in mitochondrial proteome of dark-cutting vs normal-pH beef.

Group	Proteins name	Fold Change	Protein profile in DC/NB	Protein id	Gene name
Actino-myosin cytoskeleton and filament binding proteins	Myosin light chain 1/3, skeletal muscle isoform	1.5	↓DC	A0JNJ5	MYL1
	Myosin heavy chain 9	1.7	↓DC	F1MQ37	MYH9
	Myosin light polypeptide 6	1.6	↓DC	P60661	MYL6
	Myosin light chain 6B	2.9	↓DC	Q148H2	MYL6B
	Myosine binding protein C2	1.5	↓DC	E1BNV1	MYBPC2
	MYBPC1 protein	1.6	↓DC	A6QP89	MYBPC1
	Alpha-actinin-1	1.5	↓DC	Q3B7N2	ACTN1
	Unconventional myosin-Ic	2.1	↓DC	Q27966	MYO1C
	Myozenin 3	1.5	↓DC	F1N0W6	MYOZ3
	Desmin	2.6	↓DC	O62654	DES
	Ankyrin repeat domain 2	2.7	↓DC	F1MX12	ANKRD2
	Dystrophin	3.0	↓DC	P11532	DMD
	Adducin 1	1.7	↓DC	E1BHK2	ADD1

	Coronin	2.0	↓DC	A6QLZ8	CORO6
	Myomesin 2	1,9	↓DC	E1BF23	MYOM2
	Synemin	2.7	↓DC	E1BIS6	SYNM
	Myomesin-1	1.5	↓DC	F1MME6	MYOM1
	Myozenin-1	1.5	↓DC	Q8SQ24	MYOZ1
	Meavinculin	1.7	↓DC	F1N789	VCL
	Ankyrin 3	4.1		A7Z090	ANK3
Troponin complex	Troponin I1, slow skeletal type	2.0	↓DC	G3MYN5	TNNI1
	Troponin T, slow skeletal muscle	2.0	↓DC	Q8MKH6	TNNT1
	Troponin T, fast skeletal muscle	1.4	↓DC	Q8MKI0	TNNT3
	Troponin I2, fast skeletal type	1.5	↓DC	G5E5D2	TNNI2
	Tropomyosin alpha-3 chain	2.4	↓DC	Q5KR47	TPM3
	Tropomyosin beta chain	1.5	↓DC	Q5KR48	TPM2
	Troponin C, slow skeletal and cardiac muscles	2.0	↓DC	P63315	TNNC1
	Tropomodulin-1	1.9	↓DC	A0JNC0	TMOD1
	Tropomyosin alpha-1 chain	1.6	↓DC	Q5KR49	TPM1

Collagen and fibrinogen proteins	Collagen type VI alpha 2 chain	4.2	↓DC	F1MKG2	COL6A2
	Collagen type IV apha 3 chain	2.4	↓DC	E1BB91	COL6A3
	Collagen type IV apha 1 chain	6.2	↓DC	E1BI98	COL6A1
	Fibrinogen beta chain;Fibrinopeptide B	1.5	↓DC	F1MAV0	FGB
	Spectrin beta chain	4.9	↓DC	F1MKE9	SPTB
Glycolytic and energy metabolism proteins	Glycogen phosphorylase, muscle form	1.5	↓DC	F1MJ28	PYGM
	Phosphoglycerate kinase;Phosphoglycerate kinase 1	1.5	↓DC	Q3T0P6	PGK1
	cAMP-dependent protein kinase type II-alpha regulatory subunit	1.5	↓DC	P00515	PRKAR2A
	Glyceraldehyde-3-phosphate dehydrogenase	1.6	↓DC	P10096	GAPDH
	Isocitrate dehydrogenase [NADP] cytoplasmic	2.0	↓DC	A0A140T8A5	IDH1
	3-hydroxyacyl(acyl-carrierprotein) dehydratase/ fatty acid synthase	4.9	↓DC	F1N647	FASN
	Adenylyl cyclase-associated protein	2.2	↓DC	F1N715	CAP2
	NAD-dependant protein deaetylase	1.5	↓DC	G5E521	SIRT3

	NAD-dependent protein deacylase sirtuin-5, mitochondrial	1.7	↓DC	Q3ZBQ0	SIRT5
	Oxygen-dependant coproporphyrinogen-IIIoxidase, mitochondrial	1.7	↓DC	E1BKY9	CPOX
	CSGSH iron sulfur domain 3	1.7	↓DC	G3MWJ2	CISD3
	Cytochrome c oxidase subunit 7C, mitochondrial	1.5	↓DC	P00430	COX7C
	Peptidyl-prolyl cis-trans isomerase A	2	↓DC	P62935	PPIA
	Protein phosphatase 1 regulatory subunit 3A	1.9	↓DC	E1BLN7	PPP1R3A
	Alcohol dehydrogenase [NADP(+)]	1.7	↓DC	Q3ZCJ2	AKR1A1
	14 kDa phosphohistidine phosphatase	1.6	↓DC	Q32PA4	PHPT1
	Carbonic anhydrase 3	2	↓DC	Q3SZX4	CA3
	Guanidinoacetate N-methyltransferase	1.5	↓DC	Q2TBQ3	GAMT
Others	Protein unc-45 homolog B(UNC45B protein)	1.8	↓DC	F1MFZ5	UNC45B
	GTP-binding nuclear protein Ran	1.6	↓DC	Q3T054	RAN
	Probable C->U-editing enzyme APOBEC-2	1.9	↓DC	Q3SYR3	APOBEC2
	Poly(RC) binding protein 2	1.6	↓DC	Q3SYT9	PCBP2
	SET and MYND domain containing 1	2.2	↓DC	F1MZS3	SMYD1

	Ribonuclease inhibitor	1.8	↓DC	H9GW43	RNH1
	General vesicular transport factor p115	2.1	↓DC	P41541	USO1
	SH3 domain binding glutamate rich protein	1.5	↓DC	F1MRQ7	SH3BGR
	CAP-Gly domain containing linker protein 1	2.3	↓DC	E3W9A2	CLIP1
	Muscle-related coiled-coil protein	1.9	↓DC	A5PJI6	MURC
	Spectrin alpha chain	1.8	↓DC	E1BFB0	SPTAN1
	Caveolae associated protein 1	2.3	↓DC	A1L578	CAVIN1
	Clathrin light chain B	2	↓DC	P04975	CLTB
	Clathrin heavy chain 1	1.9	↓DC	P49951	CLTC
	Perilipin 4	1.9	↓DC	F1MNM7	PLIN4
	Immunoglobulin like and fibronectin type III domain containing 1	4.2	↓DC	G3MZU6	IGFN1
	LIM and cysteine-rich domains protein 1	1.5	↓DC	Q17QE2	LMCD1

APPENDIX B: CHAPTER IV SUPPLEMENTAL FILES

Figure B.1: Box and whisker plots of non-significantly abundant (P > 0.05) glycolytic metabolite present in dark-colored beef at slightly elevated pH (ADC) compared with normal-pH (N).

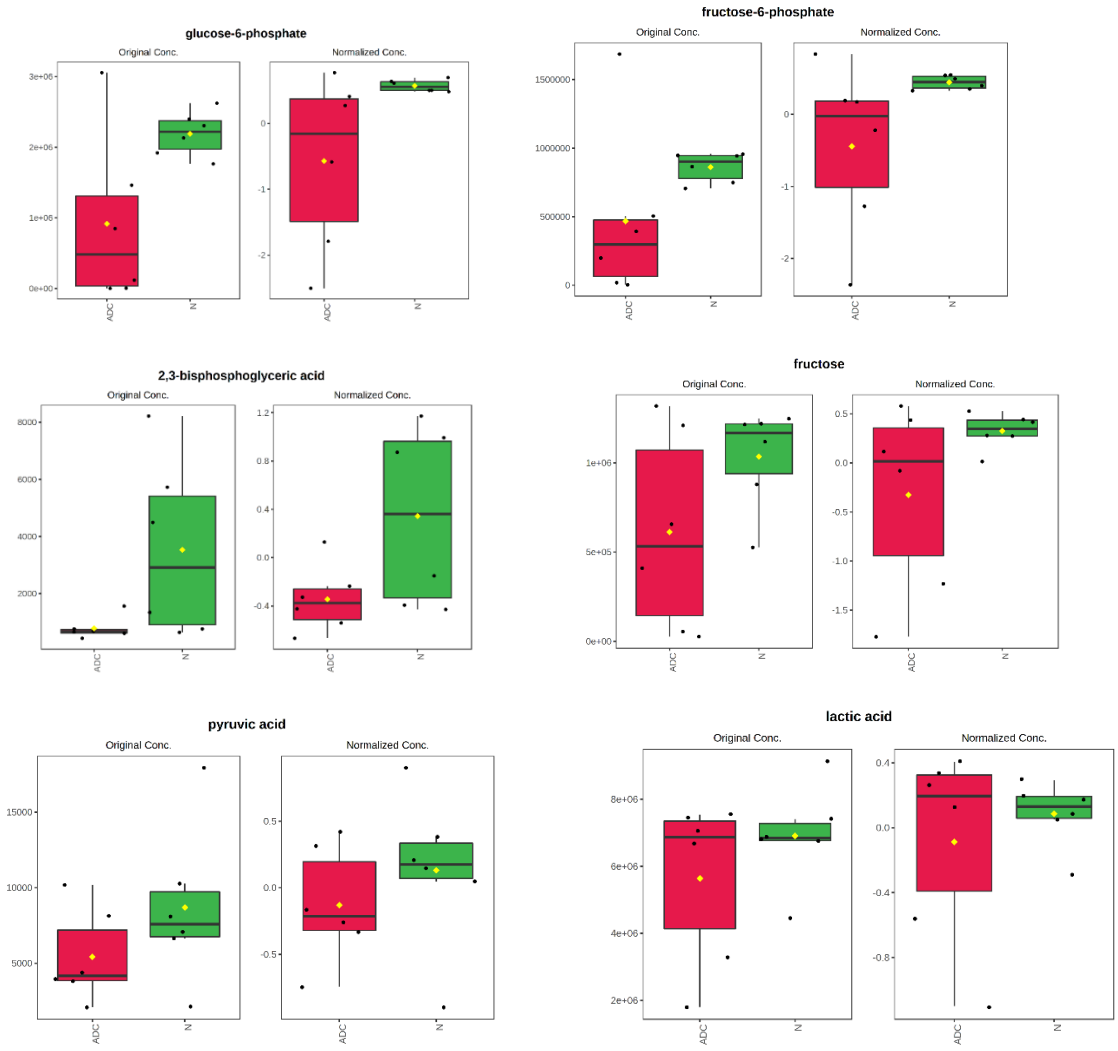

Figure B.2: Box and whisker plots of non-significantly abundant (P > 0.05) tricarboxylic acid cycle (TCA) metabolites present in dark-colored beef at slightly elevated pH (ADC) and normal-pH (N).

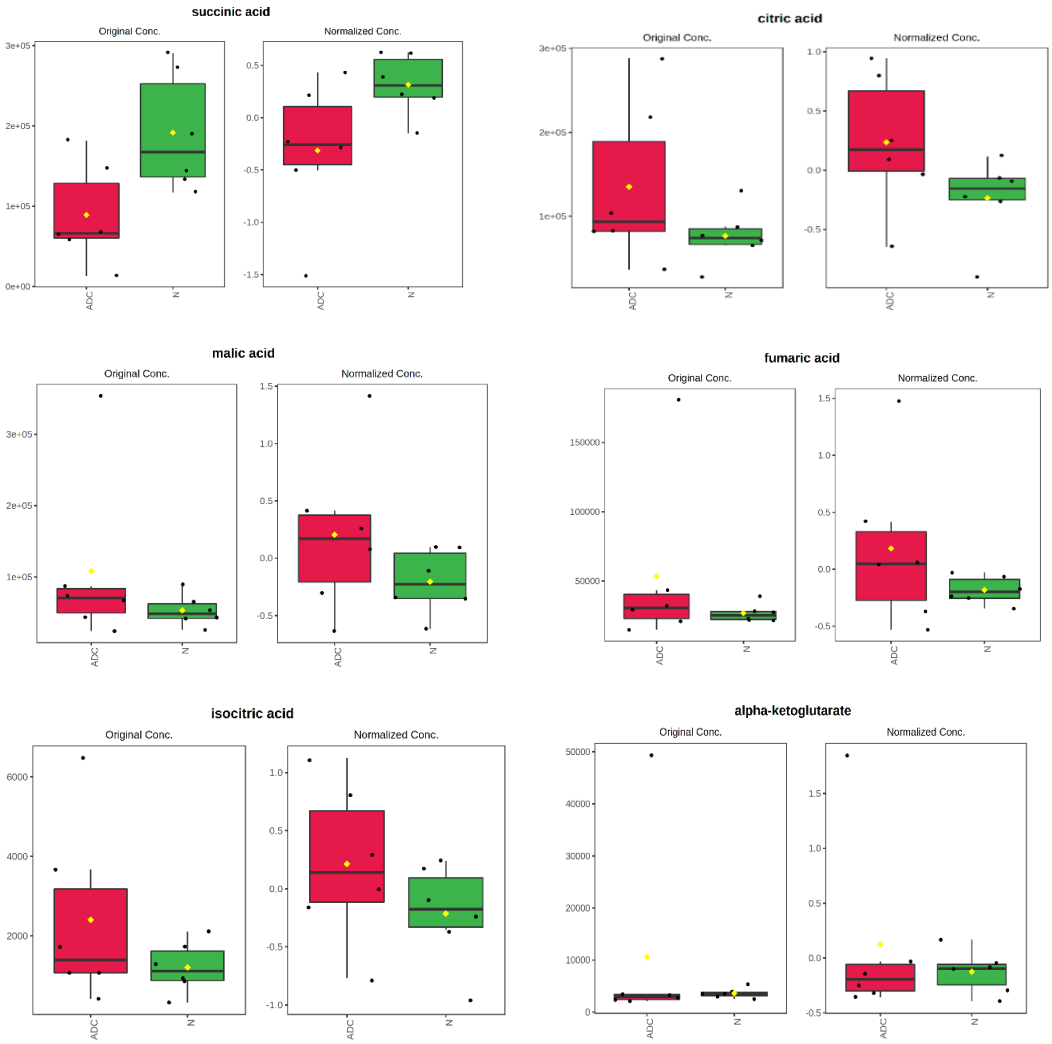

Figure B.3: Box and whisker plots of non-significantly abundant (P > 0.05) adenine nucleotide metabolites present in dark-colored beef at slightly elevated pH (ADC) and normal-pH (N).

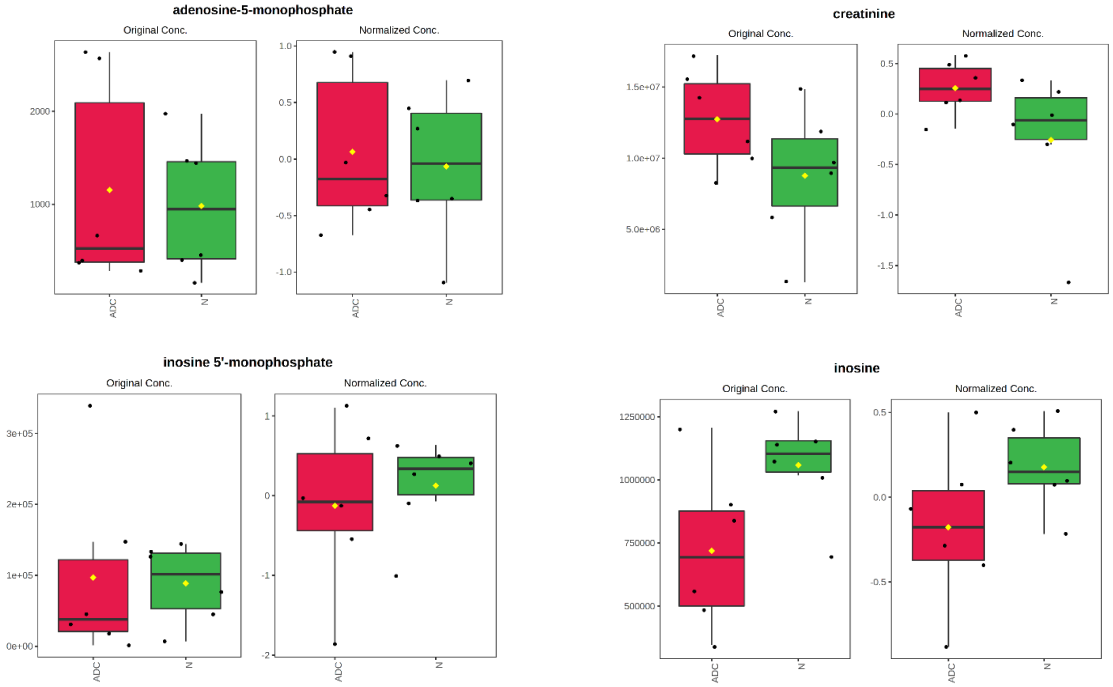

Table B.1: Comparison of color and biochemical properties of normal-pH and dark-colored beef at slightly elevated pH

Parameters		Normal-pH	Dark-colored beef	SEM	P-value
b) Proximate composition[1]	Moisture (%)	71.7	71.2	1.2	0.22
	Protein (%)	23.7	23.7	0.8	0.51
	Fat (%)	4.7	4.8	0.2	0.21
b) Surface color[2]	*L**	43.59	38.48	0.31	< 0.001
	*a**	28.05	25.28	0.28	< 0.001
	b*	21.42	18.94	0.24	< 0.001
c) Biochemical properties[3]	pH	5.57	5.70	0.10	< 0.01
	Oxygen consumption	0.66	0.86	0.058	0.03
	Metmyoglobin reducing activity	0.82	1.32	0.012	0.02

[1]Proximate composition was determined using a NIR-based Food Scan.

[2] Surface color was measured using a HunterLab MiniScan spectrophotometer after exposing the steaks to atmospheric oxygen for 1 h at 4 °C. *L** represents lightness, and a lower number represents darker meat color; *a** value represents redness, and a lower number indicates less red color.

[3] pH was measured using a probe-type pH meter; Deoxymyoglobin content of bloomed and vacuum packaged steaks was used as OC. A greater number indicates more oxygen consumption; Metmyoglobin reducing activity was determined as resistance to form initial metmyoglobin formation, and a greater number indicates greater metmyoglobin reducing activity.

Table B.2: Proteins up-regulated in dark-colored beef at slightly elevated pH compared with normal-pH beef (fold-changes: dark color/normal $P < 0.05$).

Gene name	Protein name	Molecular function	Regulation	Fold change (dark color/normal pH)	P-value
ATP1A2	Sodium/Potassium-transporting ATPase subunit alpha-2	ATPase, ATPase-coupled cation transmembrane transporter activity	↑	1.7	0.02
CYB5R3	NADH-Cytochrome b5 reductase 3	ADP, AMP, FAD, and NAD binding	↑	1.4	0.02
NDUFA7	NADH dehydrogenase[Ubiquinone] 1 alpha sub-complex subunit 7	NADH dehydrogenase(ubiquinone) activity, mitochondrial electron transport	↑	1.5	0.02
OXCT1	Succinyl-CoA:3-ketoacid coenzyme A transferase 1, mitochondrial	CoA transferase activity	↑	1.4	0.005
ACTN4	Alpha-actin-4	Actin-binding, muscle contraction	↑	1.3	0.02
TPM2	Tropomyosin beta chain	Actin binding, muscle contraction	↑	1.3	0.002

XIRP1	Xin actin-binding repeat-containing protein 1	Actin filament binding, muscle contraction, structure, and associated activity	↑	5.0	0.01
SYNPO2L	Synaptopodin 2-like protein	Actin binding, sarcomere organization, muscle contraction	↑	1.5	0.02
SLMAP	Sarcolemmal membrane-associated protein	Muscle contraction	↑	1.5	0.01
JSRP1	Junction sarcoplasmic reticulum protein 1	Skeletal muscle contraction	↑	1.3	0.01
LDB3	LIM domain-binding protein 3	Actin binding and muscle structure development	↑	1.3	0.03
CSRP3	Cysteine and glycine-rich protein 3	Actin-binding, skeletal muscle development	↑	2.1	0.03
HSPB7	Heat shock protein beta-7	Protein C-terminus binding and response to unfolded protein	↑	1.8	0.02
DNAJB4	DNAJ homolog subfamily B member 4	ATPase activator, chaperon, and unfolded protein binding	↑	1.3	0.008
GLRX3	Glutaredoxin-3	Glutathione oxidoreductase activity	↑	1.3	0.05
ANXA3	Annexin A3	Calcium ion binding	↑	1.3	0.03
S100A2	Protein S100-A2	Calcium-dependant protein binding	↑	2.4	0.05

REEP5	Receptor expression-enhancing protein 5	Endoplasmic reticulum organization	↑	1.7	0.016
RBM10	RNA-binding protein 10	miRNA, RNA ,and metal ion binding	↑	1.6	0.007
MAPRE2	Microtubule-associated protein RP/EB family member 2	Microtubule, protein kinase and identical protein binding	↑	1.5	0.03
CNBP	CCHC-type zinc finger nucleic acid-binding protein	mRNA binding and translation regulatory activity	↑	1.4	0.02
DTNA	Dystobrevin alpha	PDZ, phosphate and Zinc ion binding	↑	1.5	0.007
IPO5	Importin-5	GTPase inhibitor activity, nuclear import signal receptor activity, and RNA binding	↑	1.6	0.03

Table B.3: Proteins down-regulated in dark-colored beef at slightly elevated pH compared with normal-pH (fold-changes: dark color/normal $P < 0.05$).

Gene name	Protein name	Molecular function	Regulation	Fold change (dark color/normal pH)	P-value
PYGM	Glycogen phosphorylase, muscle form	Glycogen phosphorylase activity, glycogen metabolic process	↓	-1.4	0.004
PFKM	ATP-dependant6-phosphofructokinase, muscle type	Canonical glycolysis, AMP, ATP binding, and 6-phosphofructokinase activity	↓	-1.3	0.02
PHKB	Phosphorylase b kinase regulatory subunit beta	Glycogen metabolic process, calmodulin-binding	↓	-1.3	0.004
PHKA1	Phosphorylase b kinase regulatory subunit alpha, skeletal muscle	Glycogen metabolic processes, calmodulin binding, and phosphorylase activity	↓	-1.3	0.003
PHKG1	Phosphorylase b kinase gamma catalytic chain, skeletal muscle	Glycogen biosynthesis activity and phosphorylase kinase activity	↓	-1.5	0.001
AGL	Glycogen debranching enzyme	Glycogen biosynthesis activity	↓	-1.3	0.001
EPM2A	Protein-tyrosine-phosphatase	Glycogen binding and glycogen synthase activity	↓	-1.6	0.02

CALM1	Calmodulin-1	Adenylate cyclase activator, calcium ion binding, and channel inhibitor activity	↓	-1.3	0.006
GC	Vitamin D binding protein	Vitamin D binding	↓	-1.4	0.02
BANF1	BAF nuclear assembly factor 1	DNA binding	↓	-1.3	0.04
FBN1	Fibrillin 1	Calcium ion, heparin binding and hormone activity	↓	-1.3	0.004
SDR39U1	Epimerase family protein SDR39UI	Oxidoreductase activity	↓	-1.8	0.006
CZIB	CXXC motif-containing zinc binding protein	Zinc ion binding	↓	-1.7	0.03

Table B.4: Differentially present metabolites in normal-pH and dark-colored beef at slightly elevated pH (fold-changes: dark color/normal > 2 or < 0.5, $P < 0.05$).

metabolite	fold change (darker/normal)	expression	P-value	FDR	role
1-monopalmitin	2.31	up	0.0001	0.02	Fatty acid
1-monostearin	2.27	up	0.002	0.14	Fatty acid
aconitic acid	2.01	up	0.02	0.35	TCA metabolite
cellobiose	0.36	down	0.02	0.35	carbohydrate metabolism
lactose	0.30	down	0.05	0.35	carbohydrate metabolism
maltose	0.35	down	0.02	0.35	carbohydrate metabolism
raffinose	0.34	down	0.04	0.35	galactose metabolism
sophorose	0.35	down	0.04	0.35	galactose metabolism

FDR – false discovery rate P-value

APPENDIX C: CHAPTER V SUPPLEMENTAL FILE

Figure C.1: Box and whisker plots of significantly abundant (P > 0.05) tricarboxylic acid cycle (TCA) metabolites present in dark-colored beef and normal-pH (N) during postmortem storage (Day 7 and 14). The green color represents normal-pH beef and the red color represents dark-colored beef at slightly elevated.

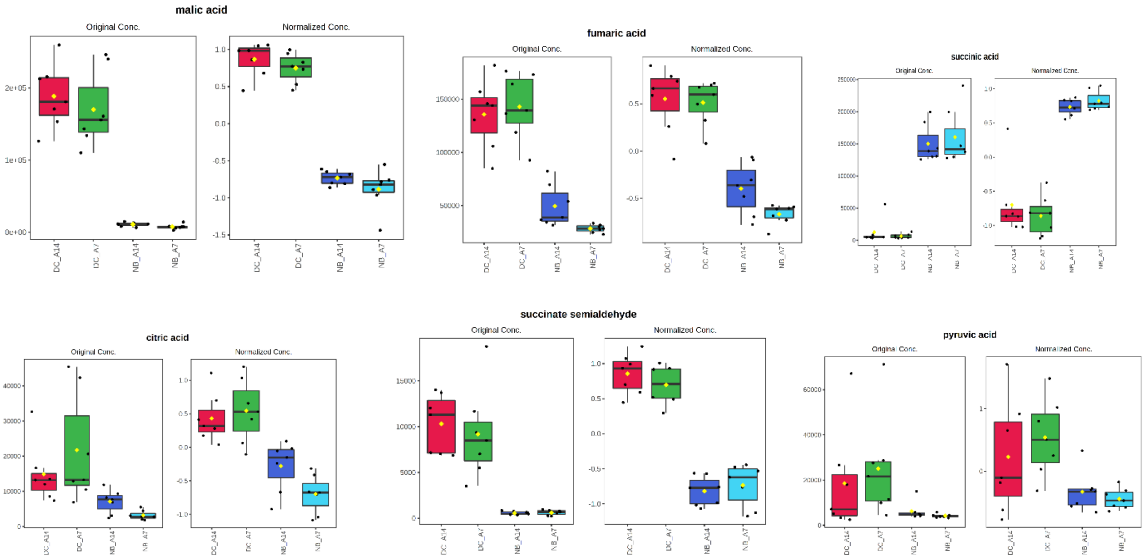

Figure C.2: Box and whisker plots of significantly abundant (P > 0.05) Nucleotide metabolism metabolites present in dark-colored beef and normal-pH (N) during postmortem storage (Day 7 and 14). The green color represents normal-pH beef and the red color represents dark-colored beef at slightly elevated.

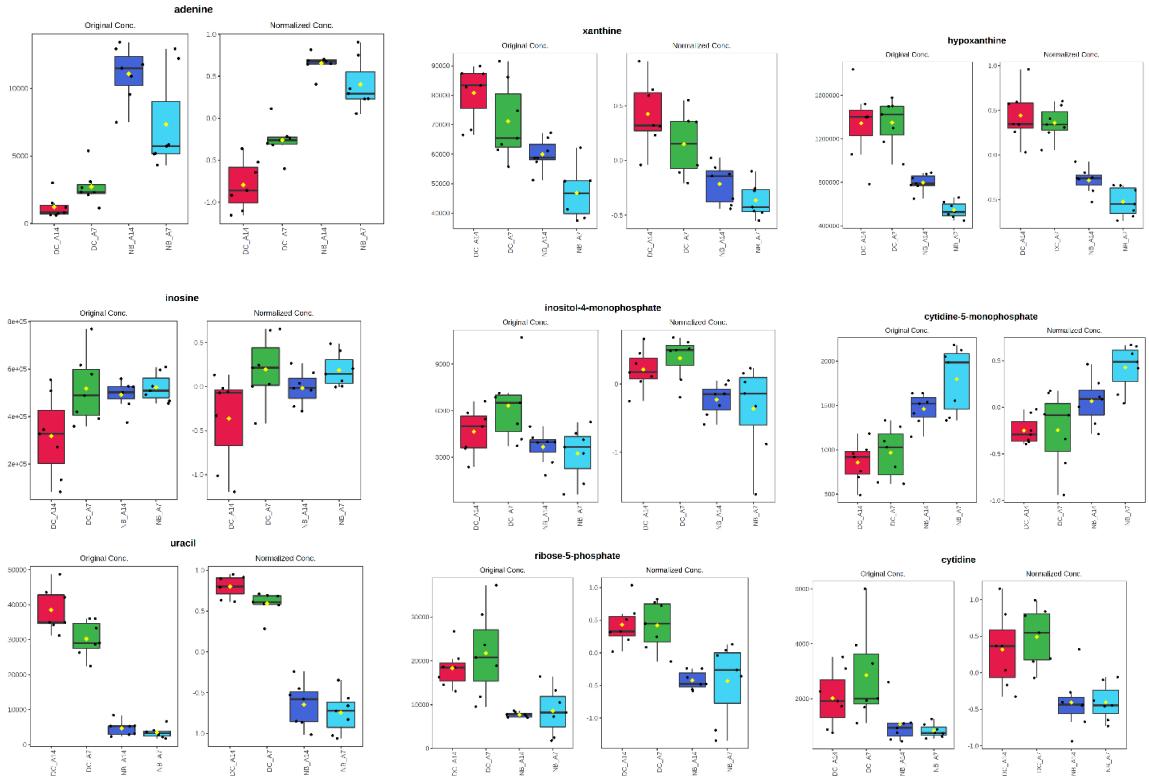

Figure C.3: Box and whisker plots of significantly abundant (P > 0.05) Amino acid metabolism metabolites present in dark-colored beef and normal-pH (N) during postmortem storage (Day 7 and 14). The green color represents normal-pH beef and the red color represents dark-colored beef at slightly elevated.

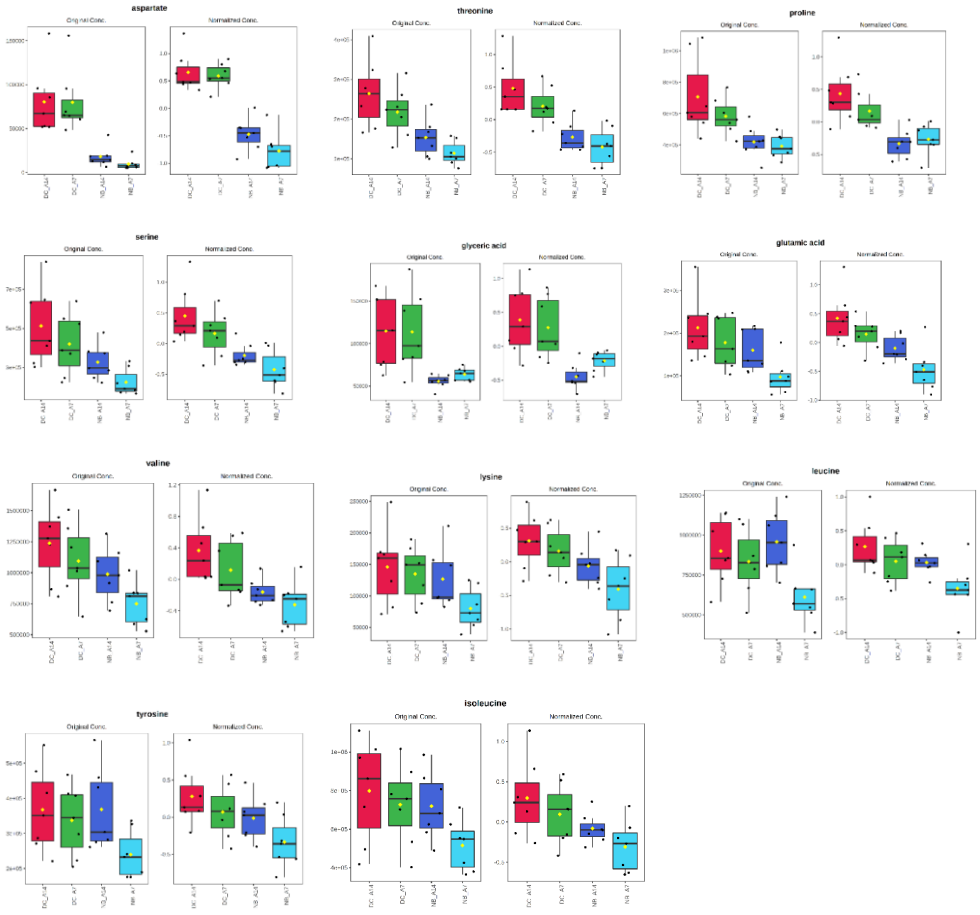

Figure C.4: Box and whisker plots of significantly abundant (P > 0.05) glycogen metabolism metabolites present in dark-colored beef and normal-pH (N) during postmortem storage (Day 7 and 14). The green color represents normal-pH beef and the red color represents dark-colored beef at slightly elevated.

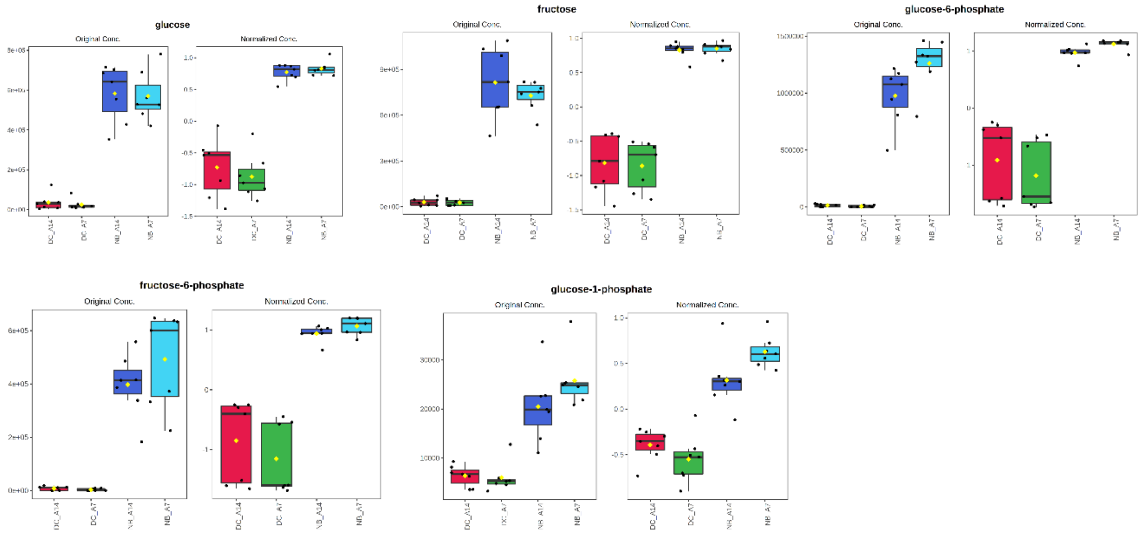

Figure C.5: Protein-protein interaction network of changes in protein abundance within wet-aged dark-cutting beef. (a) Protein-protein interaction networks showing changes in protein abundance at 7 days of aging. (b) Protein-protein interaction networks showing changes in protein abundance at 14 days of postmortem wet-aging.

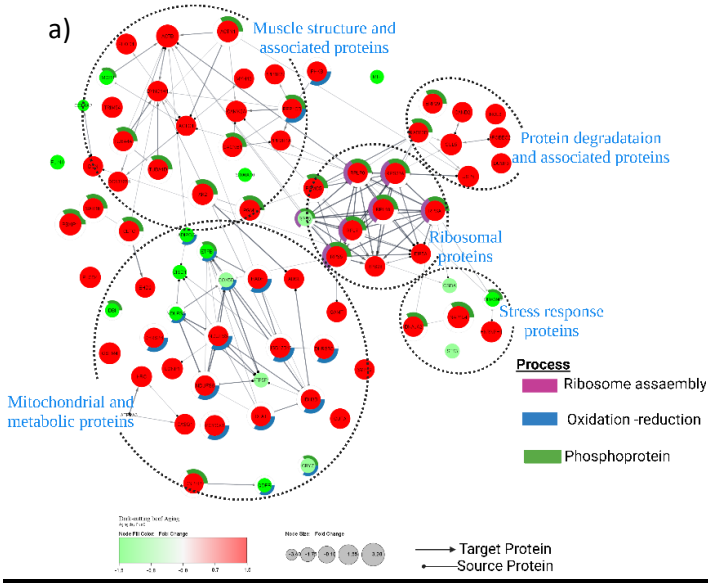

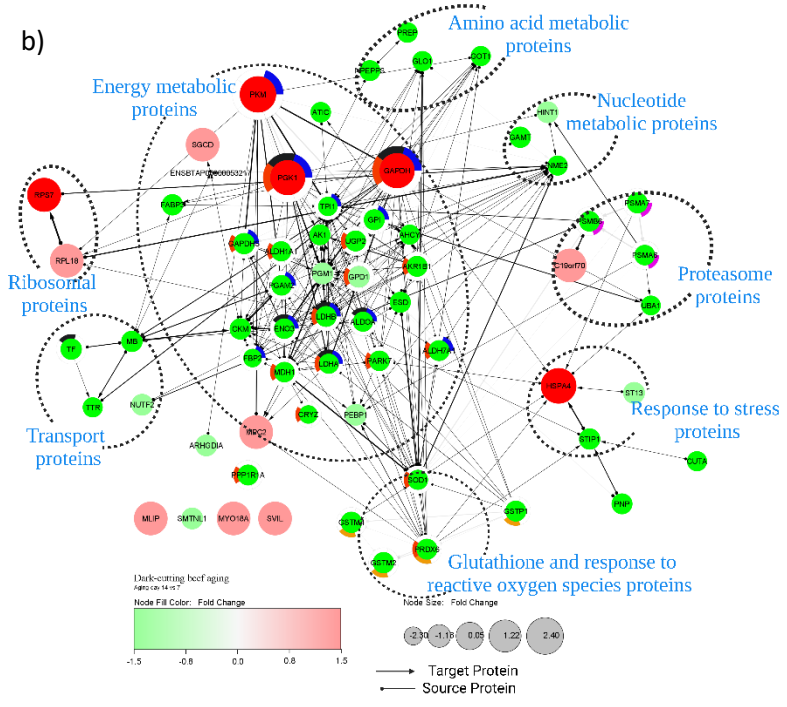

Figure C.6: Analysis of non-semi trypsin specific cleavage peptide profiles in dark cutting compared with normal-pH beef during postmortem storage for 0, 7, and 14 days. (a) Relative abundance median peptide ratios of non-specific trypsin cleavage peptides (N- and C-termini specific) in dark-cutting beef compared with normal-pH beef during postmortem aging. (b) Volcano plot of differentially abundant non-specific peptides in dark-cutting relative to normal-pH beef at 14 days of postmortem storage. (c and d) Pie charts showing the role of the proteins associated with the differentially abundant peptides down-regulated and up-regulated in dark-cutting beef, respectively. (e, f, and g) Protein sequences and structural visualization of the differentially down-regulated peptides in dark-cutting compared with normal-pH beef at day 14 of storage. Protein structures of proteins with ≥5 peptides are represented. The 3D models were constructed using PYMOL as described in the Methods. The green color represents the location of the non-specific peptides with in the protein structures.

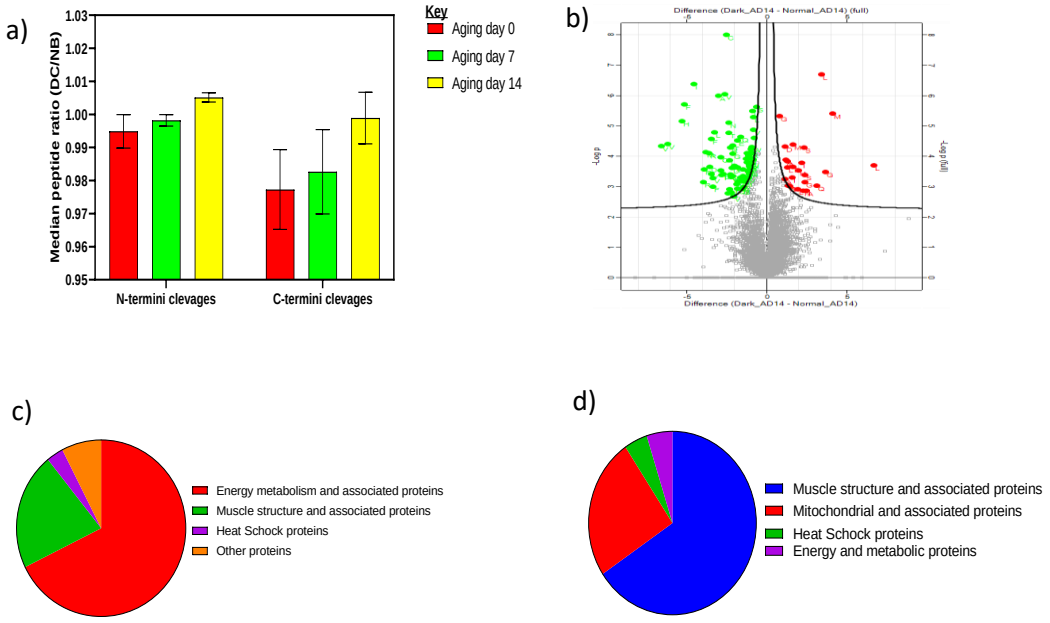

e)Glycogen phosphorylase, muscle isoform-97,293Da

MSRPLTDQEKRKQISVRGLAGVENVTELKKNFNRHLHFTLVKDRNVATPRDYYFALAYTVRDHLVGRWIRTQQ
HYYEKDPKRIYYLSLEFYIGRTLQNTMVNLALENACDEATYQLGLDMEELEEIEEDAGLGNGGLGRLAACFL
DSMATLGLAAYGYGIRYEFGIFNQKISGGWQMEEADDWLRYGNPWEKARPEFTLPVHFYGRVEHTSQGAK
WVDTQVVLAMPYDTPVPGYRNNVVNTMRLWSAKAPNDFNLKDFNVGGYIQAVLDRNLAENISRVLYPND
NFFEGKELRLKQEYFVVAATLQDIIRRFKSSKFGCLDPVRTNFDAFPDKVAIQLNDTHPSLAIPELMRILVD
QERLEWEKAWEVTVKTCAYTNHTVLPEALERWPVHLIETLLPRHLQIIYEINQRFLNRVAAAFPGDVDRLRR
MSLVEEGAVKRINMAHLCIAGSHAVNGVARIHSEILKKTIFKDFYELEPHKFQNKTNGITPRRWLVMCNPG
LAEIIAERIGEEYIADLDQLRKLLSYVDDESFIRDVAKVKQENKLKFSAYLEKEYKVHINPNSLFDIQVKRI
HEYKRQLLNCLHVITLYNRIKKEPNKFFVPRTVMIGGKAAPGYHMAKMIIKLITAIGDVVNHDPVVGDRLR
VIFLENYRVSLAEKVIPAADLSEQISTAGTEASGTGNMKFMLNGALTIGTMDGANVEMAEEAGEENFFIFGM
RVEDVERLDQKGYNAQEYYDRIPELRHVIDQLSSGFFSPKQPDLFKDIVNMLMHHDRFKVFADYEEYIKCQ
ERVSALYKNPREWTRMVIRNIATSGKFSSDRTIAQYAREIWGVEPTRQRMPAPDEKI

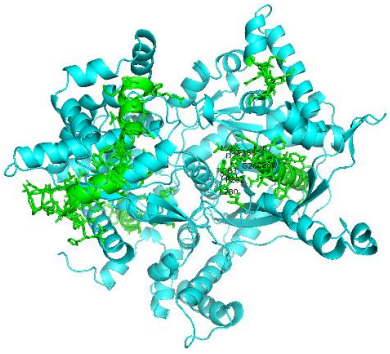

f) Creatine kinase M-type, 42,989Da

MPFGNTHNKHKLNFKAEEEYPDLSKHNNHMAKALTLEIYKKLRDKETPSGFTLDDVIQTGVDNPGHPFIMTVGC
VAGDEESYTVFKDLFDPIIQDRHGGFKPTDKHKTDLNHENLKGGDDLDPNYVLSSRVRTGRSIKGYALPPHC
SRGERRAVEKLSVEALNSLTGEFKGKYYPLKSMTEQEQQQLIDDHFLFDKPVSPLLLASGMARDWPDARGI
WHNDNKSFLVWVNEEDHLRVISMEKGGNMKEVFRRFCVGLQKIEEIFKKAGHPFMWNEHLGYVLTCPSN
LGTGLRGGVHVKLAHLSKHPKFEEILTRLRLQKRGTGGVDTAAVGSVFDVSNADRLGSSEVEQVQLVVD
GVKLMVEMEKKLEKGQSIDDMIPAQK

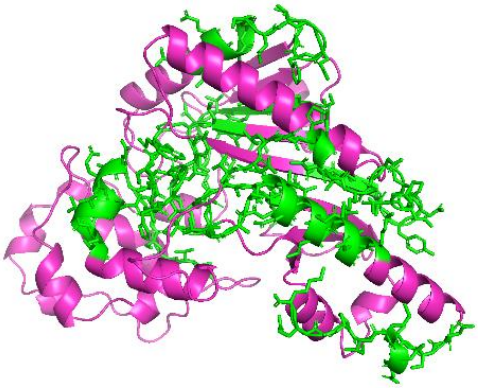

g) Glyceradehyde-3-phosphate, 35,868Da

[1]MVKVGVNGFG[10]RIGRLVTRAA[20]FNSGKVDIVA[30]INDPFIDLHY[40]MVYMFQYDST[50]HGKFNGTVKA[60]ENGKLVINGK[70]AITI
FQERDP[80]ANIKWGDAGA[90]EYVVESTGVF[100]TTMEKAGAHL[110]KGGAKRVIIS[120]APSADAPMFV[130]MGVNHEKYNN[140]TLKI
VSNASC[150]TTNCLAPLAK[160]VIHDHFGIVE[170]GLMTTVHAIT[180]ATQKTVDGPS[190]GKLWRDGRGA[200]AQNIIPASTG[210]AAK
AVGKVIP[220]ELNGKLTGMA[230]FRVPTPNVSV[240]VDLTCRLEKP[250]AKYDEIKKVV[260]KQASEGPLKG[270]ILGYTEDQVV[280]SCD
FNSDTHS[290]STFDAGAGIA[300]LNDHFVKLIS[310]WYDNEFGYSN[320]RVVDLMVHMA[330]SKE

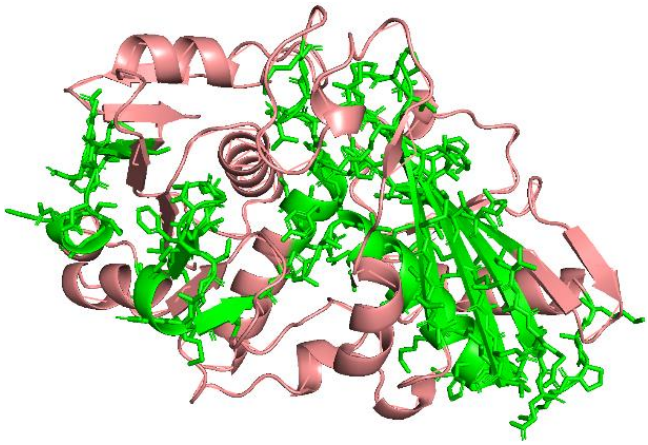

Figure C.7: GO Slim summery of biological processes (Red), cellular component (blue) and molecular functions (green) respectively. (a-c) Categories of differentially abundant proteins in dark-cutting compared with normal-pH beef at day o, 7, and 14 of postmortem wet aging. The height of the bars represents the number of IDs in each category.

a)

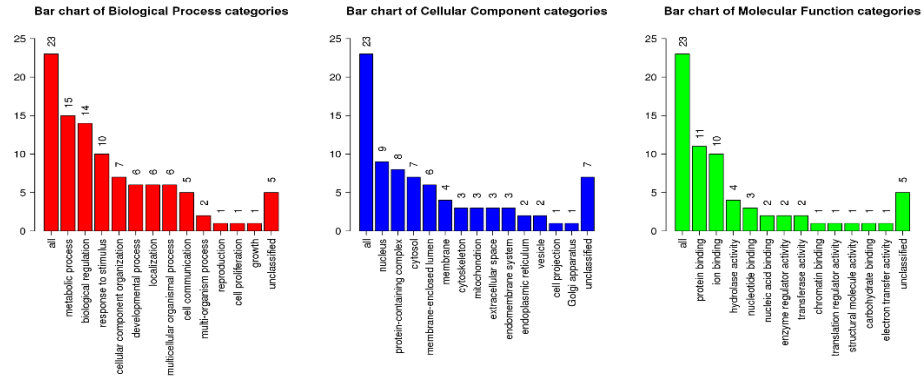

b)

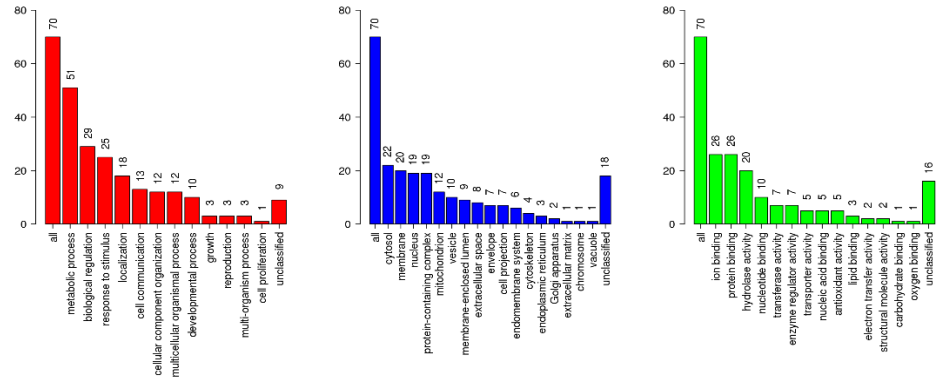

c)

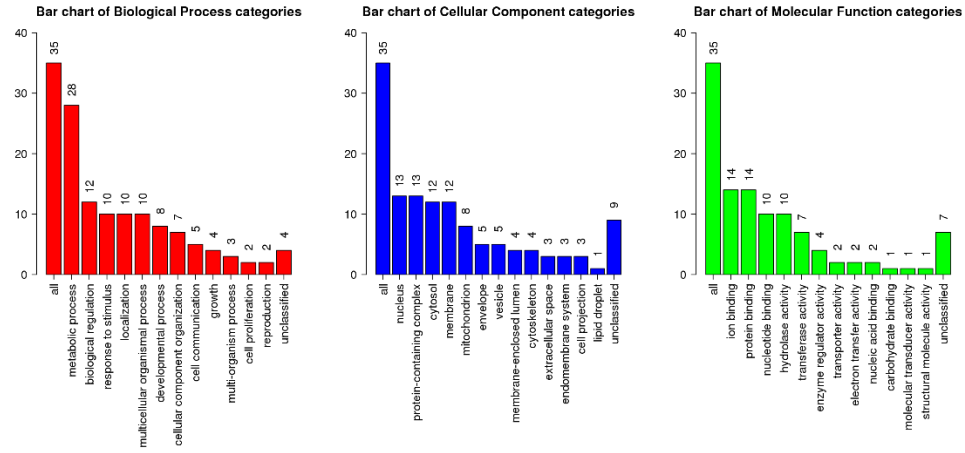

Table C.1: Differentially abundant proteins down-regulated (↓) and up-regulated (↑) in dark-cutting compared with normal-pH beef at day 0 of postmortem aging

Protein name	Fold change	Protein profiles in DC/NB	Protein ID	Protein name
GTP-binding protein SAR1b	-1.7	↓DC	Q3T0T7	SAR1B
Protein-tyrosine-phosphatase	-1.6	↓DC	A5PK37	EPM2A
Myosin-1	-1.6	↓DC	Q9BE40	MYH1
Phosphorylase b kinase regulatory subunit	-1.5	↓DC	A0A3Q1LNY7	PHKG
Phosphorylase b kinase regulatory subunit	-1.5	↓DC	A0A3Q1LYW4	PHKB
Collagen alpha-1(IV) chain	-1.5	↓DC	A0A3Q1LZV6	COL4A1
COP9 signalosome complex subunit 8	-1.5	↓DC	A4FV74	COPS8
Bisphosphoglycerate mutase	-1.5	↓DC	F1MX69	BPGM
Sarcoglycan alpha	-1.5	↓DC	A0A3S5ZPC5	SGCA
Glutaredoxin-3	1.5	↑DC	F1ML12	GLRX3
Peptidyl-prolyl cis-trans isomerase D	1.5	↑DC	P26882	PPID
LIM and cysteine-rich domains protein 1	1.5	↑DC	Q17QE2	LMCD1
Complement component 1 Q subcomponent-binding protein, mitochondrial	1.5	↑DC	Q3T0B6	C1QBP
UTP--glucose-1-phosphate uridylyltransferase	1.6	↑DC	Q07130	UGP2
Alpha-actinin-4	1.6	↑DC	A5D7D1	ACTN4
Myomesin 3	1.6	↑DC	E1BCU2	MYOM3
Fibrinogen gamma-B chain	1.6	↑DC	Q3SZZ9	FGG
Retinal dehydrogenase 1	1.6	↑DC	P48644	ALDH1A1
Succinyl-CoA:3-ketoacid-coenzyme A transferase	1.6	↑DC	Q24JZ7	OXCT1
Cysteine and glycine-rich protein 3	1.7	↑DC	Q4U0T9	CSRP3
Serpin A3-2	1.8	↑DC	Q3ZEJ6	SERPINA3-2
Complement C3	1.8	↑DC	Q2UVX4	C3
Ig-like domain containing protein	2.1	↑DC	F1MLW7	IGLL1
Fructose-biphosphate aldolase	3.7	↑DC	A0A3S5ZPB0	ALDOC
Xin actin-binding repeat-containing protein 1	4.9	↑DC	E1AXU0	CMYA1

Table C.2: Differentially abundant proteins down-regulated (↓) and up-regulated (↑) in dark-cutting compared with normal-pH beef at day 7 of postmortem aging

Protein name	Fold change	Protein profiles in DC/NB	Protein IDs	Gene name
Heat shock protein beta-6	-1.8	↓DC	Q148F8	HSPB6
Proteasome (Prosome, macropain) 26S subunit	-1.7	↓DC	A4FUZ3	PSMC1
Protein phosphatase 1 regulatory subunit 3A	-1.7	↓DC	E1BLN7	PPP1R3A
Bisphosphoglycerate mutase	-1.7	↓DC	Q3T014	BPGM
GTP-binding protein SAR1b	-1.7	↓DC	Q3T0T7	SAR1B
Importin 5	-1.6	↓DC	A0A3Q1LV36	IPO5
Sarcoglycan delta	-1.6	↓DC	E1BPR7	SGCD
Cytosol aminopeptidase	-1.6	↓DC	P00727	LAP3
Bifunctional purine biosynthesis protein PURH	-1.6	↓DC	Q0VCK0	ATIC
Tubulin polymerization-promoting protein family member 3	1.5	↑DC	Q3ZCC8	TPPP3
Superoxide dismutase [Mn], mitochondrial	1.5	↑DC	P41976	SOD2
Phosphoglucomutase-1	1.5	↑DC	Q08DP0	PGM1
Radixin	1.5	↑DC	Q32LP2	RDX
Heat shock protein beta-1	1.5	↑DC	Q3T149	HSPB1

Beta-enolase	1.5	↑DC	Q3ZC09	ENO3
Eukaryotic translation initiation factor 1	1.5	↑DC	Q5E938	EIF1
Peroxiredoxin-2	1.5	↑DC	Q9BGI3	PRDX2
Bridging integrator 1	1.6	↑DC	F6R9I4	BIN1
AHNAK nucleoprotein	1.6	↑DC	A0A3Q1MHT0	AHNAK
Histidine triad nucleotide-binding protein 1	1.6	↑DC	A0A3Q1MQJ9	HINT1
Lumican	1.6	↑DC	Q05443	LUM
Protein CutA	1.6	↑DC	P69678	CUTA
Superoxide dismutase [Cu-Zn]	1.6	↑DC	P00442	SOD1
Aspartate aminotransferase, mitochondrial	1.6	↑DC	P12344	GOT2
Proteasome subunit alpha type-6	1.6	↑DC	Q2YDE4	PSMA6
Protein deglycase DJ-1	1.6	↑DC	Q5E946	PARK7
Apolipoprotein A-I	1.7	↑DC	P15497	APOA1
Serotransferrin	1.7	↑DC	Q29443	TF
Hydroxyacyl-CoA dehydrogenase	1.7	↑DC	F1N338	HADH
Peroxiredoxin-6	1.7	↑DC	O77834	PRDX6
Myoglobin	1.7	↑DC	P02192	MB

L-lactate dehydrogenase A chain	1.7 ↑DC	P19858	LDHA
Complement C3	1.7 ↑DC	Q2UVX4	C3
Hemopexin	1.7 ↑DC	Q3SZV7	HPX
Triosephosphate isomerase	1.8 ↑DC	Q5E956	TPI1
Glutathione S-transferase P	1.8 ↑DC	P28801	GSTP1
Adenosylhomocysteinase	1.8 ↑DC	Q3MHL4	AHCY
Proteasome subunit alpha type-1	1.8 ↑DC	Q3T0X5	PSMA1
Phosphatidylethanolamine-binding protein 1	1.9 ↑DC	P13696	PEBP1
Proteasome subunit beta type-6	1.9 ↑DC	Q3MHN0	PSMB6
Nucleoside diphosphate kinase B	1.9 ↑DC	Q3T0Q4	NME2
L-lactate dehydrogenase B chain	2.0 ↑DC	Q5E9B1	LDHB
S-formylglutathione hydrolase	2.0 ↑DC	Q08E20	ESD
Fructose-bisphosphate aldolase	2.0 ↑DC	A6QLL8	ALDOA
Uncharacterized	2.1 ↑DC	G3N0V0	
Pyruvate kinase	2.1 ↑DC	A5D984	PKM2
Transthyretin	2.1 ↑DC	O46375	TTR
Aspartate aminotransferase, cytoplasmic	2.1 ↑DC	P33097	GOT1

UTP--glucose-1-phosphate uridyl transferase	2.3	↑DC	Q07130	UGP2
Retinal dehydrogenase 1	2.3	↑DC	P48644	ALDH1A1
Fructose-1,6-bisphosphatase isozyme 2	2.4	↑DC	Q2KJJ9	FBP2
Malate dehydrogenase, cytoplasmic	2.5	↑DC	Q3T145	MDH1
Zeta-crystallin	2.5	↑DC	O97764	CRYZ
Serpin A3-2	3.4	↑DC	A2I7M9	SERPINA3-2

Table C.3: Differentially abundant proteins down-regulated (↓) and up-regulated (↑) in dark-cutting compared with normal-pH beef at day 14 of postmortem aging

Protein name	Fold change	Protein profiles in DC/NB	Protein ID	Gene name
Bifunctional purine biosynthesis protein PURH	-3.2	↓DC	Q0VCK0	ATIC
Gp_dh_N domain-containing protein	-2.8	↓DC	A0A3Q1LPH5	g.52082
Cytosol aminopeptidase	-2.5	↓DC	P00727	LAP3
Glyceraldehyde-3-phosphate dehydrogenase	-2.5	↓DC	P10096	GAPDH
Creatine kinase M-type	-2.2	↓DC	Q9XSC6	CKM
Guanidino-acetate N-methyltransferase	-2.0	↓DC	Q2TBQ3	GAMT
Protein phosphatase 1 regulatory subunit 3A	-1.9	↓DC	E1BLN7	PPP1R3A
Glyceraldehyde-3-phosphate dehydrogenase, testis-specific	-1.9	↓DC	Q2KJE5	GAPDHS
Ubiquitin carboxyl-terminal hydrolase isozyme L3	-1.9	↓DC	Q2TBG8	UCHL3
Glycogen phosphorylase, muscle form	-1.8	↓DC	P79334	PYGM
COP9 signalosome complex subunit 3	-1.7	↓DC	A6H7B5	COPS3
Heat shock 70 kD protein binding protein	-1.7	↓DC	A7E3S8	ST13
Phenylalanine--tRNA ligase beta subunit	-1.7	↓DC	A8E4P2	FARSB
COP9 signalosome complex subunit 2	-1.7	↓DC	G3X736	COPS2
cAMP-dependent protein kinase catalytic subunit alpha	-1.7	↓DC	P00517	PRKACA
cAMP-dependent protein kinase type I-alpha regulatory subunit	-1.6	↓DC	P00514	PRKAR1A
Aspartyl aminopeptidase	-1.7	↓DC	Q2HJH1	DNPEP
Uncharacterized	-1.6	↓DC	A0A3Q1NI96	
Adenylosuccinate synthetase isozyme 1	-1.6	↓DC	A5PJR4	ADSSL1
Phosphotriesterase-related protein	-1.6	↓DC	A6QLJ8	PTER
Ubiquitin carboxyl-terminal hydrolase 14	-1.6	↓DC	Q0IIF7	USP14
Trans-1,2-dihydrobenzene-1,2-diol dehydrogenase	-1.6	↓DC	Q148L6	DHDH
Heat shock protein HSP 90-beta	-1.6	↓DC	Q76LV1	HSP90AB1
Vinculin	-1.5	↓DC	A0A3Q1MN97	VCL
Importin subunit alpha	-1.5	↓DC	A0A3Q1MUS6	KPNA3
Uncharacterized	-1.5	↓DC	A0A3Q1NFY4	

Elongation factor 1-gamma	-1.5	↓DC	Q3SZV3	EEF1G
Glycogen debranching enzyme	-1.5	↓DC	F1MHT1	AGL
COP9 signalosome complex subunit 4	-1.5	↓DC	Q3SZA0	COPS4
Heat shock protein HSP 90-alpha	-1.5	↓DC	Q76LV2	HSP90AA1
Succinate dehydrogenase [ubiquinone] iron-sulfur subunit, mitochondrial	1.6	↑DC	Q3T189	SDHB
Cytochrome c oxidase subunit 7A1, mitochondrial	1.6	↑DC	P07470	COX7A1
Myomensin 3	1.6	↑DC	E1BCU2	MYOM3
ADP/ATP translocase 3;ADP/ATP translocase 3, N-terminally processed	1.7	↑DC	P32007	SLC25A6
Uncharacterized	1.8	↑DC	G3N0V0	
Complement C3	1.9	↑DC	Q2UVX4	C3
CDGSH iron-sulfur domain-containing protein 1	1.9	↑DC	Q3ZBU2	CISD1
Coenzyme Q10 homolog A	2.0	↑DC	Q1RMM6	COQ10A
Protein S100-A2	2.3	↑DC	P10462	S100A2

Table C.4: Differentially abundant non-specific N-termini peptides down-regulated (↓) in dark-cutting compared with normal-pH beef at day 14 of postmortem aging

Protein name	Peptide Sequence	[1]First AA	[2]Last AA	Fold Change	Protein profiles in DC/NB	Peptide Mass
Creatine Kinase M-type	VAGDEESYTVFK	V	K	-93.6	↓DC	1344
	TVGCVAGDEESYTVFK	T	K	-4.4	↓DC	1761
	LSVEALNSLTGEFKGK	L	K	-2.9	↓DC	1692
	MWNEHLGYVLTCPSNLGTGLR	M	R	-2.79	↓DC	2417
	SFLVWVNEEDHLR	S	R	-2.3	↓DC	1643
	VLTCPSNLGTGLR	V	R	-2.4	↓DC	1387
	SSEVEQVQLVVDGVK	S	K	-2.4	↓DC	1615
	LGSSEVEQVQLVVDGVK	L	K	-2.2	↓DC	1785
	TDLNHENLKGGDDLDPNYVLSSR	T	R	-2.1	↓DC	2571
	GQSIDDMIPAQK	G	K	-2.0	↓DC	1302
	LSVEALNSLTGEFK	L	K	-2.0	↓DC	1507
Glyceraldehyde-3-phosphate	VVESTGVFTTMEK	V	K	-2.8	↓DC	1427
	VPTPNVSVVDLTCRLEKPAK	V	K	-2.8	↓DC	2222
	LTGMAFRVPTPNVSVVDLTCR	L	R	-4.4	↓DC	2332
	FRVPTPNVSVVDLTCR	F	R	-34.8	↓DC	1859
	AFRVPTPNVSVVDLTCR	A	R	-4.6	↓DC	1930

	IVSNASCTTNCLAPLAK	I	K	-2.4	↓DC	1819
	VPTPNVSVVDLTCR	V	R	-2.1	↓DC	1556
	AITIFQERDPANIK	A	K	-2.3	↓DC	1615
	LISWYDNEFGYSNR	L	R	-2.3	↓DC	1763
	VIHDHFGIVEGLMTTVHAITATQK	V	K	-2.2	↓DC	2617
Glycogen phosphorylase, muscle isoform	VHINPNSLFDIQVK	V	K	-72.1	↓DC	1623
	MSLVEEGAVKR	M	R	-5.0	↓DC	1218
	DIVNMLMHHDR	D	R	-4.6	↓DC	1380
	QPDLFKDIVNMLMHHDR	Q	R	-3.1	↓DC	2108
	VLYPNDNFFEGKELR	V	R	-2.4	↓DC	1840
	WLVMCNPGLAEIIAER	W	R	-2.1	↓DC	1871
	LITAIGDVVNHDPVVGDRLR	L	R	-2.1	↓DC	2158
	CNPGLAEIIAER	C	R	-2.2	↓DC	1342
	QEYFVVAATLQDIIRR	Q	R	-2.2	↓DC	1921
Glycogen debranching enzyme	NDLGHPFCDNLR	N	R	-5.1	↓DC	1457
	LNLQQAGSFQYYFLQGNEK	L	K	-2.8	↓DC	2247
	ALWHLSCDVAEGK	A	K	-3.9	↓DC	1485
	QLRPNFTIAMVVAPELFTTQK	Q	K	-4.8	↓DC	2403
Alpha-actinin-3	MVLQPEGLGTGEGPFAGGR	M	R	-13.9	↓DC	1872
	LQPEGLGTGEGPFAGGR	L	R	-7.2	↓DC	1642

	VLQPEGLGTGEGPFAGGR	V	R	-6.1	↓DC	1741
	GLEQAEKGYEDWLLSEIR	G	R	-2.8	↓DC	2135
	ILAGDKNYITAEELR	I	R	-2.3	↓DC	1705
Myosin-1	FSGPASGEAEGGPK	F	K	-10.2	↓DC	1290
	LFSGPASGEAEGGPK	L	K	-9.6	↓DC	1403
Myosin heavy chain 13	LDEAEQLALKGGK	L	K	-6.6	↓DC	1371
Myosin heavy chain 7	FANYAGFDTPIEK	F	K	-10.9	↓DC	1472
MYBPC1 Protein	CSTELFVREPPVMVTK	C	K	-5.7	↓DC	1892
T-complex protein 1 subunit eta	GGAEQFMEETER	G	R	-2.2	↓DC	1383
Filamin C	HIPGSPFTAK	H	K	-38.6	↓DC	1054
Nebulin	TSDYEQSETSRPALAQPVPEKPVER	T	R	-5.2	↓DC	2813
Dystrophin	GSWQPVGDLLIDSLQDHLEK	G	K	-3.4	↓DC	2249
MGC166429 protein	LAAVEVTEQETK	L	K	-2.0	↓DC	1317
Adenylosuccinate synthatase isozyme 1	YAHMVNGFTALALTK	Y	K	-2.0	↓DC	1636
	ICDLLSDFDEFSSR	I	R	-2.0	↓DC	1703
Phosphorylase kinase	TLLAGSPPFWHRK	T	K	-2.6	↓DC	1509
Pyruvate dehydrogenase E1 component subunit beta, mitochondrial	TIRPMDIETIEGSVMK	T	K	-5.1	↓DC	1819
Beta-enolase	VGDEGGFAPNILENNEALELLK	V	K	-10.1	↓DC	2341

Sarcoplasmic/endoplasmic reticulum calcium ATPase 1	VGTTRVPMTGPVK	V	K	-2.3	↓DC	1342
Aldehyde dehydrogenase, mitochondrial	VVGNPFDSR	V	R	-4.7	↓DC	989.5
Aldehyde dehydrogenase 1A1	LECGGGPWGNK	L	K	-2.3	↓DC	1174
Cytosol aminopeptidase	LILADALCYAHTFNPK	L	K	-2.7	↓DC	1846
Ryanodine receptor 1	YYCLPTGWANFGVTSEEELHLTR	Y	R	-4.0	↓DC	2742
Nucleosome assembly protein-like 4	QVPNDSFFNFFSPLR	Q	R	-3.5	↓DC	1814
Transitional endoplasmic reticulum ATPase	ETVVEVPQVTWEDIGGLEDVK	E	K	-3.5	↓DC	2341
Ubiquitin carboxyl-terminal hydrolase isozyme L3	FLEESASMSPEER	F	R	-3.5	↓DC	1511
SET and MYD domain containing 1	QEPVFADTNIYTLR	Q	R	-7.2	↓DC	1666
Heat shock 70kD protein binding protein	LLGHWEEAAHDLALACK	L	K	-4.9	↓DC	1933

[1]Represents first amino acid in the peptide sequence cleavaged at the N-termini

[2]Represents last amino acid in the peptide sequence cleavaged at the C-termini

Table C.5: Differentially abundant non-specific N-termini peptides up-regulated (↑) in dark-cutting compared with normal-pH beef at day 14 of postmortem aging

Protein name	Peptide Sequence	First AA	Last AA	Fold Change	Protein profiles in DC/NB	Peptide Mass
	HRPDLIDYSK	H	K	2.5	↑DC	1242.64
	HEAFESDLAAHQDR	H	R	2.5	↑DC	1624.72
	QLVPIRDQSLQEELAR	Q	R	2.5	↑DC	1894.03
Alpha-actin-2	ISSSNPYSTVTVDEIR	I	R	2.6	↑DC	1766.87
Alpha-actinin-3	MMMVLQPEGLGTGEGPFAGGR	M	R	165	↑DC	2134
Myosin-2	GIFSILEEECMFPK	G	K	6362.6	↑DC	1698.8
	PLNETVVDLYKK	P	K	3.1	↑DC	1417.78
	ANDDLKENIAIVER	A	R	3.1	↑DC	1598.83
	MFVLEQEEYK	M	K	2.6	↑DC	1314.62
Myosin-heavy chain 7	GSSFQTVSALHR	G	R	37.9	↑DC	1288.65
Myosin light chain kinases 2, Skeletal	EEDCFQILDDCPPPPAPFPHR	E	R	3.5	↑DC	2536.12
Myosin heavy chain 11	QANPILEAFGNAKTVK	Q	K	4.8	↑DC	1699.93
Myomesin 1	FPVTGLIEGR	F	R	2.3	↑DC	1087.6
Myomesin 2	LRSHTVWER	L	R	4.9	↑DC	1182.63
	VSNLHEGHFYEFR	V	R	3.6	↑DC	1633.76
Myomesin 3	SVSEAGVGESSAVTEPIR	S	R	3.5	↑DC	1773.87

	AINQYGMSDPSEPSEPIALR	A	R	4.7	↑DC	2174.03
	VNNITSER	V	R	2.4	↑DC	931.472
Nebulin	GMGCFLYDTPDMVR	G	R	3.4	↑DC	1660.7
Troponin C, skeletal muscle	NNDGRIDYDEFLEFMK	N	K	2.9	↑DC	2004.89
Tropomyosin alpha-1 chain	ENALDRAEQAEADKK	E	K	3.1	↑DC	1686.82
Troponin I1	AKECWEQEHEEREAEK	A	K	46.3	↑DC	2086.9
	LVDYLDVGFDTTR	L	R	1626.4	↑DC	1512.75
Collagen type VI alpha 3 chain	LQASVTPLTTPVVSSK	L	K	4.1	↑DC	1626.92
Junctional sarcoplasmic reticulum	DVEAPAPVPESWASSSSSPK	D	K	4	↑DC	2026.95
F-actin-capping protein subunit alpha-2	EATDPRPYEAENAIESWR	E	R	2.4	↑DC	2132.98
Filamin C	DGTCTVSYLPTAPGDYSIIVR	D	R	4.6	↑DC	2284.1
Pelctin	DGRHPQGEQMYR	D	R	2.4	↑DC	1472.66
Cofilin-2	ASGVTVNDEVIK	A	K	2.6	↑DC	1230.65
Phosphate carrier protein, mitochondrial	AVEEQYSCDYGSGR	A	R	4.9	↑DC	1619.65
ADP/ATP translocase	AAYFGVYDTAK	A	K	5.4	↑DC	1204.58
Succinate dehydrogenase[ubiquinone]iron-sulfur subunit	CHTIMNCTQTCPK	C	K	6.5	↑DC	1649.68
Succinate dehydrogenase[ubiquinone] flavor-protein subunit	TYFSCTSAHTSTGDGTAMVTR	T	R	3.1	↑DC	2249.97

ATP synthase subunit alpha, mitochondrial	VVDALGNAIDGK	V	K	2.7	↑DC	1170.62
ATP synthase subunit f, mitochondrial	LGELPSWILMR	L	R	13.8	↑DC	1313.72
Electron transfer flavor-protein subunit alpha, mitochondrial	HLGGEVSCLVAGTK	H	K	15.7	↑DC	1426.72
NADH dehydrogenase[ubiquinone] 1 beta subunit 9	HLESWCIHR	H	R	29.7	↑DC	1236.58
Cytochrome b-c1 complex subunit 7	DDTIHENDDVKEAIR	D	R	8.7	↑DC	1768.82
Voltage-dependent anion-selective channel protein 3	ICNYGLTFTQK	I	K	2.7	↑DC	1343.65
	LTFDSSFSPNTGK	L	K	4	↑DC	1399.66
60kDa heat shock protein, mitochondrial	VGGTSDVEVNEK	V	K	2.4	↑DC	1232.59
Heat shock cognate 71 kDa protein	STAGDTHLGGEDFDNR	S	R	33.7	↑DC	1690.72
CDGSH iron-sulfur domain-containing protein 1	HNEETGDNVGPLIIKK	H	K	3.5	↑DC	1762.92
Glycogen debranching enzyme	SGDWMIDYVSNR	S	R	35.9	↑DC	1441.63
Alpha -enolase	AAVPSGASTGIYEALELRDNDK	A	K	2.6	↑DC	2276.13
MYBPC1 Protein	NSETDTIVFIR	N	R	2.4	↑DC	1293.66
	FTITGLPTDSR	F	R	2.5	↑DC	1206.62
	ENYAGNYR	E	R	2.7	↑DC	985.425
	DDSGVYHINLK	D	K	2.7	↑DC	1259.61
Four and a half LIM domains 1	FVFHQEQVYCPDCAK	F	K	2.7	↑DC	1926.84

PDZ and LIM domain 5	GCTGSLNMTLQR	G	R	2.8	↑DC	1336.62
PDZ and LIM domain 5	ILAQITGTEHLK	I	K	24.2	↑DC	1322.76
DLST protein	AEAGAGVGLR	A	R	2.8	↑DC	899.482
	AFTMTAAETAR	A	R	3.5	↑DC	1168.55
Ryanodine receptor 1	ISQSAQTYDAR	I	R	7.8	↑DC	1238.59

[1]Represents first amino acid in the peptide sequence cleavaged at the N-termini

[2]Represents last amino acid in the peptide sequence cleavaged at the C-termini

Peptide sequences within the same row originated from the same protein

APPENDIX D: COPY RIGHTS

A: JOURNAL PROTEOMICS:

Dear Frank Kiyimba,

Thank you so much for contacting us.

Please note that, as one of the authors of this article, you retain the right to reuse it in your thesis/dissertation. You do not require formal permission to do so. You are permitted to post this Elsevier article online if it is embedded within your dissertation. Kindly cite with full acknowledgement to the article as mentioned below:

Example: “This article/chapter was published in Publication title, Vol number, Author(s), Title of article, Page Nos, Copyright Elsevier (or appropriate Society name) (Year).”

Please feel free to contact me if you have any queries.

All our best wishes for your dissertation submission!

Kind regards,

Kaveri Thakuria

Senior Copyrights Coordinator

ELSEVIER | HCM - Health Content Management

B: JOURNAL ANIMAL SCIENCE:

Dear Frank Kiyimba,

Thank you for your email.

As an Oxford author, you retain the right to include the article in full or in part in a thesis or dissertation, provided that this not published commercially. For more information, please see the following page:
https://academic.oup.com/pages/authoring/journals/production_and_publication/online_licensing

If you have any further queries, please do not hesitate to contact us.

Kind regards,

Olivia Wignall
Author Support | Oxford Journals
Oxford University Press

VITA

Frank Kiyimba

Candidate for the Degree of

Doctor of Philosophy

Dissertation: THE MOLECULAR AND BIOCHEMICAL BASIS OF DARK-CUTTING BEEF

Major Field: Animal Science

Biographical:

Education:

Completed the requirements for the Doctor of Philosophy in Animal Science at Oklahoma State University, Stillwater, Oklahoma in December, 2022.

Completed the requirements for the Master of Science in Animal Science at Oklahoma State University, Stillwater, Oklahoma in 2019.

Completed the requirements for the Bachelor of Science in Agriculture at Makerere University, Kampala, Uganda in 2017.